Observations of Snow and Ice Formation on Solar Photovoltaic Panels and an Enhanced Method
of Modelling Snow Melting from Solar Photovoltaic Panels

by

Robert Elliott Pawluk

A thesis submitted in partial fulfillment of the requirements for the degree of

Master of Science

in

Civil (Cross-Disciplinary)

Department of Civil and Environmental Engineering
University of Alberta

Abstract

One of the fundamental limitations of solar photovoltaic (PV) generating systems in cold regions is snow accumulations blocking irradiance from reaching the PV cells. Snow accumulations on PV panels result in both reduced electricity generation and increased uncertainty in electricity generation predictions.

A comprehensive literature review summarizes existing research that is targeted at quantifying and modelling the impact of snow on the electricity generation of PV systems. Furthermore, it analyses factors that influence the effect snow has on PV panels and mitigation methods to reduce the effect of snow.

In order to better understand the formation of snow accumulations and improve the prediction of snow clearing on PV panels, an experiment was set up in Edmonton, Canada. The experimental setup gathered data that served as the foundation for the remaining analyses in the thesis.

Observations of the formation of ice between the snow accumulations and the panel surface are presented, and analysis identifies the sources of moisture for icing: snow melting on contact with a warm panel, ice pre-existing on the panel before the snow accumulation formed, and partial melting of the existing snow accumulation. The formation of ice provided evidence that adhesion between the panel, ice, and snow acts together with friction to prevent snow accumulations from sliding clear of PV panels.

An enhanced empirical model is presented to predict the meteorological conditions under which snow accumulations will likely begin sliding or melting from PV panels. The key enhancement is using an estimation of the radiation being absorbed by the panel rather than the plane-of-array irradiance on a snow-covered panel. This empirical model is evaluated using data collected

through experimentation. The proposed changes increase the modelling precision by up to a factor of four.

Lastly, a simple first-principle model to predict PV panel temperature is established. The model is a transient state model and accounts for the heat capacity of the PV panels. The model was employed to further enhance the developed empirical threshold models by accounting for the heat capacity of the panels. The heat capacity was accounted for in the threshold by using time dependent-weighted values of the current and preceding irradiance, for which the weighting coefficients were determined with the first principle model.

Preface

This thesis contains three manuscripts described below, the remainder of this thesis is an original manuscript for which the research and writing were done by Robert Pawluk.

Chapter 2 of this thesis has been accepted as Robert E. Pawluk, Yuxiang Chen, and Yuntong She, "Photovoltaic Electricity Generation Loss Due to Snow – A Literature Review on Influence Factors, Estimation, and Mitigation," *Renewable & Sustainable Energy Reviews*. I was responsible for the research as well as the manuscript construction. Yuxiang Chen and Yuntong She acted as the supervisory authors and aided in the development of concepts & structure as well as editing.

Chapter 4 of this thesis was presented as Robert Pawluk, Yuxiang Chen, and Yuntong She, "Observations of Ice at the Interface Between Snow Accumulations and Photovoltaic Panel Surfaces," at the *6th International Renewable and Sustainable Energy Conference*, Rabat Morocco, Dec 5-8, 2018 and may be published on IEEE Xplore. I was responsible for the experimental design & construction, performing the experiments, analysis, and manuscript construction. Yuxiang Chen and Yuntong She acted as the supervisory authors and aided in the development of concepts & structure as well as editing.

An adaptation of Chapter 5 will be submitted as Robert Pawluk, Yuxiang Chen, and Yuntong She, to the journal *Solar Energy.* I was responsible for the experimental design & construction, data collection, analysis, and manuscript construction. Yuxiang Chen and Yuntong She acted as the supervisory authors and aided in the development of concepts & structure as well as editing.

Acknowledgments

This work would not have been possible without the assistance and support of many people, for which I am enormously thankful.

I am particularly thankful to my co-supervisor Dr. Y. Chen for his selfless devotion to developing his students and providing me with the opportunity and ongoing support to develop and adapt my research. I am deeply grateful to Dr. Y. She for the guidance she provided me that led me to develop more meaningful research, and the considerable time she has spent developing my technical writing skills.

Although it would not be possible to thank all of the people who have directly and indirectly assisted me to develop this thesis, I would like to extend a thank-you to the following people.

- Zequn Wang, a close friend, for his endless encouragement, support, and assistance in all forms
- My father, Ronald Pawluk, for the extensive amount of thought and effort he devoted to helping me construct the experiment
- My peers, Behnaz Hesaraki, Regina Celi Dias Ferreira, Jiacheng Yao, Stephan Fan, Marko Spasojevic, Anni Wei, Maysoun Ismaiel, Yue Shao, and Ahmed Al-Tamimi for their compassion as well as the knowledge they shared about building science and the specifics of their research

Finally, I would like to say thank you to my entire family for the sacrifices they have made to open doors for me time and time again. Without their unwavering commitment it would not have been possible to pursue this research.

Table of Contents

List of Tables

List of Figures

Chapter 1: Introduction

Increasingly renewable energy contributes to meeting global energy needs; renewable energy sources (e.g., solar, wind, hydro, and biomass) was responsible for 24% of global electricity generation in 2016, contributing more than natural gas [1]. Furthermore, the installed electricity generating capacity of renewable energy has outpaced the growth in any individual fossil fuel [1]. The application of solar photovoltaic (PV) is increasing exponentially (Figure 1.1); the installed capacity has more than doubled in the three years between 2014 and 2017, to 404.5 GW [2]. The growth in solar PV has been driven by a decrease in system cost, and high levels of scalability. The costs of PV modules and the associated hardware has decreased significantly, between 2010 and 2018 the installed cost of PV systems decreased by more than a factor of three [3]. The scalability allows for small point-of-use PV systems (less than 10 kW) and large utility scale systems (greater than 100 MW) to both be feasible. Furthermore, PV systems can stand alone or be integrated into other land uses (e.g. buildings and parking lots) and have a minimal effect on the usability of the surrounding areas.
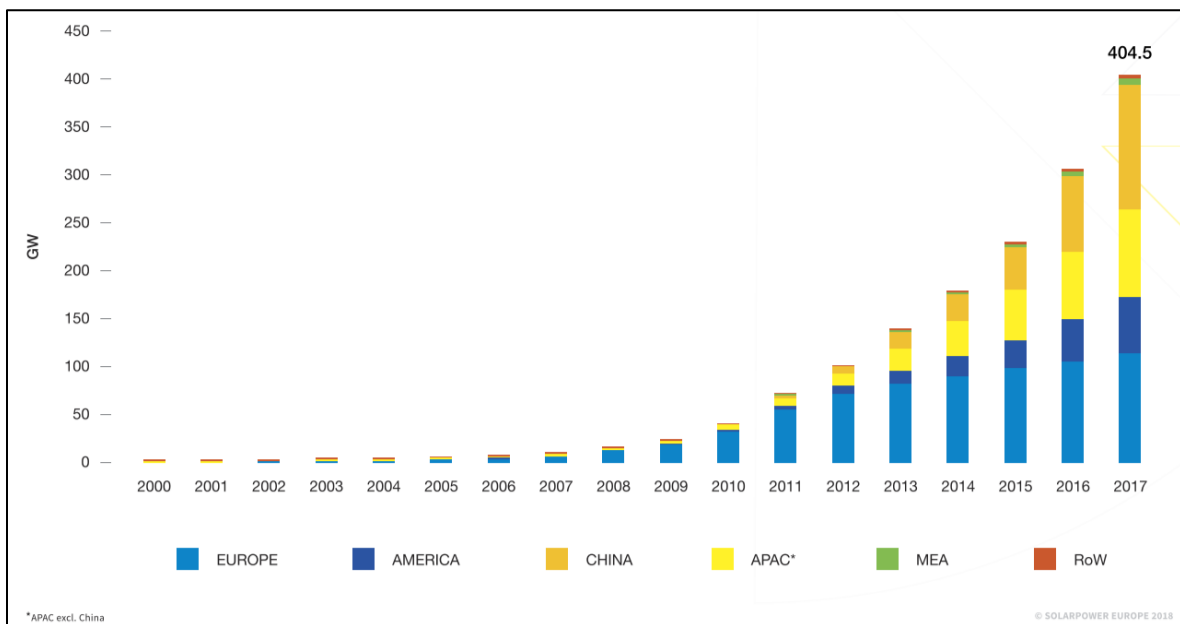
Figure 1.1 Global Total Solar PV Installed Capacity 2000-2017 [2]

Unlike traditional forms of electricity generation, the electricity generation from certain renewable energy forms (e.g., wind and solar) is not consistent and varies with meteorological conditions. To effectively integrate PV solar into electricity grid management, their generation must be highly predictable. Without being effectively integrated into the grid the benefits that PV solar provides are severely limited, as it does not replace the need for other generating sources, and their associated fixed costs (e.g., maintenance, borrowing costs, and administrative costs).

Throughout winter months, in regions of high latitude, PV system electricity generation is challenged by lower solar exposure and snow cover, at the same time these regions have the highest energy demands during the winter. Snow cover on PV panels reduces the amount of solar irradiance reaching the PV cells, resulting in significantly less, or no electricity generation. Research has reported that snow can reduce the annual electricity generation by up to 34% [4], but generally less than 10% [5-9]. However, up to 90% to 100% of electricity generation during winter months can be lost [5,10,11]. Furthermore, snow can remain on panels for days or weeks [5,10,12], significantly reducing the predictability and consistency of PV system electricity generation during winter months. The loss in generation and lack of predictability in winter months make it difficult to consider PV systems, in their current state, as an effective replacement for traditional energy sources in regions of high latitude. However, reducing the effect of snow on the electricity generation from PV systems, and increasing its predictability would enhance the integration of PV systems into electricity grids, and allow them to offer more value to regional electricity grids.

Currently, there is extensive multidisciplinary work towards improving the applicability and efficiency of solar PV. A portion of the research has been focused on developing accurate electricity generation prediction models. Modelling efforts are broad, from increasing the accuracy of irradiance predictions to understanding the interaction between meteorological conditions and

PV panel generation. A small part of the research effort is focused on understanding how snow effects electricity generation. It is the author's belief that developing a thorough understanding of what causes snow to remain on PV panels, developing methods of mitigating the impact of snow, and being able to adequately model its impact is critical for the broad adoption of PV generation to be possible in cold regions that experience snow.

1.1. Objective and Scope of the Research

This thesis was created to serve three purposes. The first purpose was to highlight the current level of understanding of the interaction between PV systems and snow. The second was to increase the understanding of the cause of snow accumulations. The third purpose was to improve the modelling methods used to approximate the effect of snow on PV system generation.

The scope of this thesis was limited in three ways. First, the scope was limited to the direct effect of snow on PV system generation, and not the long-term effect that snow can have on the degradation of PV panels. Second, throughout this thesis the analyses are supported by studies and experimental observations related to PV systems, avoiding tangential information; this was done to ensure the analysis remained focused and comprehensible. Third, the research presented focusses on the enhancement of the thresholds that define when clearing begins in empirical threshold type snow cover prediction models; it does not focus on the development of a first-principle model (based purely on known thermal heat transfer relationships) that can be used independently.

1.2. Outline of Thesis

- Chapter 2: Photovoltaic Electricity Generation Loss Due to Snow – A Literature Review on Influence Factors, Estimation, and Mitigation, thoroughly explores previous research related to quantifying the electricity generation loss caused by snow, influence factors

affecting the loss, loss estimation techniques, and mitigation methods with potential to effectively reduce loss. The literature review highlights i) that there is a limited understanding of the interactions at the interface between the snow and the panel, and ii) the importance of accurately modelling the snow clearing process. The remainder of the research presented in this thesis is targeted at addressing these two topics.

- Chapter 3: Experimental Setup, provides an in-depth explanation of the testing apparatus and data measurement and logging equipment. The use of non-conventional data logging and measurement equipment is analyzed. The data collected from the experimental setup was used as the foundation for the analyses in the remaining three chapters.

- Chapter 4: Observations of Ice at the Interface Between Snow Accumulations and Photovoltaic Panel Surfaces, presents observations of the formation of ice between PV panel surfaces and snow accumulations, and analyses the source of moisture for ice formation. These observations further highlight the complexity of the interactions occurring at the panel-snow interface by suggesting that the adhesion of the ice on the PV panel surface is contributing to snow accumulations remaining on the panels. If this hypothesis is correct, then models that approximate when panel temperatures reach 0°C—when the ice would melt—are correctly simulating the thermal processes causing sliding. Bosman [13], Marion et al. [5], and Lorenz et al. [14] developed empirical threshold models to predict the snow cover clearing off PV panels by indirectly simulating panel temperature.

- Chapter 5: Empirical Threshold Modelling, presents a unique way to calculate absorbed irradiance from standard meteorological observations. This chapter also demonstrates

that the use of an approximated value of the absorbed irradiance by the panel to develop threshold type empirical snow cover prediction models can significantly improve the modelling precision.

- Chapter 6: First Principle Model, presents the development of a simple first-principle thermal heat transfer model that predicts PV panel temperature. Empirical models are beneficial to system designers and operators; however, first-principle models offer more adaptability, which can be useful for researchers. The developed model simulates when melting is expected to begin given ambient temperature, irradiance conditions, and PV characteristics. In this analysis, the first-principle model is used to quantify the impact of preceding irradiance values on the PV panel temperature, as a result of the thermal heat capacity of the panel. The relative impacts of the current and preceding irradiance values are then used to establish weighted absorbed irradiance threshold models. The weighted absorbed irradiance models offered a modest improvement over the absorbed irradiance models discussed in Chapter 5.

- Chapter 7: Conclusions, summarizes the previous chapters, highlights the important findings of the thesis, and provides suggestions for future research in the field.

Chapter 2: Photovoltaic Electricity Generation Loss Due to Snow – A Literature Review on Influence Factors, Estimation, and Mitigation

This paper provides a critical literature review of the impact of snow accumulations on photovoltaic (PV) system electricity generation. The review quantifies the impact of snow, identifies factors that influence the generation loss, examines existing snow impact estimation techniques, and identifies mitigation strategies to reduce the impact of snow accumulations. Reported annual and monthly electricity generation losses resulting from snow accumulations on photovoltaic systems show that annual electricity generation losses were less than 10% in most climates; however, monthly generation losses throughout the winter were generally higher than 25%. The influences of climatic characteristics and system characteristics on the impact of snow were examined individually, and the codependence between influence factors was also discussed where relevant. Estimation techniques for electricity generation loss due to snow cover were summarized. Relatively accurate estimates are achievable by several models when considering ambient temperature, solar irradiance, and snow depth. Ten mitigation methods were identified as having the potential to reduce the impact of snow on PV system electricity generation and were discussed qualitatively. This review provides system designers and operators with the information required to identify how to manage the effect of snow on PV systems and highlights the need for researchers to develop ways to reduce and predict the impact.

2.1. Introduction

The dependence on renewable energy to satisfy global energy needs is increasing. Renewable energy sources (e.g., solar, wind, hydro, and biomass) contributed to 24% of total power generation in 2016 and has been contributing more to global electricity generation than natural gas since 2013 [1]. Furthermore, the growth in renewable energy's electricity generating capacity has outpaced the growth in any fossil fuel's electricity generating capacity[1]. Solar photovoltaic (PV)

installations have increased rapidly; in the five years between 2011 and 2016, the installed capacity of solar PV systems increased by a factor of four, to 303 Gigawatts [15]. The rate of growth of solar PV far exceeds that of other renewable energy sources [15], for two primary reasons: reductions in system costs and scalability. Between 2012 and 2017 the installed cost of utility-scale PV systems decreased by over a factor of two, due in large part to reductions in PV module costs [16]. The unique scalability of solar PV makes it cost-effective to build relatively small PV systems for point-of-use electricity generation (less than 10 kW) or large utility-scale projects (greater than 100 MW), and neither have a substantial impact on the neighbouring area.

Because of the current financial framework used by most electricity grids, PV system designs are not purposefully optimized to generate electricity during times with the highest electricity demand. As a result, PV is not replacing alternative generating sources, and the associated fixed costs (e.g., maintenance, borrowing costs, and administrative costs) and the environmental impacts of maintaining alternative generating capacity remain. PV systems would offer more financial and environmental value to electricity grids if they could be depended on during periods of peak demand. Additionally, the electricity generation should be predictable and frequent to effectively use existing energy storage and perform offsettable energy uses (e.g., drying clothes, pre-heating buildings, or pumping to fill reservoirs) when energy is plentiful, cutting the requirement for backup electricity generating infrastructure.

Communities at high latitudes have the largest energy requirements during the winter, due in large part to space heating needs. However, PV systems at high latitudes are subject to snow cover as well as less solar exposure. Furthermore, snow cover reduces the amount of solar irradiance that reaches the PV cells, resulting in significantly less, or no electricity generation. The amount of electricity generation loss caused by snow cover has been found to be as high as 34% of the annual

generation [4] but is typically less than 10% [5-9]. However, during winter months, 90% to 100% of expected generation can be lost due to snow cover on PV panels [5,10,11]. Snow cover, which can last for several days or weeks [5,10,12], increases the uncertainty and reduces the frequency of PV electricity generation throughout the winter. The geographical factor and snow impact all contribute to PV systems not being effective replacements, in their current state, for traditional energy sources in regions of high latitude. Focusing on improving winter electricity generating capacity and dependability, rather than maximizing overall generation in the design of PV systems could result in PV systems offering more value to electricity grids.

The objective of this paper is to provide a better understanding of the effects of snow cover on PV system electricity generation, influencing factors, and provide insight into how winter PV electricity generation can be predicted and increased for regions with snow events. The paper first quantifies the impact of snow on PV system electricity generation by reviewing the results of past studies. The variance in these results is then examined quantitatively and qualitatively to identify the influence factors including ambient temperature, snowfall amount, solar irradiance, friction and adhesion, obstructions to sliding, tilt angle, and the array arrangement. Next, existing modelling techniques that predict snow cover and the amount of electricity generation loss due to snow cover are described and contrasted. Finally, mitigation methods that have the potential to reduce the snow-caused generation loss are identified and evaluated qualitatively. From this point forward, loss will mean electricity generation loss of PV systems due to snow cover unless specified otherwise.

2.2. Quantifying the Electricity Generation Loss Caused by Snow Cover

Many studies have assessed the loss of fixed PV panels [4-6,8-11,17,18]. Table 2.1 summarizes the impact of snow on PV panel monthly and annual electricity generation reported in previous

studies. No studies, to the authors' knowledge, have reported the loss of PV systems mounted on solar trackers; it is believed that their loss is considerably smaller than that of fixed systems [11,19].

Table 2.1 Monitored Electricity Generation Loss Caused by Snow Cover in Past Studies

Climate[1]	Location	Annual Snowfall	Tilt Angle	Snow Sliding Obstructed	Annual Electricity Generation Loss	Winter Month Electricity Generation Loss
Severe	Truckee, California [10]	487 cm Measured	0°	No[2]	18%	10% to 100% Avg: 42%[4]
			24°	Yes	15%	8% to 90% Avg: 33%[4]
			39°	Yes	12%	6% to 80% Avg:25%[4]
	Truckee, California [11]	610 cm Measured	0°	No[2]	26%	10% to 100%[3, 4]
			24°	Yes	17%	8% to 90%[3, 4]
			39°	Yes	13%	6% to 80%[3, 4]
		610 cm[5]	35°	No	6%	2% to 31%[3, 4]
	Calumet, Michigan [4]	530 cm Measured	0°	No[2]	34%	Avg: 68%[4]
			15°	Yes	34%	Avg: 63%[4]
			30°	Yes	29%	Avg: 60%[4]
			45°	Yes	31%	Avg: 62%[4]
			15°	No	12%	Avg: 26%[4]
			30°	No	10%	Avg: 23%[4]
			45°	No	5%	Avg: 13%[4]
Moderate	White Bear Lake, Minnesota [6]	105 cm	22.6°	Yes	3%	N/A
	Boulder, Colorado [5]	2 Year Average: 97 cm	18.4°	Yes	2 Year Average: 5.9%	0% to 48%[6]
		2 Year Average: 89 cm	15°	Yes	2 Year Average: 6.0%	0% to 67%[6]
	Lafayette, Colorado [5]	2 Year Average: 81 cm	30°	No	2 Year Average: 1.9%	0% to 27%[6]

Climate[1]	Location	Snowfall	Tilt[2]	Obstruction	Loss	Monthly Loss
	Kenosha, Wisconsin [5]	2 Year Average: 50 cm	35°	Yes	2 Year Average: 4.3%	0% to 47%[6]
	Janesville, Wisconsin [5]	2 Year Average: 50 cm	26°	Yes	2 Year Average: 9.3%	0% to 92%[6]
		2 Year Average: 91 cm	22.5°	Yes	2 Year Average: 5.5%	0% to 60%[6]
	Grand Prairie, Alberta, Canada [9]	Long term Average: 154 cm [20]	14°	No	0.4%	Avg: 15.7%[7]
			18°	No	0.7%	Avg: 14.5%[7]
			27°	No	2.3%	Avg: 11.7%[7]
			45°	No	3.4%	Avg: 6.8%[7]
			53°	No	3.8%	Avg: 2.0%[7]
			90°	No	3.9%	Avg: 0.8%[7]
	Edmonton, Alberta, Canada [9]	Long term Average: 124 cm [20]	14°	No	4.5%	Avg: 16.8%[7]
			18°	No	4.7%	Avg: 16.9%[7]
			27°	No	4.0%	Avg: 13.2%[7]
			45°	No	1.7%	Avg: 5.0%[7]
			53°	No	0.8%	Avg: 2.2%[7]
			90°	No	0.3%	Avg: 0.5%[7]
Mild	25 Sites in Japan [8]	0 cm to 650 cm	Various	No	24 Sites <=1.0%, 1 Site 3.5%	N/A
	Munich, Germany [17]	5 to 31 cm[3]	28°	Yes	0.3% to 2.7%	N/A
	Kingston, Ontario, Canada [18]	Year 1: 58 cm[5]	10°	No	~3.2%	N/A
			20°	No	~2.5%	N/A
			40°	No	~1.5%	N/A
			60°	No	~1.0%	N/A
		Year 2: 49 cm[5]	5°	No	<0.9%	N/A
			10°	No	<1.25%	N/A
			15°	No	<0.9%	N/A
			20°	No	<0.9%	N/A
			30°	No	<0.3%	N/A
			40°	No	<0.9%	N/A
			60°	No	<0.9%	N/A

Table Notes:

N/A: winter monthly electricity generation loss values or means were not reported

[1] See further definition of climate types in Section 2.3.1

[2] Obstructions to sliding do not affect tilt angles of 0°

[3] Approximate value, visually taken from a graph

[4] Monthly loss reported between November and May

[5] Measured snow-fall at a nearby location

[6] Monthly loss reported between November and March

[7] Monthly loss reported between October and March

In an attempt to provide a general sense of the impact of snow on electricity generation, Ryberg and Freeman [19] developed charts of the United States (US) that show regional trends in the estimated annual loss. Slightly less than half the US is estimated to experience annual losses greater than 2% with only about one-tenth estimated to experience more than 10% loss. Ryberg and Freeman's [19] charts do not show microclimates caused by, for example, large elevation changes or local geography, which can be better identified by high-resolution annual ground snow cover maps (maps for Europe and the US in Wirth et al. [21]). An excellent example of a microclimate is Truckee, California, located within the Sierra Nevada Mountain Range. Truckee experiences large amounts of snowfall and, as a result, up to 18% annual snow-induced electricity generation loss [10,11] whereas its surrounding region is only estimated to experience at most a 2% loss in electricity generation based on Ryberg and Freeman's [19] charts.

Winter electricity generation, in daily, weekly, and monthly resolutions, is critical to consider when assessing the feasibility of using solar energy to replace existing energy sources at high latitudes. Brench [22] reported that in the day following a snowfall, the electricity generation from PV systems was reduced by between 4% and 56% because of snow cover, even in a relatively mild climate. No studies have reported weekly generation losses, but it is not uncommon for snow to remain on PV panels for more than several days or weeks [5,10,12]. Table 2.1 contains the winter monthly electricity generation losses that have been reported by previous studies. For the range of tilt angles most commonly used in PV systems, the monthly loss is over 25% and can be as high as 100% [5,10,11].

2.3. Influence Factors

The combined effects of climate and the PV system design characteristics affect the level of electricity generation loss resulting from snow cover. In this section, an effort is made to discuss the individual impacts and their interactions.

2.3.1. Climate

The main climatic influence factors are snowfall and ambient temperature. Both frequent and substantial snowfalls can increase the impact of snow. Frequent snowfalls hamper the electricity generation to some degree for many winter days. Substantial snowfalls reduce the penetration of solar irradiance to PV panels and its contribution to the warming and shedding of snow accumulations [22,23]. As a result, the panels may remain covered with snow until the ambient temperature becomes warm enough for clearing to occur. Ambient temperatures approaching $0°C$, as expected, have shown a strong relationship with the clearing of PV panels [5,13,14,19,24].

The two primary modes of snow clearing are melting and sliding. With thicker snow accumulations, the snow tends to slide, rather than completely melt [18,25]. With lighter snowfalls and warmer temperatures, the snow cover typically melts entirely, or significant amounts melt before sliding occurs [18,25]. The relationship between ambient temperature reaching $0°C$ and snow clearing suggests that sliding occurs once melting begins. However, sliding has been observed at module temperatures as low as $-10°C$ [17]. Three climate types that have different combinations of ambient temperature and snowfall characteristics in the winter months and their impacts on loss are presented in this sub-section.

2.3.1.1 Mild Climates

The electricity generation loss is typically small in climates that experience either or both: ambient temperatures frequently higher than $0°C$ and small amounts of annual snowfall. Low amounts of

annual snowfall typically result in thin snow cover. Thin snow cover and high ambient temperatures lead to snow cover remaining on panels for only short periods. Additionally, in mild climates, snow cover typically clears by melting in place, and not sliding [18,25].

Four studies provide evidence that in mild climates, the time required for snow accumulations to clear from PV panels is minimal. Andrews et al. [18] showed that throughout a winter that the ambient temperature averaged -1.0°C, the time required for panels to clear of snow was generally less than 8 hours; with colder weather, averaging -4.2°C, clearing took four times longer. Brench [22] studied PV systems subject to mild winter temperatures and an average annual snowfall of 102 cm [26] in Natural Bridges National Monument (Utah, US). Brench [22] found the electricity generation loss for the day following a snowfall was between 4% and 14% with light snowfalls (less than 2.5 cm in thickness) but was approximately 3 to 8 times greater with more significant snowfalls. In a two-day experiment performed in March 1995, Ross [23] documented the snow clearing process of PV panels in Varennes, Quebec, Canada. Over 65% of the possible electricity generation was lost throughout the two-day snow clearing process. The ambient temperature was only slightly below freezing (warmer than -5°C), and the sky was overcast. Becker et al. [17] studied a 1 Megawatt PV system in Munich, Germany and reported that it only experienced snow cover for 5 to 17 days per year in the winters between 1999 and 2004. In Munich, throughout the winter months, the ambient temperature daily high is frequently above 0°C, and the average annual snowfall is only between 5 cm and 31 cm [27].

Snow has a relatively small impact on PV electricity generation in mild climates, electricity generation loss is typically less than 2% or 3% of the expected annual electricity generation (Table 2.1). Becker et al. [17] found that snow only accounted for a reduction in annual electricity generation of 0.3% to 2.7% in Munich between 1999 and 2004. Comparable values were found in

a two-year study performed in Kingston, Ontario, Canada which experienced similar snowfall amounts: 49 cm and 59 cm for the winters of 2010/2011 and 2011/2012 respectively [18]. This study showed that 0.1% to 3.5% of the annual electricity generation was lost to snow cover for 70 PV modules varying in tilt angle (between 5° and 60°) and technologies (crystalline silicon and amorphous) [18]. Sugiura et al. [8] studied 25 PV systems in a mild climate, 23 of the sites had less than a 0.7% loss in annual generation attributable to snow cover. The two remaining sites in this study experienced approximately 1.0% and 3.5% annual loss.

2.3.1.2   Severe Climate
Severe climates exhibit both of the following characteristics: wintertime ambient temperatures consistently well below 0°C and significant amounts of snowfall. There are two unique studies performed in climates that experience significant snowfalls. The first study was performed in Truckee, California over two consecutive years [10,11]. Truckee experienced 483 cm of snowfall in the first year of the experiment [10] and 711 cm during the second year [11]. Throughout the two year period, the PV panels that were left to be covered with snow had an annual electricity generation of between 6% and 26% less than an adjacent panel that was kept clear of snow [11]. In a second study performed in Calumet, Michigan, US, between 5% and 34% of expected annual generation was lost to snow coverage on PV panels [4]. Throughout the study period, Calumet experienced 531 cm of snow. The ambient temperature in Calumet only occasionally is above 0°C [28].

Both studies were performed in regions that experienced significantly more snow than most PV installations. The results of these studies likely represent the upper limit of electricity generation loss resulting from snow cover. However, both these studies were performed in regions where the ambient temperatures are not typically severely cold for extended periods, increasing the frequency

of opportunities for snow to clear. No research has been conducted in winter climates with both cold ambient temperatures and significant snowfalls.

2.3.1.3 Continental Moderate Climates

Many regions experience cold winter temperatures, but due to a continental climate, they receive only modest amounts of snowfall, between 100 cm and 200 cm annually. Most of the Canadian Prairies and the Northern US experience this type of climate. Two studies have been performed in regions that experience cold continental climates. PV systems located in Colorado and Wisconsin experienced an estimated annual electricity generation loss of 1.9% to 9.3% [5]. These systems experienced 38 cm to 126 cm of snow annually [5]. In a second study performed in Edmonton and Grande Prairie, Alberta, Canada, snow reduced the annual electricity generation by 0.25% to 4.70% [9]. Edmonton and Grande Prairie experience an average of only 124 cm and 154 cm of annual snowfall respectively. The daily maximum ambient temperature is above 0°C for approximately one-third of the days from December to February but can remain well below 0°C for several consecutive weeks [20]. As a result, panels may remain snow-covered for extended periods, leading to PV systems generating nearly no electricity for days or even up to an entire month [5].

2.3.2. Friction and Adhesion

Friction and adhesion between the snow and the top surface of the PV panel work together to prevent snow from sliding off the PV panel surface. Both are affected by the weather and PV panel surface characteristics.

The process of sliding can occur either when the interface between the panel and snow is dry, or when it is wet. The process of dry sliding is not well understood. With wet sliding, water acts to lubricate the interface between the PV panel and the snow accumulation resting on top, reducing the friction to a point where sliding can occur. Rohm et al. [29] showed that the dynamic coefficient

15

of friction between a ski and snow decreases as the snow temperature increases towards 0°C, hypothesizing that the coefficient of friction decreased as the amount of water at the interface increases. Marion et al. [5] hypothesized that the static coefficient of friction between snow and a PV panel could be as high as 0.14 (comparable to the coefficient of friction of a waxed wooden ski on wet snow). Marion et al. [5] also considered the dynamic coefficient of friction of polyethylene skis as a lower bound for the coefficient of friction between snow and PV panels. The coefficient of friction for a polyethylene ski at temperatures near the melting point of snow has been found to be 0.02 [29,30]. Additionally, Jelle [31] suggests a tentative coefficient of friction between glass and snow of 0.003 when the interface was warmed by room temperature (i.e., the interface is likely wet). Similar values were attained by Mellor [32]. The wide range of values of the coefficient of friction found in the literature can be attributed to the changing properties of snow, including shape [31] and moisture content [23,33]. However, all of the values suggested by past literature are so low that snow would clear from panels tilted beyond 10° [5], which does not represent reality [4,5,7,9-11,18,25,31,34,35].

Adhesion, caused by the formation of ice on the PV panel surface, could explain why snow accumulations remain on PV panels [23]. The moisture that freezes to the PV panel, anchoring the snow accumulation, can come from several sources: melting of snowfall on contact with the panel, sublimation of snow and deposition of the resultant water vapor [36], water on the surface prior to snowfall, excess moisture in the snow, melting of snowfall from previous days, and rain falling on the snow accumulation [23]. The force required to break the bond between the panel surface and the snow, which can be several orders of magnitude higher than the frictional forces [31], must be overcome before the snow can begin to slide. As such, reducing the adhesion between the PV panel and the snow could reduce or eliminate snow accumulations on tilted panels. Techniques to reduce

16

the adhesion between snow and PV panels include: stopping snow from settling on PV panels [31,37], reducing the formation of ice between the snow and the panel, and reducing the adhesion strength between the ice and the panel [38-41].

2.3.3. System Characteristics

Unlike climate, system characteristics can be optimized to reduce the impact of snow on electricity generation. In this section, the impact of different system characteristics on the resultant snow-induced electricity generation loss is discussed, and where possible, their impact is quantified.

2.3.3.1 Obstructions to the Path of Sliding Snow

Obstructions in the path of sliding snow can either entirely prevent snow from sliding or cause it to slump and build up along the bottom of the panel. Additionally, obstructions can create catchment areas for snow accumulations to begin forming from [23]. Melting of built-up snow can take a considerable amount of time and can result in the panel not functioning correctly for an extended period. Obstructions can include flat surfaces below the panels (the ground or roof) on rack mounted systems [4,10], high-friction surfaces below the panels such as roofing shingles in many residential applications [5,42], PV panel framing [23,25,43,44], or mounting hardware that protrudes beyond the front surface of the panel.

Heidari et al. [4] used a side by side experiment to quantify the maximum effect of obstructed snow sliding paths. This study employed three sets of tilted PV panels (15°, 30°, and 45° tilt angles). In each set of PV panels, there was an unobstructed panel and a panel with the snow sliding path obstructed by the ground. The obstructed panels experienced losses throughout the snow season of between 60% and 63%, while the unobstructed panels experienced one third the losses (12% to 26%). Similar findings were reported by Townsend and Powers [11]; the loss for an obstructed panel tilted at 39° was 15% of annual generation versus 6% for an unobstructed system with a tilt angle of 36°.

2.3.3.2   Tilt Angle

In general, the tilt angle of a PV system is negatively correlated with the loss [5,9-12,18,22,34,45,46]. Higher tilt angles can aid in the clearing of snow from PV panels in the following two ways. At high latitudes, the solar altitude during the winter is low, and higher tilt angles result in more irradiance on the PV panel, increasing the potential for warming, which can aid in melting and sliding. For sliding of the snow to occur, the driving forces (force component of the weight of the snow cover along the PV surface) pushing the snow down the panel must overcome the frictional (a product of the friction coefficient and the force component of the weight of the snow cover perpendicular to the PV surface) and adhesive forces holding it on the PV panel. The driving forces increase with tilt angle while the frictional forces decrease. As a result, higher tilt angles will contribute to sliding in more circumstances.

The quantitative relationship between tilt angle and the amount of electricity generation loss attributable to snow cover is much less defined. Brench [22] showed that a panel tilted at 40° experienced only 55% of the loss of a panel tilted at 30°. Powers et al. [10] and Townsend and Powers [11] proposed an empirical equation (Eqn. (2.1)) to estimate the impact of PV system tilt angle on the annual loss. The constant in Eqn. (2.1) is an empirically fitted value, and the snow depth is the annual depth of snowfall in inches.

$$\% \ annual \ loss = Constant \times Snow \ depth \times \cos^2(tilt \ angle) \tag{2.1}$$

Under certain circumstances, the tilt angle may have no impact on loss, namely under warm climatic conditions with light snowfalls, and when the path of sliding snow is severely obstructed. In warmer weather, Andrews et al. [18] showed no correlation between loss and PV panel tilt angle, but the relationship is much clearer with colder temperatures. Heidari et al. [4] showed that

PV systems with severely obstructed sliding paths had no appreciable loss reduction as tilt angle increased. Marion et al. [5] and Townsend and Powers [11] also showed the smaller impact of tilt angles in obstructed PV setups. The reason for this is because in cases where snow is built-up on the lower part of the panel it is cleared primarily through melting instead of sliding.

The perceived impact of tilt angle on reducing the portion of annual electricity generation lost due to snowcover can be small or negative in cases where the solar altitude is extremely low during winter months (e.g., arctic regions) [19]. In these cases, increases in tilt angle result in significantly more incident sunlight, and as a result, significantly more potential electricity generation during the winter. The effect is that even though a panel at a higher tilt angle will be covered with snow for less time, the portion of the potential annual electricity generation lost may be higher.

2.3.3.3   Array Arrangement

The impact of snow on PV panels is related to the array arrangement and the amount of sunlight incident on each cell. The maximum throughput current (I) of a cell is strongly correlated with the solar irradiance reaching the cell [47]. With snow accumulations thicker than 2 cm, the sunlight penetrating the snow and reaching the PV panel is negligible—less than 25% [23]. Within a PV panel, cells are arranged in series to create arrays. The result is that shading (which has a similar effect to snow) of a single cell significantly impedes the current throughput and performance of the entire array [47]. For example, shading one cell by between 60% and 70% reduced the electricity generation of a 36-cell array by 43% [23]. Several studies have shown that shading part of a PV panel by any amount reduces the electricity generation of the entire panel by a disproportionally high amount [19,23,25,47-51].

Because of the codependence of cells, partial shading results in significantly more electricity generation loss when shading obstructs more arrays [13,48,52]. Barreiro et al. [48] showed PV

panels with shading oriented parallel to the arrays generated 430% the electricity generated by a

panel with shading oriented perpendicular to the arrays when one-eighth of the panel was shaded

(both mono-crystalline and poly-crystalline PV panels were tested). This discrepancy is because

shading parallel to the longest dimension of the arrays affects the minimum number of arrays, and

the other arrays in the panel function normally. In warm weather, snow tends to slide down a PV

panel with the bottom edge of the panel being the last to clear [18]. As such, in climates with warm

snow, the loss could be minimized by mounting PV panels with the longest dimension of the arrays

running horizontally.

2.4. Estimating Techniques

Models predicting the electricity generation of PV panels have existed since the development of

PV systems. However, models that estimate the impact of snow cover on PV panel generation have

only been established recently. Snow cover blocks solar irradiance from reaching the PV panel. If

neglected in generation prediction models, generation can be over predicted [53-57].

2.4.1. Prediction Resolution

Kostylev and Pavlovski [58] outlined five essential electricity generation prediction time-steps as

described in Figure 2.1. These five time-steps can be divided into short-term and long-term

predictions. In general, short-term models are used for grid management and fault detection, and

long-term models are used in PV system design [58,59].

Prediction Length	**Purpose**	
Intra-hour • 15 to 120 minute forecast • Approximately 1 minute time-step	• Ensuring enough electricity supply for momentary variations in demand	Short-Term
Hour • 6 hour forecast • 1 hour time-step	• Ensure enough electricity supply for routine load changes • Control of peak shaving intensity • System fault detection	Short-Term
Day • 1 to 3 day forecast • 1 hour time-step	• Ensure capability of meeting output commitments • Management of electrical transmission system • Electrical price forecasting • System fault detection	Short-Term
Week • 2 to 9 week forecast • 1 day time-step	• For hedging electricity production • Optimization of existing generation systems	Long-Term
Month • 1 to several years forecast • Monthly or annual production	• Assess location suitability • Evaluate projects financially	Long-Term

Figure 2.1 Electricity Generation Forecasting Timeframes (information from [58,59])

Existing long-term models can adequately estimate the statistical distribution of the impact of snow on PV panel electricity generation. Since precise estimation of the duration of snow coverage is not essential in long-term predictions, long-term models only need to predict the effect of snow cover with sufficiently small bias [59]. Long-term models are based on historical data only, but due to year-to-year variations in weather, there can be a significant amount of uncertainty. Thevenard and Pellard [53] reported that the standard deviation of loss was 75% of the mean value.

Short-term predictions must be accurate and precise. Short-term models use weather forecasts, meaning they are subject to inaccuracies in the forecasted weather parameters. As an example, the root-mean-square-error (RMSE) of solar irradiance predictions is around 7.5% for intraday predictions and increases to between 16% and 40% for inter-day predictions (0 to 48 hour) [14,54]. Short-term models have also been paired with historical data to provide an understanding of the short-term variability that can be expected in a PV system's electricity generation [24,60]. This provides valuable information for designers of PV systems that will be depended on to provide energy (by a contract, or in off-grid applications).

2.4.2. Modeling Methods

More than ten models have been created to estimate the PV electricity generation loss caused by snow. They can be grouped into direct electricity generation loss prediction models and snow cover prediction models. In addition, ground snow observations either through meteorological stations, or satellite observations [59] can be used to infer the current snow cover condition of PV panels when it is unknown.

2.4.2.1 *Direct Electricity Generation Loss Prediction Models*

The reported direct loss prediction models use system and weather characteristics in a data-driven approach and directly output the predicted loss for timesteps between one day and one year in length. Two approaches have been used to develop these models. The stochastic approach only

requires historical PV system electricity generation quantities to account for the loss in existing electricity generation predictions [61]; the curve fitting approach associates PV system characteristics and weather parameters with the amount of loss [10,11,34,62].

Table 2.2 lists the input parameters used in all types of data-driven models. Several models use only widely available weather parameters, while others utilize more complex parameters that are only available from advanced weather observation stations. Additionally, the use of site-specific weather and design characteristics as model inputs is critical to accurate model results [25,34]. However empirical constants established at one site can be applicable to other similar sites [25,34].

Table 2.2 Input Parameters for Direct Electricity Generation Loss Prediction Models

Author	Powers et al. [10]	T. Townsend and Powers [11]	Andrews and Pearce; Andrews [25,34]	Hong et al. [61]	Zamo et al. [62]	Shishavan et al. [45]
Model Type	Curve Fitting	Curve Fitting	Curve Fitting	Stochastic	Curve Fitting	Curve Fitting
Minimum Prediction Resolution	Monthly	Monthly	Daily	Monthly	Yearly	Monthly
PV System Properties:						
Clear System Electricity Generation Prediction				✓		
Tilt Angle	✓	✓				✓
Historical Electricity Generation				✓		
Obstructions to Sliding						
Array Length		✓				
Minimum Array Height		✓				

Physical Properties of Panel					
Physical Properties of Surroundings					
Weather Parameters:					
Ambient Temperature		✓	✓		✓
Irradiance		✓	✓		✓
Humidity Characteristics		✓			✓
Wind Characteristics					✓
Cloud Characteristics					✓
Air mass Characteristics					✓
Precipitation Amount					✓
Solar Height					✓
Properties of Snow:					
Snow Depth on Panel					
Snowfall Quantity	✓	✓	✓		✓
Ground Snow Depth					✓
Days of ground snow cover					✓
Physical properties of snow					
Repose Angle of Snow		✓			
Date of Snowfalls		✓			

Both the curve fitting and the stochastic approach significantly reduced the modeling error of electricity generation predictions. Without considering snow, errors in monthly electricity

generation predictions during winter months can be nearly 100% [5,11,45,61]. Hong et al.'s [61] stochastic model reduced electricity generation forecasts to be within 34% of actual generation on a month to month basis, down from up to 103% without the stochastic model.

2.4.2.2 Snow Coverage Prediction Models

Snow cover prediction models simulate the snow clearing process to estimate the snow-covered portion of the panel. This information can then be used to determine the generation loss. Two unique approaches have been taken to estimate the snow coverage on PV panels: threshold type models [5,13,14,19,24], and first-principle thermal and mass transfer [23,63]. Table 2.3 tabulates several models and outlines their input variables.

Table 2.3 Input Parameters for Snow Cover Prediction Models

Author	Ross [23]	Lorenz et al. [14]	Marion et al. [5]; Pisklak [24]; Ryberg and Freeman [19]	Bosman and Darling [13]	Rahmatmand et al. [63]
Model Type	First-Principle	Threshold	Threshold	Threshold	First-Principle
Minimum Prediction Resolution	Intra-hour	Intra-day	Hourly	Intra-day	Intra-hour
PV System Properties:					
Clear System Electricity Generation Prediction	✓	✓	✓	✓	
Tilt Angle	✓		✓		✓
Historical Electricity Generation					
Obstructions to Sliding			✓		
Array Length	✓				✓
Minimum Array Height	✓				
Physical Properties of Panel	✓				

25

Physical Properties of Surroundings	✓				✓
Weather Parameters:					
Ambient Temperature	✓	✓	✓	✓	✓
Irradiance	✓		✓		
Humidity Characteristics	✓				
Wind Characteristics	✓				
Cloud Characteristics	✓				
Air mass Characteristics	✓				
Precipitation Amount					
Solar Height	✓				
Properties of Snow:					
Snow Depth on Panel	✓	✓			✓
Snowfall Quantity			✓		
Ground Snow Depth	✓	✓		✓	
Days of ground snow cover					
Physical properties of snow	✓				✓
Repose Angle of Snow					
Date of Snowfalls				✓	

Threshold type models define threshold limits, which, if surpassed, the snow is assumed to clear from the panel, either entirely or at a defined rate. Threshold limits can be applied to a single variable such as the ambient temperature or ground snow depth [13,14] or combinations of system and weather parameters [5,14,19,24]. Ground snow cover depth is necessary to identify when new snow has fallen and create the initial snow cover condition in snow cover prediction models. Threshold models are best suited for short time-step predictions because they attempt to simulate the behavior of the snow.

The accuracy of threshold type models has been well tested. In intraday predictions of single-site electricity generation, a threshold model reduced the electricity generation prediction RMSE to

less than 7%, which is around the RMSE in the irradiance forecasts being used [14]. Results for regional forecasts had an error of less than 5%. These types of models can also enhance longer-term forecasts [5,13,19,24], reducing annual electricity generation forecast error by over 40% [19].

First-principle models make use of energy balance equations to predict PV panel temperatures and snow melting. These models predict when snow clearing will occur, either through complete melting or sliding. Complex first-principle models can require over 25 input parameters that wholly define the PV system characteristics, current weather conditions, and surrounding conditions [23,63]. To the authors knowledge a thorough validation of first principle models has never been reported.

A key assumption for first-principle models is the conditions under which snow will slide. Most of the research publications indirectly conclude that melting or sliding would begin at PV temperatures above 0°C. For example, threshold type forecast models, that correlated clearing with ambient temperatures higher than 0°C, reduced forecast error by over 40% [5,19], Lorenz [14] also reduced error substantially with a threshold that considered only ambient temperature. However, Becker et al. [17] reported a weak correlation between clearing and module temperature, observing sliding at module temperatures as low as -10°C and much higher than 0°C.

Snow cover prediction models that do not reference current snow cover conditions are subject to sustained under predictions of the loss by falsely predicting snow clearing, followed by prolonged periods (days or weeks) of cold temperatures [5]. This has resulted in an error of up to 90% for monthly electricity generation predictions [5]. The model developed by Lorenz et al. [14] is the only model that considers the current snow cover condition of the PV system. The most readily available method to identify snow cover condition is to compare current electricity generation with

the expected generation of a snow-free panel, if the panel is not clear of snow, then there will be a substantial difference between the two.

2.5. Mitigation Methods

Mitigation methods must exhibit minimal maintenance, low cost, minimal energy use, and low impact on electricity generation. One advantage of PV systems is that they typically require little maintenance over the life of the system. Frequent maintenance would be bothersome to system operators, especially small-scale operators. The total cost of installing and maintaining a mitigation method must be justified by the value of the loss that is avoided. For example, if the snow removal action consumes energy, the cost of the required energy must be less than that of the additional amount generated by clearing the panels. Finally, the system used to get rid of snow accumulations from PV modules must not substantially reduce the amount of electricity generated; this is a crucial concern with various films applied to the front surface of the panels [64]. In addition to the mitigation methods discussed in this section, the PV system characteristics (e.g., obstructions to the path of sliding snow, tilt angle, and array arrangement) should also be considered to mitigate loss.

2.5.1. Increasing Overnight Tilt Angle

For tracking PV systems, if mild climates exist after a snowfall, increasing the tilt angle can reduce the amount of electricity generation loss resulting from snow cover [19]. Threshold models suggest that if the ambient temperature is greater than 0°C then sliding will occur [5,13,14,19,24]. Increasing the tilt angle leads to more rapid sliding [5,18,22], which can lead to the panels being clear before sunrise. Increasing the overnight tilt angle to 20° versus the typical 5° was simulated to increase annual electricity generation by 1% to 2% as a result of snow accumulations sliding overnight [19].

2.5.2. Reflection on back

In rack mounted PV systems (used on flat roofs, and ground mounting) diffuse light reflected from the ground behind the panels is absorbed by the back surface of the panel, which is always clear of snow. Freshly fallen snow has an albedo of about 0.8 which decreases to about 0.65 after two days [65]. In contrast, bare soil has an albedo of approximately 0.2 [25]. Because of the differences in the albedo of ground and snow, the intensity of irradiance reaching the back surface of the panel in the winter has been reported to be 2.5 times as high as the intensity in the summer [10]. Ross [23] and Powers et al. [10] found that when the ground was covered with snow, the irradiance on the back of the panel was around 25% of the front surface irradiance. The absorbed light results in increased PV temperature, which can quicken the melting or sliding of accumulated snow on the front of the PV panel [23,66-69].

Ross' study [23] is the only published work which endeavored to enhance the utilization of the reflected light reaching the back surface to reduce the loss. Ross [23] applied a high absorptivity coating directly to the back of a PV panel. Also, to reduce the convective heat loss from the back of the PV panel, an offset piece of Lexan glazing was added behind the coating to create an air cavity, as depicted in Figure 2.2. Electricity generation was recorded for a 2-day snow clearing period after one snowfall event; the modified panel generated three times more electricity than a standard panel. A physics-based model developed by Ross [23] estimated that the modification reduced the average duration of snow cover to between 4% and 83% that of an unmodified panel for various locations across Canada.
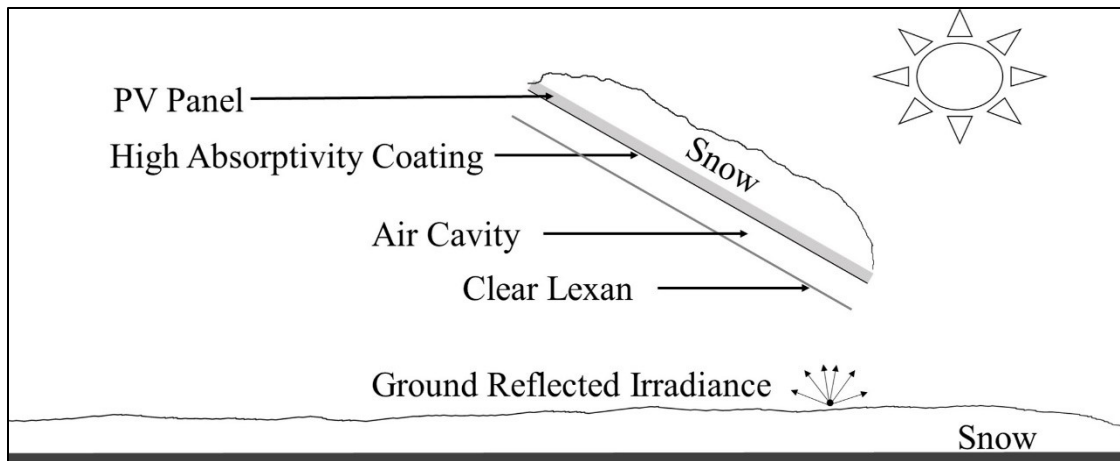
Figure 2.2 Back Surface Absorption Schematic [23]

However, testing the modified PV panels showed that applying a high absorptivity coating and glazing on the back of PV panels resulted in substantially higher PV panel temperatures [23]. The higher temperatures would reduce electricity output in hotter summer months [70,71], and could also contribute to degradation. Ross [23] observed that in warm months, the modified PV panels could become 23°C warmer than the standard panels. This temperature difference could result in electricity generation being reduced by between 5% and 25% [70,71]. The reduced electricity generation makes this mitigation method not advantageous in most grid-tied PV systems. However, it may have an application in PV systems where the consistency of winter electricity generation is more critical than the overall electricity generation, for example where solar energy is depended on for heating or charging batteries in remote facilities.

2.5.3. Surface Coatings

Surface coatings reduce the impact of snow cover on PV panels either by reducing adhesion and friction or by absorbing portions of the solar irradiance to break down the snow cover. Coatings require no additional infrastructure and have a relatively low unit cost. Coatings must be able to withstand adverse conditions including UV rays, hail, snow, ice, and dust throughout the life of the PV system (approximately 25 years). Snow and hail degrade existing coatings [39,41,72], but

enhancements have been made with regards to self-healing and more durable coatings [39,41,73,74].

The second requirement is that a surface coating must have a high transmittance in the spectral range used by PV cells [0 nm to 1200 nm [75]] [64]. Even a small decrease in transmittance due to a coating could result in, a net negative impact on electricity generation throughout the year. However, several coatings have been shown to increase the overall transmittance of solar irradiance [76].

2.5.3.1 Coatings to Reduce Friction and Adhesion

Reduced friction and adhesion between snow and PV panels can reduce loss when sliding is the mode of clearing. Friction relates to the interaction between snow and the PV panel. Adhesion is caused by the bonding strength of ice that forms at the interface between the panel and the snow. There are three scales on which the surface can be modified to reduce the strength of friction and adhesion: nano, micro, and macro scales. The interaction of snow and PV panels has only been researched explicitly on the micro level by examining hydrophobic and hydrophilic coatings. However, the interaction between ice and PV panels has been evaluated on all three scales.

2.5.3.1.1 Nanoscale Coatings

The primary method of reducing nanoscale adhesion between ice and a PV panel is to apply a coating that is made up of a material that exhibits weak atomic level interactions with ice and water [77]. The interface material can change the shearing stress required by a factor of over 100 [77]. The most common way to reduce the strength of adhesion is the silanization process, which results in between an 11% and 32% decrease [38]. However, even with treated glass, the adhesion strength can remain over 162 kPa [38], which is stronger than the driving forces behind sliding in almost any snow cover scenario.

2.5.3.1.2 Microscale Coatings

Microscale surface coatings typically work by modifying the way that water droplets interact with the surface by changing their contact angle. There are two types of microscale coatings. The hydrophobic coatings act to increase the contact angle θ (as depicted on the left of Figure 2.3). For a tilted surface, the higher the contact angle, the more likely water is to run down the surface, resulting in less water accumulation. Hydrophobic coatings increase the surface roughness on the micrometer scale, decreasing the contact area between the water and the panel. In contrast hydrophilic coatings work to retain water, by increasing the contact area, and resultant contact angle (as depicted on the right of Figure 2.3).
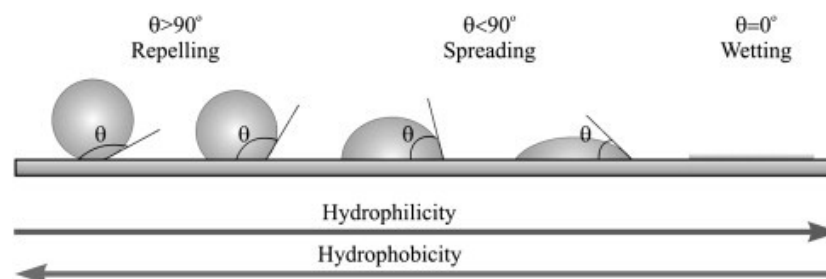
Figure 2.3 The Contact Angle Associated with Different Types of Surface Coatings [78]

The effectiveness of using hydrophobic coatings to reduce water accumulations on surfaces has been proved; however, very few studies report the effectiveness with freezing rain and snow. Hydrophobic coatings have been shown to be effective in preventing the accretion of freezing rain[73]. Some research has suggested that hydrophobic and hydrophilic coatings are designed to work in specific ice and snow conditions and as a result, have adverse effects in conditions other than what they were designed for [38,72,79]. For example, the results of Kako et al. [79] show that neither hydrophobic nor hydrophilic coatings perform well with all snow conditions (wet and dry snow).

Hydrophilic coatings accelerated the snow sliding process with wet snow but performed poorly with dry snow [79]. The hypothesis is that with wet snow, the hydrophilic coating forms a lubricating surface by attracting the water in the snow, making it easier for sliding to occur [7,79]. The use of hydrophobic coatings with wet snow is hypothesized to cause water to be repelled from accumulating on the surface; a lubricating layer is less likely to form and therefore sliding is less likely [7,79]. Another theory why hydrophobic coatings do not work with wet snow is that water vapor can condense and freeze in between the surface roughness features that make it hydrophobic, allowing ice to become more anchored than with a smooth surface [38]. When there is no adhesion, dry snow slides based on the characteristics of solid-on-solid friction [72]. Hydrophobic coatings accelerated the snow sliding process for dry snow because of reduced contact points between the snow and the surface [72]. Conversely, hydrophilic coatings increased adhesion with dry snow, resulting in less tendency for the snow to slide clear of the panel [7,79].

As such, the use of hydrophobic or hydrophilic coatings to reduce snow accumulation on PV panels is complex for regions that experience both wet and dry snow. In a previous study, the snow clearing effectiveness of PV panels with prismatic glass, three post-production hydrophobic surface coatings, and one post-production hydrophilic coating were tested [7]. These coatings yielded only minor benefits at large tilt angles and showed no measurable benefit at tilt angles less than 40° [7]. The reduced clearing time at large tilt angles (60°) yielded only minor increases in the electricity generation because the time required for snow to clear was short, regardless of coating [7]. However, it was suggested that creating hydrophilic channels in a hydrophobic surface could potentially achieve the benefits of both hydrophobic and hydrophilic surfaces [33]. Based on existing research, the durability and the limited range of effectiveness prevent micro-scale coatings from being a practical solution for reducing the impact of snow on PV panels.

2.5.3.1.3   Macroscale Coatings

Macroscale surface features are large enough to be visible. The most common macroscale difference between PV panel types is the use of textured or prismatic antireflective glass versus smooth-sheet glass on the front surface of PV panels. Visa et al. (2016) observed that smooth glass tends to clear before other types of glass. Another approach is soft films that deform non-uniformly under loading, giving the brittle ice that forms on the surface a weak foundation and allowing it to crack off more easily [38]. An optimized film can have an adhesion strength as low as 0.2 kPa to 10 kPa, substantially lower than the 200 kPa to 300 kPa range reported for standard films [38-41,74].

2.5.3.2   Self-Cleaning Surfaces
Self-cleaning surfaces are used on windows and work by using incident UV rays to decompose organic matter settled on them [31,64]. Theoretically, the use of a similar coating to melt snow is much more straightforward, as the coating would only need to absorb a part of the spectrum not used for electricity generation and convert the absorbed energy to heat. However, PV panels convert a wide range of wavelengths into electricity, leaving only longwave radiation usable by the coating [75], which has lower transmittance through snow [80], making this type of coating relatively ineffective without them gravely reducing electricity generation when the panels are free of snow.

2.5.4.   Heating
Heating PV panels is the most straightforward approach to remove snow from PV panels. The idea is to generate enough heat that a layer of water can form on which the snow can slide, or if sliding is not possible, sustain the heat long enough that complete melting occurs. A general assumption within the field is that sliding occurs at module temperatures of 0°C, although some skepticism exists. There are many commercially available and implementable methods of adding heat to PV

panels to clear snow accumulations. However, the energy input required to warm a panel to the point of clearing in a cold climate may outweigh the energy that would be generated as a result of the clearing. The primary types of heating systems are voltage application to the PV panels and using an external heating apparatus.

2.5.4.1 Voltage Application Heating

The voltage application method makes use of the resistive properties of PV panels [81-85]. Voltage is applied to the PV panels after a snowfall, causing them to generate heat. This method is advantageous over external heat sources because the only additional hardware required is controllers and modifications to the array wiring. One disadvantage is the heat output is limited to the electricity generation rating of the PV panel (approximately 150 W/m^2) [83]. In cold climates, these systems may not have sufficient heat output to warm the panel to a point where sliding can occur. Additionally, the low heat output results in a slow temperature rise and more heat is wasted dissipating into the snow layer and air rather than melting snow.

2.5.4.2 External Heating Source

External heat sources can take two forms: adding resistive heaters to the front [86-89] or back surfaces of the PV panel [44,90-94]. Both types of external heating source systems benefit from having the potential to deliver heat to the panels at a faster rate as compared to voltage application heating; this reduces the amount of heat lost to the surrounding air and makes this system more applicable to colder climates. Both types have the disadvantage of requiring additional hardware (electrical or plumbing) to transmit and transfer the energy to the PV panels. With front heaters, as with anything that goes on the front of the panel, care must be taken to ensure the heater has a high transmittance and it is durable. Additionally, back mounted heaters have the advantage over others of being able to use many different types of energy to warm the panels (e.g., thermal, waste heat) [95], which may have a significantly lower cost than electricity.

2.5.5. Electrostatic Forces

Extensive effort has been placed in developing a means of clearing dust from PV panels using electric fields. By integrating conductors in the glass and charging them with high alternating voltages, electrostatic repulsion between dust and the conductors occurs. The result is the dust being "lifted" from the glass surface [96] and progressing down the tilted panel with each alternating charge, similar to what would occur with dust on a vibrating surface. Electrostatic forces have also been shown to elevate or convey water on a surface [97-99] and could be useful for clearing snow and preventing ice from forming on the PV panel surface. Although this technology is not yet commercially available, the use of electrostatic forces has the advantages of having very low energy consumption (because only capacitive current is required to charge the conductors), and very little maintenance because there are no moving parts.

2.5.6. Thermal Collector

The use of a solar thermal collector attached to a tilted snow-covered solar panel has been tested and discussed on the internet [100]. The logic is that snow will not accumulate on a vertical thermal collector, and as such it will be exposed to absorb solar irradiance when the remainder of the panel is covered with snow. The absorbed irradiance causes the absorber to warm up and transfer heat through conduction to the snow-covered solar panel. The solar panel will warm, and the snow will melt (Figure 2.4 depicts this process). In a brief testing period, Dufresne [100] showed the thermal collector did cause the snow on the panel to begin melting, but it did not reach a point where the panel cleared. The results of this test failed to conclusively show the thermal collector as a suitable solution for clearing snow. If it could be shown to be effective, this would provide an excellent solution to snow melting on solar panels of all types because of its simplicity and its broad range of applicability. Care would need to be taken when designing a thermal collector to ensure it will not cause overheating of the panel during summer months.
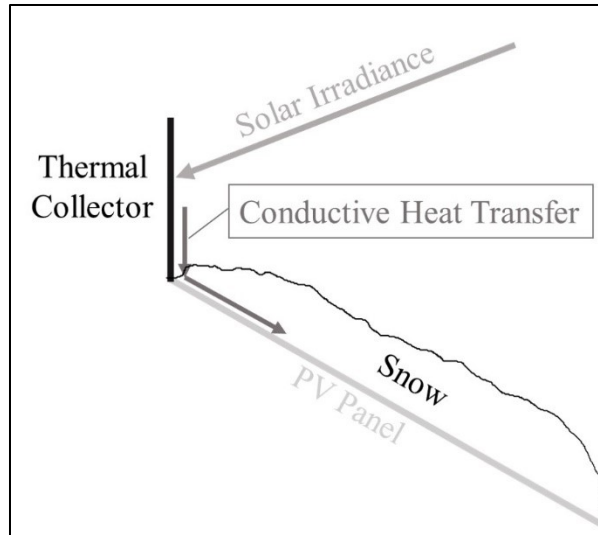
Figure 2.4 Thermal Collector Schematic

2.5.7. Venturi Deflector

In locations where the wind is typically from one direction and is consistently strong, Venturi deflectors (Figure 2.5) could be used to push air down the front of PV panels to prevent snow from accumulating. One recount of a Venturi deflector is available on the internet and described it as effective for preventing snow accumulations [37].

The Venturi deflector is a simple device with no moving parts, meaning low upfront and maintenance costs. If the wind direction is consistent and strong, deflectors could prove to be an effective means of preventing snow accumulations. Another advantage is that the active airflow down the surface of the panel could result in the panel being less warm in summer months, increasing electricity generation. However, active air circulation near the panel could possibly slow down the melting process [101], so if snow does build up on the panel, a Venturi deflector could slow the clearing process.
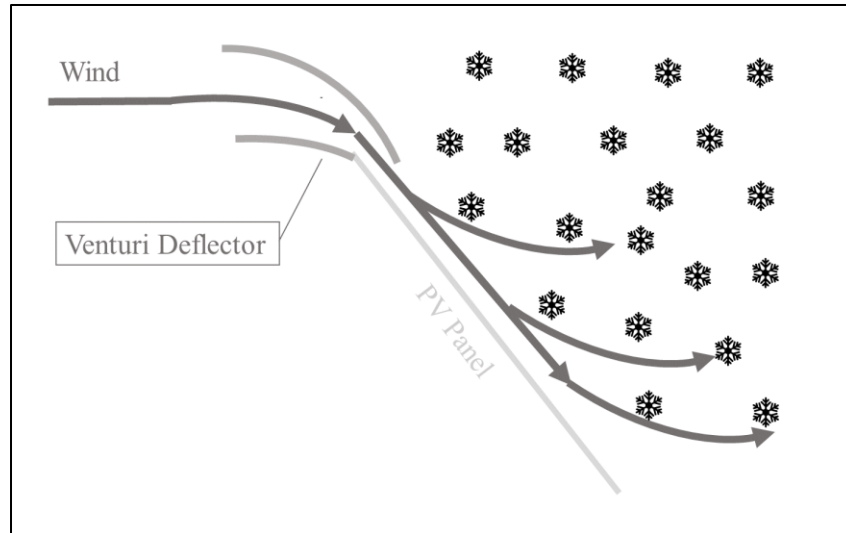
Figure 2.5 Venturi Deflector Schematic

2.5.8. Mechanical Clearing

The use of vibrations to clear snow accumulations from solar PV panels has been discussed in patents [90,102], but no publications show their effectiveness. It seems logical that these systems would be sufficient to clear dry snow off the panel. However, for wet snow or snow which freezes to the surface of the PV panel, a significant amount of strain of the panel surface would be needed to break the adhesion. Vibrations can cause cells to crack, rendering them less efficient [103]. Vibrations could be used in coordination with macro-scale coatings. The advantage of vibrations is that it would use far less energy than a heating type system.

Other mechanical clearing devices include forced air systems to blow snow clear of the panel or mechanical systems that physically move the snow clear of the panel. All mechanical devices have moving parts that will likely require maintenance over the life of a PV system, adding both nuisance and increasing the operating costs. Mechanical clearing techniques could potentially be viable if a single device, could remove snow from many panels autonomously (similar to existing dust clearing systems), concentrating the maintenance requirements. To use a single device the layout of the system must be simple, limiting it to large PV systems.

2.6. Other Observations

The process of snow accumulation formation and the mechanisms of clearing must be well understood before first principle models can be developed and used to optimize mitigation methods. For example, for a heating type system to add value to a PV system the amount of heat input required and when snow would clear naturally must be accurately predicted to use the system effectively. Further work is required to understand the snow clearing process enough to make decisions on how to design and operate mitigation methods.

The thicker the snow accumulations on PV panels, the less solar irradiance can penetrate the snow layer and be absorbed by the panel. If the depth of the snow accumulations is limited to less than 2 cm or 3 cm, the irradiance penetrating the snow accumulation is a valuable property to consider when predicting the snow clearing process, particularly in climates where the ambient temperature remains well below 0°C for extended periods. In such climates, high levels of solar irradiance reaching the panel are often the cause of snow clearing. Thinner snow accumulations allow higher levels of solar irradiance to reach the panel and warm it to a point where sliding is probable.

Taylor [104] demonstrated that the load of snow accumulating on an unheated glass roof was between 0.05 and 0.4 that of the snow accumulating on the ground, suggesting that far less snow accumulates on glass roofs than the surrounding ground. Theoretically, for PV panels with a tilt angle higher than the angle of repose of snow, once a consistent layer of snow has accumulated on the panel, no further snow will accumulate [23]. The angle of repose, as with other properties of snow can vary in a wide range. Temperature, snow impaction force, and snow crystal shape have been identified as having a significant impact on the angle of repose [105,106]. Kuroiwa et al. demonstrated that the angle of repose of natural snow was 63° at -30°C and increased to nearly 90° at -4°C [106]. Natural snow crystals had an angle of repose 40% higher than more rounded

pulverized snow [106]. Abe found the angle of repose of natural snow to be around 40° [105]. These findings suggest that with tilted PV panels there could be an upper limit to the depth of snow accumulations, but not enough research exists to develop a relationship between weather and system characteristics and the maximum snow depth. A quantitative understanding of the maximum snow depth would allow this knowledge to be integrated into snow clearing modeling and the design of mitigation methods.

Snow cover on the ground can enhance the electricity generation of PV panels because of the amount and spectral make-up of ground reflected light [107]. The albedo of snow is much higher than that of the ground. Also, the wavelengths of light reflected by snow have, in general, a higher conversion efficiency into electricity by PV panels [107]. Considering snows albedo and the spectral makeup of reflected light can result in substantially more predicted electricity generation [107], as such it is important to consider in modeling and loss estimation.

2.7. Conclusion

Snow cover induced electricity generation loss typically accounts for less than 10% of annual electricity generation from PV systems, but can make up a significant portion of the expected winter generation. Snow cover during winter months negatively impacts the quantity and reliability of PV generation. To be able to effectively incorporate PV generation into regional electricity grids and enhance the dependence that grids can have on PV systems, understanding how snow impacts PV panels and finding ways to reduce the impact are necessary.

Understanding the climatic and system characteristics, as well as, the interaction between the two is essential for design and prediction. Based on past research, the interaction between solar irradiance, ambient temperature, and snowfall quantity are the most critical climatic conditions to consider. Of the system characteristics, obstructions to the sliding path of snow cause the most

significant difference in the impact of snow on PV system generation. Modifications that reduce the obstructions to sliding can be made in all stages of PV systems, from design to operation.

For the further deployment of PV systems to be successful, high-quality modeling of both the short-term and long-term effects of snow on PV system electricity generation is required. To date, threshold type models offer the best predictions using data that is readily available from most weather stations. Threshold type models can be used by system designers and operators alike for short-term and long-term electricity generation predictions. However, a representative first principle model of the heat and mass transfer within the panel and the snow accumulation would be valuable for the development of mitigation methods, particularly those involving heat.

PV systems are used in a wide variety of environments and have different purposes (grid-tied, off-grid). Thus no single mitigation method will satisfy the needs of all PV setups. Surface coatings could prove to be extremely effective, but further research is required to ensure they have both high transmittance and durability. Electrostatic forces are also promising, although further research and development is required. Thermal absorbers also have the potential to be useful but require accurate thermal modeling to optimize performance. Heating type systems are currently commercially available but may not be cost-effective in cold climates. The remainder of the mitigation methods discussed may serve specific PV applications well. System designers should consider the climate and system characteristics, as well as the intended purpose of the PV system when deciding on the most effective mitigation strategy.

Therefore, it is critically important for researchers, designers, and operators to adequately manage the impact of snow, through accurate estimation and effective mitigation, creating a valuable asset to regional electricity grids; this begins with understanding how snow affects PV systems. The impact of snow has been studied in several climates, but there is no published research for climates

that experience both significant amounts of snowfall and wintertime ambient temperatures significantly below 0°C, such as the type of climate typically experienced in eastern Canada. A more extensive range of studied climates would give system designers a sense of the importance of managing snow cover, and help researchers understand the challenges of managing the effects of snowfall.

Chapter 3: Experimental Setup

3.1. Introduction

In order to better understand the formation of snow accumulations and improve the prediction of snow melting, an experiment was set up in Edmonton, Canada. This section provides a comprehensive description of the testing apparatus and the non-conventional data-logging and measurement equipment. Following this is a discussion of the advantages and disadvantages of using non-conventional equipment.

3.2. Testing Apparatus

The experimental setup was located in Edmonton, Canada and consisted of a framed PV panel, a piece of tempered glass, and a frameless PV panel (Figure 3.1, Figure 3.2, Figure 3.3). The framed PV panel was a Heliene 60M-270. The tempered glass was clear and had a thickness of 0.8 cm; the back surface was painted solid black to simulate the absorptivity of PV cells. Some of the paint peeled off the glass panel, however, less than 10% of the area was affected and the effect this would have on the dataset is considered minor when compared with other uncertainties involved with an outdoor experiment. The frameless panel was a Lumos LSX280-60M-C. The framed panel had a white plastic film back surface with an estimated albedo of 0.8; the black painted glass had an estimated albedo of 0.2. The back surface of the frameless panel was a transparent film under which was the back of the PV cells; the average albedo was estimated to be 0.2. The framed PV panel and tempered glass sheet were set up on October 30, 2017; the frameless panel was installed on December 14, 2017. Both the framed panel and the frameless panel were left with the circuit open. Three different types of panels were used to potentially understand how each panel surface and framing type contributed to the retention of snow on PV panels.

Figure 3.1 Experimental Test Frame

Figure 3.2 View of the Experimental Setup Towards the South-East (frameless panel, pneumatic actuation, and instrumentation were not yet been installed)

Figure 3.3 View of the Experimental Setup Towards the East (frameless panel, pneumatic actuation, and instrumentation were not yet been installed)

The three panels were mounted on a frame that allowed the tilt angle to be pneumatically adjusted between 13° and 71°. The tilt angle was varied on several occasions; Figure 3.4 is a histogram of the tilt angles utilized when natural snow clearing was observed. The majority of the observations were at tilt angles near 30° (between 27° and 31°) and 45° because those are commonly used angles for rail mounted systems on roofs and rack-mounted systems. The frame was south facing, and the panels were unaffected by shading except in the final stages of sunset (30 minutes before sunset). The wind was obstructed by trees and buildings on the east, west, and north of the apparatus, which were between 10 m and 50 m away from the testing apparatus. The frame was constructed of wood to reduce the heat transmission between the panels and the frame. To prevent additional obstructions to the path of sliding snow the panels were installed with no hardware protruding beyond the front surface of the panels and the mounting frame was not in the path of the sliding snow. Furthermore, ground interference to sliding was prevented by ensuring a sufficient distance between the panel and the snow accumulated on the ground.
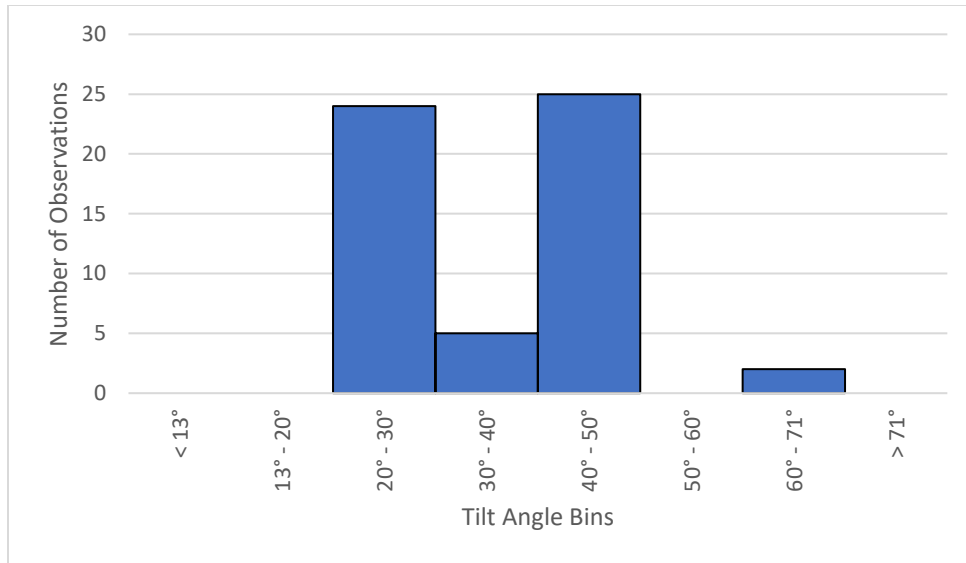
Figure 3.4 Histogram of the Tilt Angles of the Observations

3.3. Data Recording

Data recording was accomplished in two ways. A variety of onsite observations were taken with a data logger at the location of the experiment. Further observations were taken by a weather station operated by Alberta Agriculture which was 930 m south-west of the site (ID# 3012220) [108]. Table 3.1 outlines the meteorological parameters measured by the weather station as well as the interval at which they were measured. Additionally, barometric pressure was recorded at a weather station located 3.4 km from the setup [109].

Table 3.1 Weather Station Meteorological Parameters [108]

Meteorological Parameter	Measurement Interval
Instantaneous/Average/Max/Min Air Temperature	1 hour
Instantaneous/Average Relative Humidity	1 hour
Ground Snow Depth	1 hour
Instantaneous/Average/Peak Wind Direction (10m)	1 hour
Instantaneous/Average/Peak Wind Speed (10m)	1 hour
Average Wind Speed (2m)	1 hour
Average Global Horizontal Irradiance	5 minute
Water Equivalent Precipitation	1 hour

The onsite datalogger was developed using a Raspberry Pi single-board computer, and a variety of sensors and other hardware. Table 3.2 outlines the data recorded by this data logger and the measurement intervals. Unfortunately, the temperature and irradiance measurements were not reliable, and as a result, these measurements only exist for small portions of the period of the experiment. The reason for this unreliability is believed to be due to the long cable length over which signals were required to travel between the sensors, the signal converters, and then to the Raspberry Pi. Furthermore, the number of sensors assigned to each of the communication circuits was near the maximum allowable in some cases, and the sequencing of communication may not have been well executed.

Table 3.2 Data logger Measured Parameters

Data Type	Number of Sensors	Measurement Interval
Panel Temperature	33	1 minute
Plane-of-Array Irradiance	1	1 minute
Still Images	1	2 minute

It is worth noting that although in this case, the implementation of the datalogger was not perfect, the Raspberry Pi and peripheral components can be reliable. The Raspberry Pi was generally reliable at recording still images, which were transmitted over a cellular network to cloud storage. The Raspberry Pi could also be interfaced with remotely via a personal computer or a cellular device. The datalogger continued to function at ambient temperatures below -30°C, and throughout rain/snow even in a precariously sealed box.

3.4. Discussion

The use of a framed PV, glass, and frameless PV panels was done to observe the differences in snow clearing between the panel types. The hypothesis was that the framing would pose an obstruction to sliding snow. On several occasions, particularly with ambient temperatures near 0°C, the sliding of the snow accumulation was obstructed by the frame. However, in general, the impact of the frame was small.

Although the data logging system used for the collection of experimental data was not without flaws, non-conventional systems are of high merit. The flaws in this experiment were likely due to the implementation of the hardware, and not due to inherent problems with the hardware. It is difficult to conclude how much of the issue with robustness was the result of this specific assembly and how much is a result of the hardware being potentially less reliable, though there is some evidence to prove that these devices can be extremely robust [110].

Conventional sensors can be integrated into a non-conventional data recording system; also, a wide variety of sensors are available that allow a system to measure a nearly limitless set of parameters. Aside from the ability to measure nearly any parameter, a key advantage of using non-conventional measurement and data-logging equipment (like the Raspberry Pi computer used in this analysis) is cost. The data logging system used in this experiment was approximately one order of magnitude less expensive than a system with the same functionality. However, there was a significant amount of time that was invested in developing the system, but this time was justified as an opportunity to learn and develop an aptitude for programming and complex problem-solving. Creating the script to record measurements from different sensor types requires the most time investment, but this must only be performed once. If multiple data collection systems are needed with the same functionality, then only the hardware must be assembled for the remaining cases. The time required

to assemble the hardware is approximately two to three times as long as with conventional equipment. If the learning opportunity does not justify the time investment, then the ability to collect much more comprehensive data for the same equipment cost may justify the use of non-conventional hardware. For each dollar invested, there is the potential to gather data from ten locations instead of a single location. For example, with environmental modelling, rather than interpolating between several data points, the spacing of data points can match the spacing of the modelling interval. If researchers are willing to sacrifice time and some data robustness, then these systems have the potential to have a profound impact on the amount of data available to scientists. Furthermore, the development process gives junior researchers a foundation of knowledge that will undoubtedly be valuable to them in the future.

3.5. Conclusion

The use of non-conventional measurement and data logging hardware has the potential to increase the amount of data being recorded. Given the merits of non-conventional hardware, it should at least be considered when comparing the advantages and disadvantages of different types of data logging hardware.

Chapter 4: Observations of Ice at the Interface Between Snow Accumulations and Photovoltaic Panel Surfaces

4.1. Abstract

This paper presents the observation of ice formations under snow accumulations on photovoltaic (PV) panels. Five potential sources of moisture for icing were identified. An outdoor testing frame with panels was left to accumulate with snow and then manually cleared with a brush. Out of seven experimental observations, visible ice accumulations occurred five times, and the icing caused by two different sources of moisture was observed with certainty.

4.2. Introduction

In regions of high latitude, snow accumulations can have a considerable impact on PV system electricity generation, decreasing monthly electricity generation by up to 90% to 100% [5,10,11] and reducing the reliability of PV electricity generation. As a result, mitigating the impacts of snow is essential for enhancing the applicability of PV electricity generation in regions of high latitude.

Snow accumulations occur when the driving force pushing the snow down the panel (the component of the snow cover weight acting along the PV surface) is smaller than the resistive forces (frictional and adhesive). Frictional forces are believed to be small [5,31], and would result in no snow accumulations occurring on PV panels tilted beyond approximately 10° [5]. However, in actuality, snow accumulations can occur at almost any tilt angle [4,5,7,9-11,18,25,31,34,35]. As such, adhesion is believed to play a significant role in why snow accumulations remain on PV panels. Adhesion is the result of the formation of ice on the panel surface and has been shown to be several orders of magnitude stronger than the frictional force [31]. The formation of ice is the result of moisture meeting a cold PV panel. Moisture can come from a number of sources: the melting of snowfall on contact with a warm panel, sublimation of snow and deposition of the

resultant water vapor [23], water on the surface prior to snowfall, excess moisture in the snow, partial melting of snow accumulations, and rain falling on the snow accumulation [23].

This paper presents experimental observations of ice formations occurring on snow-covered PV panels. Also, an effort is made to assign the source of moisture for each of the observed ice accumulation events.

4.3. Method

4.3.1. Experimental Setup

A setup and procedure were developed to investigate the formation of ice on the PV panel surface below snow accumulations. Located in Edmonton, Canada, the setup consisted of a wooden frame to which a framed PV panel, a piece of tempered glass, and a frameless panel were mounted (Figure 4.1). The tilt angle of the panels could be varied (between 13° and 71°). The setup was south facing, and none of the panels were affected by shading, except occasionally within 30 minutes before sunset. The framed PV panel was a Heliene 60M-270. The tempered glass was clear and had a thickness of 0.8 cm; the back surface was painted solid black to simulate the absorptivity of PV cells. However, sections of the paint peeled off throughout the winter. The frameless panel was a Lumos LSX280-60M-C. The framed PV panel and tempered glass sheet were set up on October 31, 2017; the frameless panel was installed on December 14, 2017. Both the framed panel and the frameless panel were left with the circuit open. All three panels were installed with no hardware protruding beyond the front of the panel. Additionally, there were no obstructions to the path of sliding snow, and the bottom edge of the panel was sufficiently high to prevent the ground from interfering with sliding snow.

Still images of the setup were taken at 2-minute intervals. Global solar radiation, ambient temperature, precipitation water equivalent, and ground snow depth were recorded by a weather

station within 1 km from the site at 1-hour intervals [108]. The depth of snow accumulations on the PV panel surface was measured manually.

4.3.2. Procedure

Following seven snowfall events in the winter the thickness and appearance of the snow accumulations on the PV panels was observed. The tilt angle was increased in increments of approximately 10° to 71°, the maximum tilt angle the setup could achieve, to see if sliding would occur. If there were no signs of sliding the tilt angle was decreased, and the snow was manually cleared with a brush. Any ice coverage was then recorded photographically, and subjectively.

Figure 4.1 System Setup

4.3.3. Weather Characteristics

Over the duration of the experiment from October 31, 2017, to March 30, 2018, thirty snowfall events occurred at the site, totaling 87 cm, and 91 mm of water equivalent precipitation. The

average ambient temperature was -10.4°C, the daily high was -4.6°C [111]. Table 4.1 Summarizes the weather conditions for each snow event for which the procedure was performed.

Table 4.1 Weather Conditions and Concluded Source of Moisture for the Observed Events

Event #	Snow Accumulation Depth (cm)	Concluded Source of Moisture for Ice Formation	Hourly Weather Conditions Since the Beginning of the Snowfall Event			
			Ambient Temperature (°C)		*Solar Irradiance (W/m²)*	
			Maximum	*Minimum*	*Maximum*	*Daytime Average*
1	4cm	Contact Melting	0.5	-2.6	174	107
2	2 cm	Pre-Existing Ice	-2.7	-11.4	198	103
3	2 cm	Existing Snow Accumulation Melting	-5.6	-11.1	180	93
4	2 - 3 cm	No Ice Observed	-7.4	-17.3	189	117
5	2 cm	No Ice Observed	-11.2	-18.7	114	56
6	2 - 5 cm	Excess Moisture in Snow or Sublimation	-7.9	-13.1	83	31
7	0 - 3 cm	Existing Snow Accumulation Melting	-13.5	-27.3	360	168

4.4. Results

Out of the thirty snowfall events the vast majority were left to clear naturally. Sliding without melting occurred unprovoked on only two occasions (several sliding events occurred due to artificially induced vibrations). Sliding with melting was far more common, even at ambient temperatures well below -10°C. There were no cases where sliding was observed in ice affected surfaces without melting occurring in the ice affected areas. The procedure described in section 4.3.2 was performed seven times, of which visible ice buildup occurred five times. In the following sections, the appearance of ice buildups caused by different moisture sources is discussed.

4.4.1. Contact Melting

Contact melting occurs when snow falls on panels with a temperature higher than 0°C. The initial snowfall melts and forms water, as the panels cool the snow will begin to accumulate, and the water from melting will refreeze.

In one case (Event 1 in Table 4.1) contact melting was observed with certainty, the initial snowfall was observed melting on the panel, before further snow accumulated on the wet panel. The result of contact melting was a very coarse discontinuous ice build-up (Figure 4.2) which is likely the

result of water from the melted snow at the beginning of a snowfall forming large droplets, due to cohesion, and then becoming impregnated with snow and re-freezing. The frozen water droplets protruded 5 mm beyond the front surface of the panel and were abrasive to the touch.

Figure 4.2 Ice on the framed PV resulting from snow melting on contact (Event 1)

4.4.2. Pre-existing Ice

There was one occasion (Event 2) where a panel was manually cleared of snow, and the ice accumulations did not clear before the next snow accumulation formed. Pre-existing ice is an unnatural occurrence because the first snow accumulation would remain on the panel, and new snowfall would only contribute to increasing the accumulation thickness. The ice on the PV panel surface would generally be unaffected by the new snow.

4.4.3. Existing Snow Accumulation Melting

When melting occurs but is not vigorous or prolonged enough for panel clearing to occur, the melted water can refreeze and form an ice layer on the panel surface. The absorption of the solar irradiance reflected onto the back surface of the panels, as well as the light transmitted through the

snow accumulation, leads to the panel typically being warmer than the ambient temperature during the day, and as such, the snow in contact with the panel melts. The result is that most of the generated moisture is typically along the surface of the panel. As a result, when the temperature of the panel decreases, icing occurs at the interface between the PV panel and the snow accumulation. Melting was the source of moisture for icing in two cases (Event 3 & 7)

The characteristics of ice caused by previous melting are variable. Based on the observed cases the physical shape is believed to be dependent on the degree of melting and as a result the amount of available water.

In one case (Event 3) there was limited melting which led to the snow accumulation only sliding approximately 2 cm down the panel on one side of the panel. The following day when the snow coverage was removed manually, there was ice buildup. The ice was similar to that of contact melting. However, it was more consistent over the surface and had smaller protrusions beyond the surface of the panels (1-2 mm) (Figure 4.3). These characteristics are believed to be the result of the snow coverage obstructing large water droplets from forming.
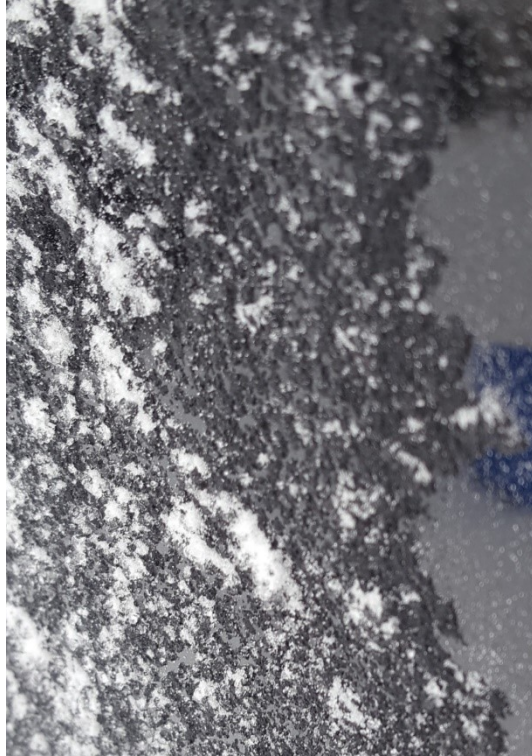
Figure 4.3 Ice on the glass panel resulting from small amounts of existing snow accumulation melting (Event 3)

In a second case (Event 7), melting took place for several days before the snow cover was removed. In this case, the ice buildup was much more substantial, with channels where water had flowed and refroze being visible. Figure 4.5 and Figure 4.4 depict the ice channels (Note: the ice was extremely brittle, and pieces of the ice broke off because of manual clearing).

Figure 4.4 Ice on framed PV panel resulting from large amounts existing snow accumulation melting (Event 7)
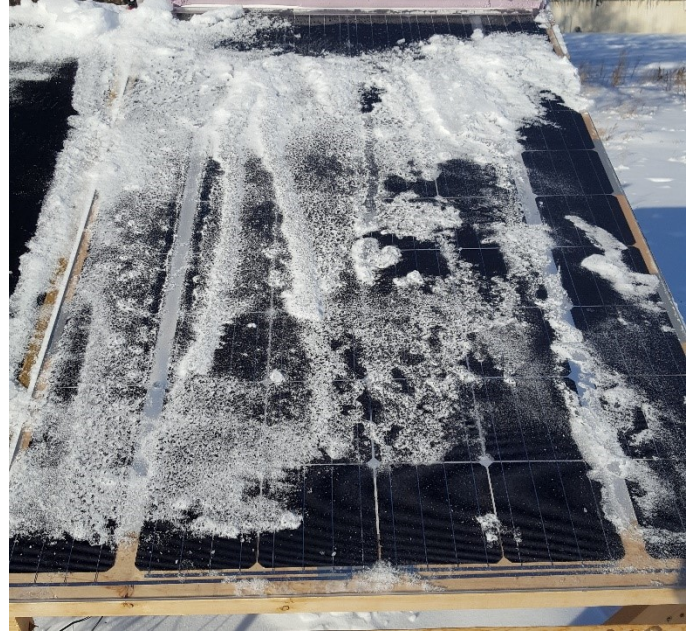
Figure 4.5 Ice on the frameless PV panel resulting from large amounts existing snow accumulation melting (Event 7)

4.4.4. Unknown Source

There was an icing event where the moisture source for the ice formation could not be determined.

In this case, a minimal amount of ice accumulated on the panels surfaces. The ice that accumulated

had extremely small protrusions, almost only a change in texture, and covered less than 10% of

the affected areas (Figure 4.6). The ice formation was determined to either be due to excess

moisture in the snow when it fell or the sublimation of the snow once it had accumulated.

<center>(A)　　　　　　　　　　　(B)</center>

Figure 4.6 Ice on the (A) frameless PV panel and (B) glass with unknown cause (Event 6)

4.5. Discussion

In warm winter conditions, where melting was believed to be actively occurring over the entire surface of the panel (due to warm ambient temperatures), sliding was observed at the minimum tilt angle setting allowable by the setup (13°), suggesting a coefficient of friction of less than 0.3. The low coefficient of friction is likely due to the interface between the panel and the snow being wetted and therefore having a smaller coefficient of friction. When melting was not occurring, sliding was only observed twice at modest tilt angles (approximately 45 degrees) out of thirty snowfall events. More often, when there was no melting sliding did not occur, even at tilt angles up to 71 degrees (the maximum tilt angle allowable by the setup), representing a coefficient of

friction of over 2.9. These results contribute to the author's belief that the adhesion caused by the formation of ice between the PV panels and snow accumulations is the primary cause of snow remaining on PV panels even at high tilt angles.

The sources of moisture for icing are very dependent on the past and present weather conditions. Melting of snowfall on contact with the panel typically occurs when snowfalls occur mid-day or shortly after sunset onto panels that have retained heat from the absorbed solar irradiance. Typically, the panels are colder than the ambient temperature at night because of radiant heat losses to the sky, so contact melting of snowfall occurring overnight is not likely. Sublimation of snow has been observed at temperatures as low as -25°C [36] making it a possible source of moisture in almost any climate. However, the sublimation process is slow [36], so it is not likely to contribute to significant ice build-up. Water on the surface can occur due to the melting of past accumulations or rainfall. If the water does not run clear of the PV panel, or evaporate before a snowfall, it can contribute to icing. Water on the surface before a snowfall can contribute to icing in two ways, it could freeze, and then snow could accumulate on top of it, or the snowfall could cool water on the surface to the point of freezing (similar to contact melting). Partial melting of snow accumulations can occur in a wide variety of climatic conditions, throughout the experiment, melting occurred at temperatures lower than -20°C on several occasions. However, at colder ambient temperatures the intensity of solar irradiance needed for sliding to occur is generally quite high. Finally, rainfall onto snow accumulations can be a source of moisture for icing in specific conditions that allow the moisture from rain to pass through the snow accumulation without freezing. When it reaches the panel, it could freeze if the panel is cold, or it could be retained in the snow until the panel temperature drops sufficiently for freezing to occur. However, if the rainfall is more significant it

can contribute to the clearing of the snow accumulation either by creating a lubricated surface for the snow to slide on or by causing it to melt in place completely.

Currently further, more advanced, research is needed to identify and understand the role ice plays in snow accumulations remaining on PV panels. Once the cause of snow accumulations remaining on panels is identified, efforts to develop mitigation methods can be better focused. Currently, as the author sees it there are several ways to prevent snow accumulations from remaining: stopping snow from settling on the panel [31,37], preventing the formation of ice between the snow and the panel, reducing the adhesion strength between the ice and the panel [38-41], and clearing the snow with mechanical or heating apparatuses.

4.6. Conclusion

This paper presents the finding of ice under snow accumulations on PV panels and suggests that ice, at the interface between the snow and the panel, may cause adhesion that results in snow accumulations remaining for extended periods. It lists five potential sources of moisture for icing and assigns the source of moisture from experimental observations of ice to melting of snow on contact with the panel, pre-existing ice on the panels, and partial melting of snow accumulations. As well, it identifies a case where either the sublimation of snow or excess moisture in the snow is believed to be the source of moisture for ice formation on the panel surface. Further, more advanced, research is required to develop a quantitative understanding of the impact of ice formations. This research can then be used to guide the development of mitigation methods to prevent snow accumulations.

Chapter 5: Empirical Threshold Modelling

5.1. Abstract

Precise and accurate predictions of the electricity generation of solar photovoltaic (PV) systems is essential for them to make up a significant portion of the generating capacity of electricity grids, and for them to be depended on as a generating source. A study was performed to enhance the methods used to predict snow cover on PV panels. Past studies have shown the effectiveness of threshold type empirical PV system snow cover prediction models that use plane-of-array irradiance as a function of ambient temperature to prescribe if sliding will occur or not. This analysis showed that considering the amount of irradiance transmitted by the snow accumulation and absorbed by the panel, rather than plane-of-array irradiance, substantially improved the modelling precision. Further improvements were achieved by considering the irradiance absorbed by the back surface of the panel. When compared to using plane-of-array irradiance, the use of absorbed irradiance increased the coefficient of determination (R^2) of the observed melting data points to the fitted line by nearly a factor of four. The improvement in modelling significantly reduces the uncertainty in the meteorological conditions that result in snow beginning to clear from PV panels and has the potential to improve the forecasting of electricity generation from PV systems in regions that experience snowfall.

5.2. Symbols

GHI	Global Horizontal Irradiance
DNI	Direct Normal Irradiance
DHI	Sky Diffuse Horizontal Irradiance
GRI	Ground Reflected Horizontal Irradiance
β	Solar altitude
α	Albedo of snow
I_F	Plane-of-array irradiance on the snow accumulation (front irradiance)
I_{BF}	Component of direct (beam) irradiance on the snow accumulation
θ_F	Angle of incidence of the front surface
Σ_F	Tilt angle of the front surface
I_{DF}	Diffuse sky irradiance on the snow accumulation

I_{RF}	Ground Reflected irradiance on the snow accumulation
Σ_B	Tilt angle of the back surface
I_B	Back irradiance
I_{BB}	Direct (beam) irradiance on the back surface
θ_B	Angle of incidence of the back surface
Σ_B	Tilt angle of the back surface
I_{DB}	Diffuse sky irradiance on the back surface
I_{RB}	Ground reflected irradiance on the back surface
C_s	Fitted shading constant
D	Shadow distance
τ	Transmittance of the snow accumulation
ε	Absorbance of snow
E_F	Irradiance absorbed by the front surface
α_B	Albedo of the back surface
E_B	Irradiance absorbed by the back surface
E_t	Total absorbed irradiance
RMSE	Root Mean Squared Error
P90	Model y-axis offset encompassing 90% of the observations
$RMSE_N$	Normalized Root Mean Squared Error
$P90_N$	Normalized model y-axis offset encompassing 90% of the observations
$P95_N$	Normalized model y-axis offset encompassing 95% of the observations

5.3. Introduction

PV systems installed in regions that experience snowfall can become covered with snow. The electricity generating capacity of a snow-covered PV panel is significantly reduced, with monthly electricity generation reduced by up to 90% - 100% during winter months [5,10,11]. Not only is the electricity generation significantly reduced, but snow accumulations also increase the challenges of predicting electricity generation during the winter months. Low levels of predictability limit the opportunity for PV systems to be fully integrated into the management of regional electricity grids. To be integrated, they should be able to be depended on to offset other forms of electricity generation. Without being fully integrated, the substantial costs (both environmental and financial) associated with maintaining alternate electricity generation types are not reduced. To integrate PV generation into electricity grids, accurate forecasts of electricity generation are required for the timestep lengths used to control the operation of electricity generation, transmission, and distribution infrastructure (15 minutes to 1 hour) [58].

For the forecasting length relevant to grid management, existing meteorological models can predict, with reasonable accuracy, when snow will begin to accumulate, how much snow will accumulate, and the intensity of solar irradiance [14]. There is much less understanding of how and when snow will clear from PV panels.

There are two primary modes of snow clearing: melting and sliding. With thicker snow accumulations, the snow tends to slide, rather than completely melt [18,25]. With lighter snowfalls and warmer temperatures, the snow cover typically melts entirely, or significant portions of it melt before sliding occurs [18,25]. The findings presented in Chapter 4 and the relationship reported by several studies between ambient temperature reaching 0°C and snow clearing suggests that sliding occurs once melting begins [112]. However, sliding has been observed at module temperatures as low as -10°C [17].

Short-term models predict the effect of snow on PV system electricity generation for periods between several minutes and several days. Accurate short-term models can go a long way to reducing the overall uncertainty in PV system electricity generation in the short-term and understanding the level of variability in the long-term [112]. Short-term models can be coupled with forecasted weather parameters to estimate the PV system electricity generation for short timesteps (15-minutes to daily). These predictions can be used to ensure enough electricity is being generated to meet momentary and routine electricity demand changes, to forecast electricity prices, and to manage electricity transmission systems [58]. Short-term models can also be coupled with historical weather data to provide an understanding of the mean value of the impact of snow for longer timesteps, as well as an understanding of the level of uncertainty in short-term electricity generation; this information is useful in the design phase, for system evaluation and optimization

[58]. The flexibility of short-term models results in them having a more diverse range of applicability when compared to longer-term models.

All of the reported short-term models depend significantly or exclusively on the ambient temperature and the plane-of-array solar irradiance to predict the effect of snow on PV panels [112]. Ambient temperature and solar irradiance have the most significant impact on the temperature of PV modules. Ambient temperature is key to determining the temperature of unheated objects, and the amount of convective and radiant heat loss. For PV panels, solar irradiance is generally the only heat input, and as a result, it is the sole cause of the panel temperature increasing above the ambient temperature. As a result, it is a crucial consideration in any snow clearing model, because snow clearing is often observed at ambient temperatures below 0°C. Snow melts at 0°C, and although complete melting (without sliding) can occur, it is not typical with thicker snow accumulations [18,25]. However, the water generated from melting is believed to lubricate the boundary between the PV panel and the snow accumulation, creating a low friction surface for the snow accumulation to slide on [112].

The existing short-term models can be grouped into two general types: direct electricity generation loss prediction models and snow cover prediction models. Direct electricity generation loss prediction models use system and weather characteristics to output the predicted electricity generation losses resulting from snow accumulations. Snow cover prediction models simulate the snow clearing process to estimate the snow-covered portion of the panel. This information can then be used to compute the generation loss. Snow cover prediction models can depend on first-principle thermal heat and mass transfer relationships (like the ones developed by Rahmatmand et al. [63] and Ross [23]), or they can be empirical models that employ a threshold of meteorological conditions to approximate when sliding occurs [5,13,14,19,24].

One of the most tested short-term models was reported initially by Marion et al. [5], and the model type has since been shown to be effective by at least three publications [19,24,45] and has been integrated into the National Renewable Energy Laboratory's System Advisor Model [113]. This model is a snow cover prediction model that uses a linear threshold between ambient temperature and plane-of-array solar irradiance to predict whether snow clearing occurs or does not occur in each hour. Furthermore, if sliding is predicted, one of two empirically fitted linear relationships, based on tilt angle and obstructions to the path of sliding snow, are used to approximate the distance that the snow slides down the length of the PV system in the hour.

Although over long timespans the model proposed by Marion et al. [5] functions exceptionally well, it is susceptible to significant errors in short-term predictions. These errors are caused by the misprediction of the clearing of individual snow accumulations. Marion et al. [5] reported that on a number of occasions clearing was predicted to occur but did not, and subsequent colder ambient temperatures prevented sliding for over a week; in these cases, the measured monthly electricity generation loss was nearly three times the predicted amount. Increasing the precision of short-term models is critical to the widespread success of PV electricity generation. As such, adapting existing snow cover prediction models to reduce the likelihood of mispredictions and improve precision was the purpose of this paper.

This study aims to share improvements for threshold type PV panel snow cover prediction models. The key change to existing models being demonstrated in this analysis is the inclusion of absorbed solar irradiance. Furthermore, a process for calculating absorbed irradiance is described.

For the purpose of this chapter, the solar radiation incident on the surface of the snow accumulated on a PV panel (plane-of-array irradiance) will be referred to as front irradiance, and the irradiance transmitted through the snow layer and being absorbed by the panel will be called front absorbed

irradiance. The irradiance received by the back surface will be referred to as back irradiance, and the amount absorbed by the panel will be referred to as back absorbed irradiance.

5.4. Methodology

This section identifies possible improvements to threshold type snow cover prediction models and justifies them with past research and principles of heat transfer. Furthermore, this section describes the dataset used and the method of calculating absorbed irradiance.

5.4.1. Model Improvements

Several changes can be made to threshold type models to enable them to better represent the first-principle thermal heat-transfer relationships occurring in a snow-covered panel. The changes outlined and analyzed in this paper are the transmittance of snow and irradiance on the back surface.

5.4.1.1 *Transmittance of Snow*

The albedo of fresh snow is as high as 0.9 [114] (albedo is the average reflectance of solar irradiance by a surface), which results in the transmittance of snow accumulations being low. The transmittance of snow accumulations decreases rapidly within the first several centimetres; 2 cm of freshly fallen snow has a transmittance of 15% to 20% [114]. Beyond 2 cm the rate at which transmittance decreases with depth (extinction coefficient) slows significantly—by over a factor of 10. The transmittance in thin snow accumulations decreases rapidly with depth because they are optically thin [115], resulting in the compound effect of absorption and increasing reflectance being realized in the value of the extinction coefficient of the first several centimetres of snow.

Because the absorptivity of snow is not high (only around 10% per cm) [114], most of the energy not reflected by the snow is absorbed by the surface of the PV panel, heating it. With high enough levels of irradiance, melting of the snow accumulation will occur at the interface between the panel and the snow. Furthermore, the low absorptivity of snow means that the radiation absorbed by the

snow is small, and except with ambient temperatures within several degrees of 0°C, significant melting at the interface would occur before melting elsewhere in the snow accumulation would occur.

In the model proposed by Marion et al. [5] as well as all other short-term models, the front irradiance plays a significant role in modelling the impact of snow on electricity generation loss. However, due to the high albedo and the resulting low transmittance, the front irradiance is only loosely correlated to the energy reaching the panel. The depth of snow, particularly for optically thin snow accumulations, plays a significant role in the portion of the front irradiance reaching the panel where it is converted to heat.

5.4.1.2 *Irradiance on the back surface*

The back surface of rack-mounted PV setups, typically found in ground mounted and flat roof-mounted PV systems, are exposed to irradiance which can contribute significantly to the warming of the PV panels. The high albedo of the snow on the ground results in high levels of ground reflected irradiance, which contributes to the irradiance on the back surface being as high as 25% of the front irradiance [10,23]. When snow accumulations do exist on the front surface, the radiation absorbed by the back surface can contribute significantly to the warming of the panel [23].

5.4.2. Data Recording

The experimental setup described in Chapter 3 was used to gather the data used in this analysis. For this analysis still images, ambient temperature, global horizontal irradiance (GHI), snow accumulation depth, and barometric pressure were used. The dataset was derived by analyzing the still images to identify the first signs of melting or sliding. Melting was defined as any visually identifiable melting over a large section of the panel. Observations, where melting was only occurring in the boundary areas between snow accumulations and clear areas, were excluded from

the analysis; this is because of the potential that heat was being conducted within the panel material from the snow-free areas to the snow-covered areas. Sliding was any displacement of snow down the PV panel surface; this included the "sagging" or "sloughing" of the snow accumulations. For each observation of clearing, the 5-minute GHI value and an interpolated value of ambient temperature (from the hourly observations) were extracted from the weather dataset.

Fifty-two observations of melting or sliding were identified. Of this dataset, five were removed leaving forty-seven in the analysis. Two observations were removed due to rapidly changing irradiance values. In these cases, the amount of irradiance on the panel changed by more than 20% in the 20 minutes preceding the observed sliding, making it difficult to pinpoint the meteorological conditions under which sliding occurred. One observation was removed because there was no possibility of melting occurring. In this case, sliding occurred rapidly during the night while the ambient temperature was less than -27.0°C. A further two observations were removed from the same day as the snow coincidently cleared shortly after the suns disc rose above the horizon when there was no considerable amount of irradiance.

Table 5.1 outlines the observed conditions under which sliding began. Throughout the experimentation, observations of clearing were made in a broad range of meteorological conditions. For the utilized observations, the ambient temperature ranged between -23.5°C and 0.5°C and GHI ranged between 36 W/m^2 and 803 W/m^2. Furthermore, cloud cover, snow characteristics, and depth of snow accumulations were variable throughout the observations.

Table 5.1 System and Meteorological Conditions During Observations

Date (YYYY-MM-DD)	Time (hh:mm)	Panel Type	Tilt angle (°)	GHI (W/m²)	Interpolated Ambient Temperature (°C)	Snow Accumulation Depth (cm)
2017-10-31	11:00	Glass	21	35.7	0.5	3
2017-11-01	15:00	Glass	33	134.6	-2.6	4
2017-11-03	11:14	Glass	45	164.2	-12.2	1
2017-11-04	10:56	Glass	45	118.1	-13.5	0.8
2017-11-04	11:28	Framed	45	173.4	-10.9	0.8
2017-11-05	10:56	Glass	31	237.5	-9.7	1
2017-11-05	11:08	Framed	31	178.8	-9.5	0.5
2017-11-05	13:24	Framed	31	251.9	-6.8	1
2017-11-08	11:54	Glass	47	134.3	-10.6	0.75
2017-11-08	12:08	Framed	71	132.8	-10.2	0.75
2017-11-14	12:38	Glass	31	182.3	-8.9	2
2017-11-16	11:21	Glass	30	212.2	-10.4	0.5
2017-11-16	11:21	Framed	30	212.2	-10.4	0.5
2017-11-17	11:09	Glass	30	182.9	-12.3	1
2017-11-18	11:04	Framed	30	301.8	-6.2	1.5
2017-11-20	11:07	Glass	30	220.3	-14.7	1
2017-11-22	10:15	Glass	30	180.0	-6.4	2.5
2017-11-22	13:05	Framed	30	227.0	-4.7	2.5
2017-11-23	10:15	Framed	30	153.8	-0.3	2.5
2017-12-24	12:37	Frameless	71	194.8	-17.2	1.5
2017-12-25	11:13	Frameless	45	161.2	-23.5	0.5
2017-12-25	11:39	Frameless	45	188.1	-23.4	0.5
2017-12-25	12:15	Frameless	45	209.5	-23.4	0.5
2017-12-27	11:24	Glass	45	129.6	-19.7	0.25
2017-12-27	11:24	Frameless	45	129.6	-19.7	0.25
2017-12-27	11:24	Framed	45	129.6	-19.7	0.25
2018-01-10	13:04	Glass	45	201.6	-23.3	0.25
2018-01-10	13:06	Frameless	45	182.6	-23.3	0.25
2018-01-10	13:14	Framed	45	172.0	-23.2	0.25
2018-01-10	13:54	Glass	45	193.9	-23.0	0.5
2018-01-10	13:54	Frameless	45	193.9	-23.0	0.5
2018-01-10	13:54	Framed	45	193.9	-23.2	0.5
2018-01-13	10:27	Glass	45	128.7	-9.5	1
2018-01-13	10:43	Framed	45	153.0	-8.7	1
2018-01-13	10:47	Frameless	45	108.7	-8.5	1
2018-01-13	12:41	Frameless	45	152.0	-3.1	0.5
2018-01-13	12:57	Framed	45	114.6	-2.4	0.5
2018-02-04	12:36	Glass	27	356.2	-16.9	3
2018-02-05	12:02	Glass	27	345.7	-16.6	2.5

2018-02-05	12:42	Frameless	27	359.3	-15.9	2.5
2018-02-20	12:05	Frameless	27	372.4	-15.1	0.75
2018-03-29	10:20	Glass	27	408.2	-9.5	2
2018-03-29	10:20	Frameless	27	408.2	-9.5	2
2018-03-29	10:28	Framed	27	474.3	-9.4	2
2018-03-30	10:30	Glass	27	238.6	-12.3	1
2018-03-30	10:32	Frameless	27	250.3	-12.2	1
2018-03-30	13:00	Framed	27	803.0	-11.8	1.5
2017-11-03[1]	12:56	Framed	45	422.2	-11.5	1
2018-01-11[2]	04:57	Framed	45	0.0	-27.0	1
2018-01-11[3]	09:52	Glass	45	95.8	-26.0	0.5
2018-01-11[3]	09:56	Frameless	45	102.4	-26.0	0.5
2018-02-20[1]	11:07	Glass	27	366.9	-13.8	0.75

Table Notes:

[1] Eliminated because of rapidly changing irradiance

[2] No melting - Cleared in the middle of the night

[3] No melting - Cleared with too low of irradiance for the ambient temperature

5.5. Irradiance and Absorbed Irradiance Calculation

In this section, a collection of methods are employed to compute the irradiance on the front and back surface of the panel, as well as the absorbed irradiance. This approach only uses commonly measured meteorological characteristics and global horizontal irradiance (GHI) but does not depend on more advanced irradiance measurements; increasing the geographic regions where it is applicable due to the higher availability of GHI measurements and forecasts. If the front (plane-of-array) irradiance is measured, then it should be used in place of the computed front irradiance.

Figure 5.1 is a flowchart of the process used to calculate absorbed irradiance. First, the components of the irradiance must be computed, following this the perpendicular component of each of the irradiance components must be determined (i.e. front irradiance and back irradiance). Finally, a computation of the portion of the irradiance being absorbed by the panel must be performed.
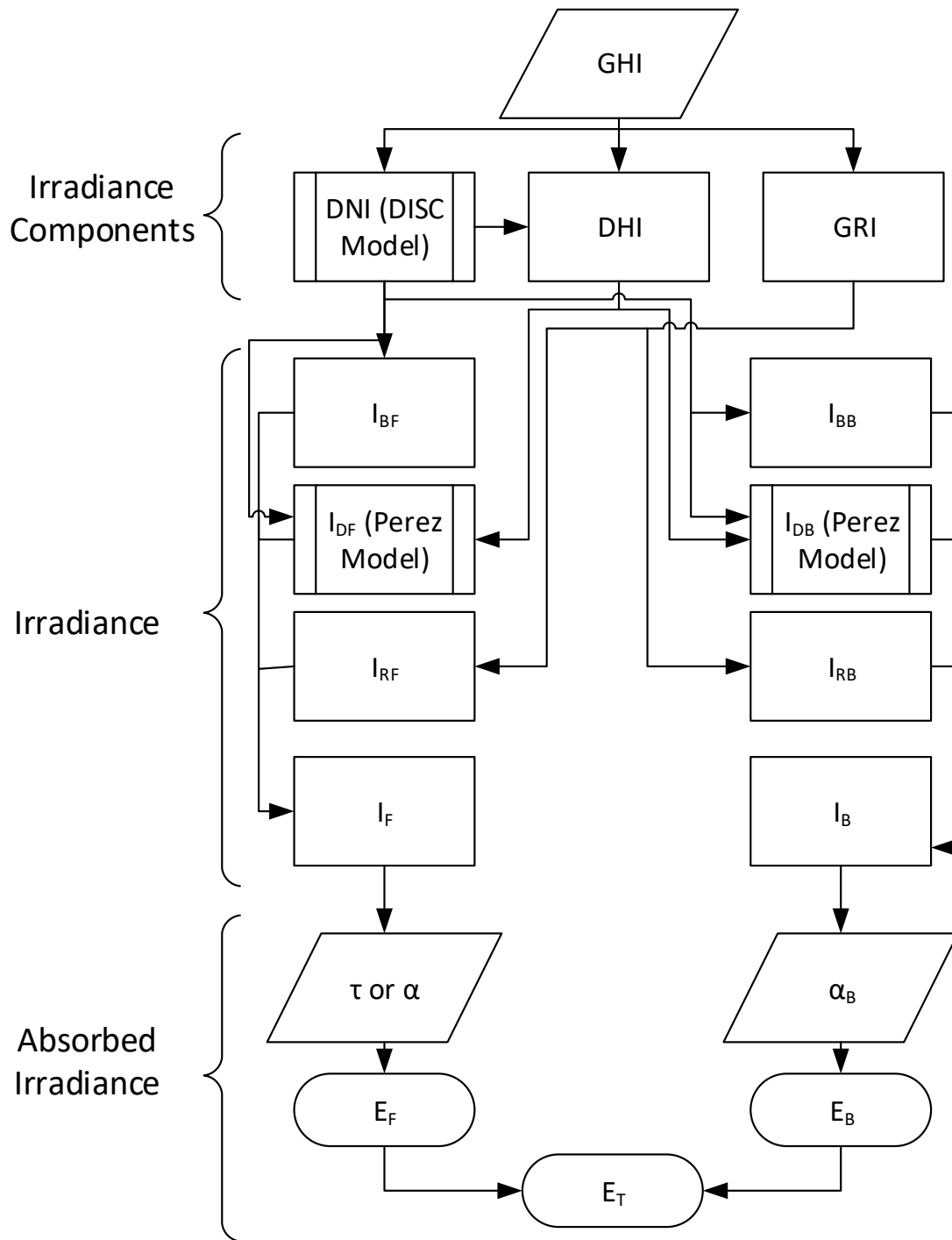
Figure 5.1 Absorbed Irradiance Calculation Flowchart

5.5.1. Components of Solar Radiation

The only solar radiation measurement taken for this study was global horizontal irradiance (GHI).

As such, the direct normal irradiance (DNI), diffuse horizontal irradiance (DHI), and ground

reflected irradiance (GRI) must be estimated before the front irradiance and back irradiance can be computed.

5.5.1.1 Direct Normal Irradiance

The direct normal irradiance (DNI) is the beam component of the sun's radiation incident on a surface oriented perpendicular to the sun's position. The intensity of DNI was computed using a modified version of the National Renewable Energy Laboratories (NREL) DISC Model, which includes a stability index, clear sky model, and airmass characteristics (as discussed in R. R. Perez et al. [116] and R. Perez et al. [117]). The random error associated with this prediction is 8.5%, and the bias is 3% [118], this level is acceptable for this analysis and likely for short-term electricity generation predictions as well. F. Holmgren et al. [119] developed the Python language code that was used to implement the modified DISC model.

5.5.1.2 Diffuse Horizontal Irradiance

The diffuse horizontal irradiance (DHI) is the diffuse sky radiation incident on the upper surface of a horizontal surface. Together DHI and the vertical component of DNI make up GHI. As a result, knowing DNI, GHI, and the solar altitude (β), DHI can be determined by Eqn. (5.1). Because a possible overestimation of DNI could result in a negative DHI, it was limited to positive numbers; this limitation was not employed with this dataset.

$$DHI = max\left\{ \begin{matrix} GHI - \cos(\beta)\,DNI \\ 0 \end{matrix} \right\}$$ (5.1)

5.5.1.3 Ground Reflected Irradiance

The ground-reflected irradiance (GRI) is the amount of irradiance that would be received by a downward facing horizontal plate (ignoring any shadowing caused by itself). The GRI was computed using the measured GHI and a ground albedo of 0.9, for fresh snow, as depicted in Eqn. (5.2).

$$GRI = \alpha \, (GHI) \tag{5.2}$$

5.5.2. Irradiance

Various irradiance models and equations can be used to determine the front irradiance and back irradiance. In this section, the front irradiance and back irradiance are computed using DNI, DHI, GRI and a variety of first-principle and empirical relationships.

5.5.2.1 Front Irradiance

The irradiance on the front surface of the panel (I_F) is the sum of the components of DNI, DHI, and GRI perpendicular to the front surface (Eqn. (5.3))

$$I_F = I_{BF} + I_{DF} + I_{RF} \tag{5.3}$$

The direct (beam) component of front irradiance (I_{BF}) was computed using Eqn. (5.4). Two conditions must be satisfied for direct irradiance to occur on the front surface; first, the sun direction must be from the front of the panel (i.e. the angle of incidence (θ_F) must be less than 90°), and second, the sun must be above the horizon (i.e. the solar altitude (β) must be greater than 0°). This excludes beam irradiance when less than half the suns disk is above the horizon, which occurs at sunrise and sunset; however, at these times, the intensity of beam irradiance is very low, and is unlikely high enough for melting to occur. Neither of these limitations was true for any of the observations utilized in this analysis.

$$I_{BF} = \begin{cases} 0, & if \; \theta_F > 90° \\ 0, & if \; \beta < 0° \\ DNI \, cos(\theta_F), & otherwise \end{cases} \tag{5.4}$$

The diffuse sky component of front irradiance (I_{DF}) was estimated using the anisotropic Perez diffuse irradiance model for tilted surfaces. The coefficients used in this analysis were derived from measurements at nine different locations [120], and to the author's knowledge are the most

73

recently updated coefficients. The reported root mean squared error (RMSE) is between 11 and 16 W/m^2 and depends on orientation, the mean bias error (MBE) is between -2 and 3 W/m^2 [120]. The reported orientation that is nearest the front surface of the panel (South facing at a tilt angle of 45°) had an RMSE of 14 W/m^2 and a MBE of -1 W/m^2. This level of certainty is not a concern for this model. Holmgren et al. [119] developed the Python code that was used to implement the Perez model.

The ground-reflected component of front irradiance (I_{RF}) was calculated using Eqn. (5.5). Eqn. (5.5) assumes that the ground is an infinitely large flat surface and computes the view factor of it to the panel surface then multiplies by GRI.

$$I_{RF} = GRI \left(\frac{1 - cos(\Sigma_F)}{2} \right)$$ (5.5)

5.5.2.2 Back Irradiance

Similar to the computations used for the front irradiance, the back irradiance (I_B) is the sum of the perpendicular components of DNI, DHI, and GRI (Eqn. (5.6)). Note that the irradiance on the back surface of the panels should only be considered if the panels are rack mounted, like the ones in the experiment. If essentially no irradiance reaches the back surface of the panels, as is the case with rail mounted systems parallel to structures, then it can be ignored.

$$I_B = I_{BB} + I_{DB} + I_{RB}$$ (5.6)

The direct (beam) irradiance on the back surface (I_{BB}) was computed by replacing θ_F with θ_B, the angle of incidence of the back surface, in Eqn. (5.4). For south-facing panels, during the winter the sun position is typically always on the front side of the panels. As a result, the component of DNI on the back surface can generally be ignored. However, the direct irradiance on the back surface

of the panel may need to be considered depending on the orientation of the panels and if snow falls occur after the Spring (Vernal) equinox for south-facing panels.

The diffuse sky irradiance on the back surface (I_{DB}) was determined with the Perez diffuse irradiance model, as it was for the front surface. The only difference is that the tilt angle of the back surface (Σ_B) was used in place of the tilt angle of the front surface (Σ_F), and $\Sigma_B=\Sigma_F+180°$.

The ground-reflected irradiance on the back surface (I_{RB}) was computed with Eqn. (5.7), which is a version of Eqn. (5.5) modified for use on the back surface and to account for shading. The panels can severely shade the area beneath and behind themselves. The most accurate way to account for shading is to simulate the location of the shaded areas and calculate the view factor of the shaded areas from the back surface of the PV panel—which varies for every point on the panel—complicating the model drastically. To account for the fact that shaded ground still receives some diffuse radiation, only the beam component on the ground ($DNIsin(\beta)$) was considered for shading. The view factor of the shadow was approximated using a fitted constant (C_s) (for this setup C_s was 2.4) and the distance between the center of the panels and the center of the shadow (D) (computed using the PV system geometry and the solar altitude angle). Solar altitude (β), and not the angle of incidence, was used for computing the shading because if the angle of incidence was used the view factor of the shadow could vary significantly depending on the computed location on the panel. A limit to the effect of shading was set to prevent negative values of back irradiance; it was only implemented in one observation.

$$I_{RB} = \max\left\{\begin{matrix}\left(\dfrac{1-cos(\Sigma_B)}{2}\right) - C_s\left(\dfrac{DNIsin(\beta)}{D}\right)\\0\end{matrix}\right\} \tag{5.7}$$

5.5.3. Absorbed Irradiance

With the front and back irradiance approximated, the amount of radiation energy being absorbed can be approximated. In this section, the absorbed irradiance for the front surface is computed based on the transmittance of the snow layer, and the absorbed irradiance on the back surface is computed using the albedo of the back surface of the panel. The equation for total absorbed irradiance is also included.

5.5.3.1 *Front Absorbed Irradiance*

The ratio between the front irradiance and the front absorbed irradiance is dependant on the transmittance of the snow layer. The albedo of PV cells is 0.1 [121]. Roughly 90% of the radiation energy that reaches the front surface of the panel is absorbed by the panel initially. The remaining 10% is reflected back to the snow accumulation—which has a high albedo—and as a result, would reflect light at the PV panel. As such, the assumption was made that the panel absorbs all the light transmitted by the snow.

To determine the amount of sunlight that penetrates the snow accumulation Perovich's [114] findings on the transmittance (τ) and albedo (α) of fresh snow were used. For snow accumulations greater than 2 cm in thickness, the average transmittance values for different wavelengths reported by Perovich [114] were used (Figure 5.2). To the author's knowledge, there is no information on the transmittance of snow accumulations less than 2 cm in thickness, and instead, in these cases, the average albedo for different wavelengths reported by Perovich [114] was used. The albedo of snow accumulations as thin as 0.25 cm were reported (Figure 5.3). Using the albedo was seen as an acceptable practice because for thin snow accumulations the transmittance is primarily driven by the albedo and not absorptivity. Notice, from Figure 5.2 and Figure 5.3 respectively, that a 2 cm snow accumulation had a transmittance of approximately 0.15 and an albedo of between 0.78 and 0.84, given Eqn. (5.8). The resulting absorbed energy by the snow in the first 2 cm is only

between 1% and 7% of the front irradiance, which is insignificant given the other unknowns in the model.
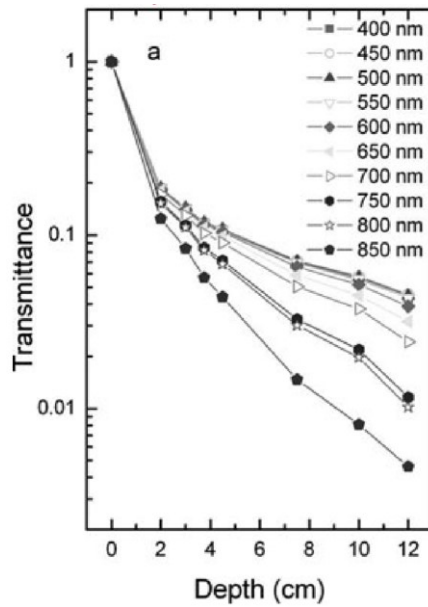

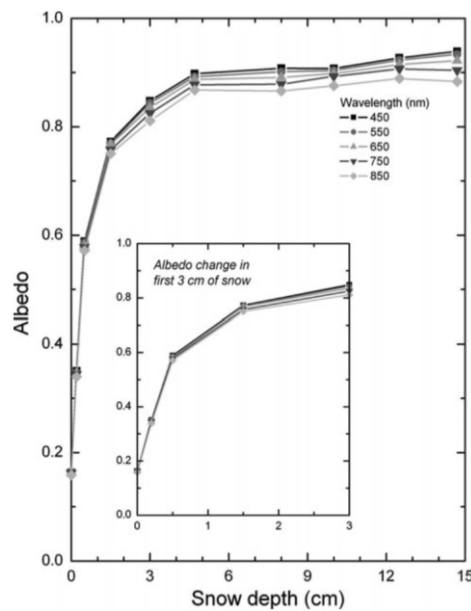*Figure 5.2 Transmittance of Fresh Snow [114]*

Figure 5.3 Albedo of Fresh Snow [114]

$$\tau = (1 - \alpha - \varepsilon) \tag{5.8}$$

With an approximated value of front irradiance (I_F), and an estimation of the transmittance of the snow accumulation (τ) the absorbed irradiance through the front surface was then computed using Eqn. (5.9).

$$E_F = \tau\, I_F \tag{5.9}$$

5.5.3.2   Back Absorbed Irradiance

With an approximation of the irradiance on the back surface (I_B) and the albedo values of the back surface of the panels (α_B), the amount of irradiance absorbed by the back surfaces of the panels was computed using Eqn. (5.10).

$$E_B = \alpha_B\, I_B \tag{5.10}$$

5.5.3.3   Total Absorbed Irradiance

The approximation of the total irradiance absorbed by the panel (E_t) is merely the sum of the irradiance absorbed by the front surface and irradiance absorbed by the back surface (Eqn. (5.11))

$$E_t = E_F + E_b \tag{5.11}$$

5.6.   Model Results

The data used in this analysis was derived differently from that of the data used in Marion et al. [5]. This analysis identifies the irradiance conditions and ambient temperature under which sliding began to occur, Marion et al. [5] made an observation every hour and determined whether sliding was occurring or not. Although the method used in the analysis presented in this paper resulted in fewer data points, it was used because the data points can be quantitatively used in a least squares regression to establish a linear threshold of the meteorological conditions under which snow clearing began.

The models discussed in this section all use meteorological conditions from the time when sliding was initially observed. The resulting model is a linear relationship with the irradiance condition

(i.e., I$_F$, E$_F$, E$_T$) as a function of ambient temperature. The models were developed using a least squares regression of the data points gathered from experimental observations, the equations of the models are shown on their respective figures. The line represents the best division between when snow clearing should be predicted and when it should not be; with meteorological conditions that are above the division, clearing of the PV panels would be predicted, and no clearing would be predicted for meteorological conditions below the division.

The least squares regression for a linear model is defined by a slope (m) and an intercept (b) which were respectively determined using Eqn. (5.12) and Eqn. (5.13). The resulting equation of the line takes the form of y=mx+b.

$$m = \frac{N \sum xy - \sum x \sum y}{N \sum x^2 - (\sum x)^2} \tag{5.12}$$

Where N is the number of observations, x is the ambient temperature, and y is the variable used in the vertical axis (i.e., I$_F$, E$_F$, E$_T$)

$$b = \frac{\sum y - m \sum x}{N} \tag{5.13}$$

Where N is the number of observations, x is the ambient temperature, and y is the variable used in the vertical axis (i.e., I$_F$, E$_F$, E$_T$)

The intercept (b) was not fixed to zero because of the potential effects of longwave radiation between the panel and the ground and sky. The ground and sky temperature can be different from the ambient temperature (generally colder); this would typically result in a positive value for the intercept (b).

Figure 5.4 shows the estimated front irradiance as a function of ambient temperature; this represents the base case, from which the improvement attained by using absorbed irradiance can

be compared. Figure 5.5 shows the estimated absorbed irradiance through the front surface of the

panel as a function of ambient temperature. Figure 5.6 shows the estimated total absorbed

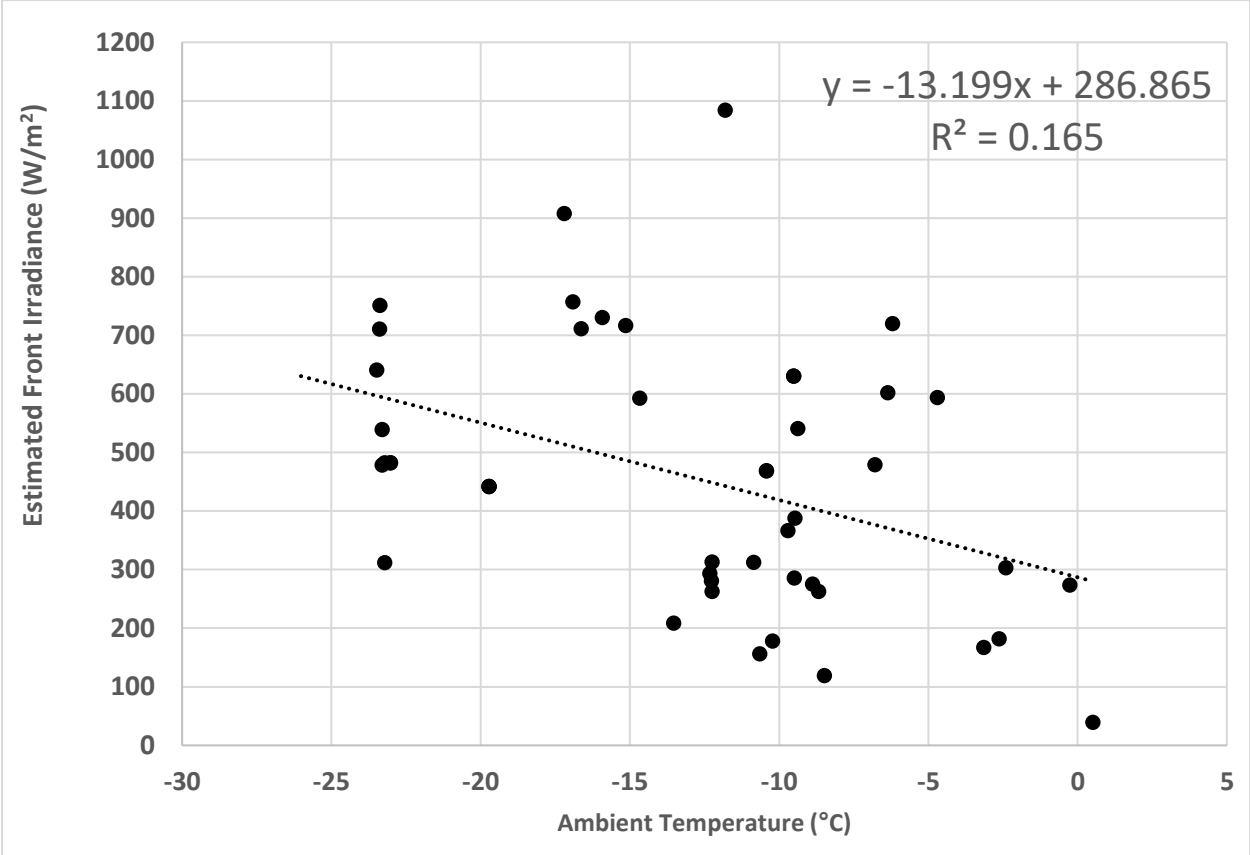irradiance as a function of ambient temperature.

Figure 5.4 Front Irradiance as a Function of Ambient Temperature
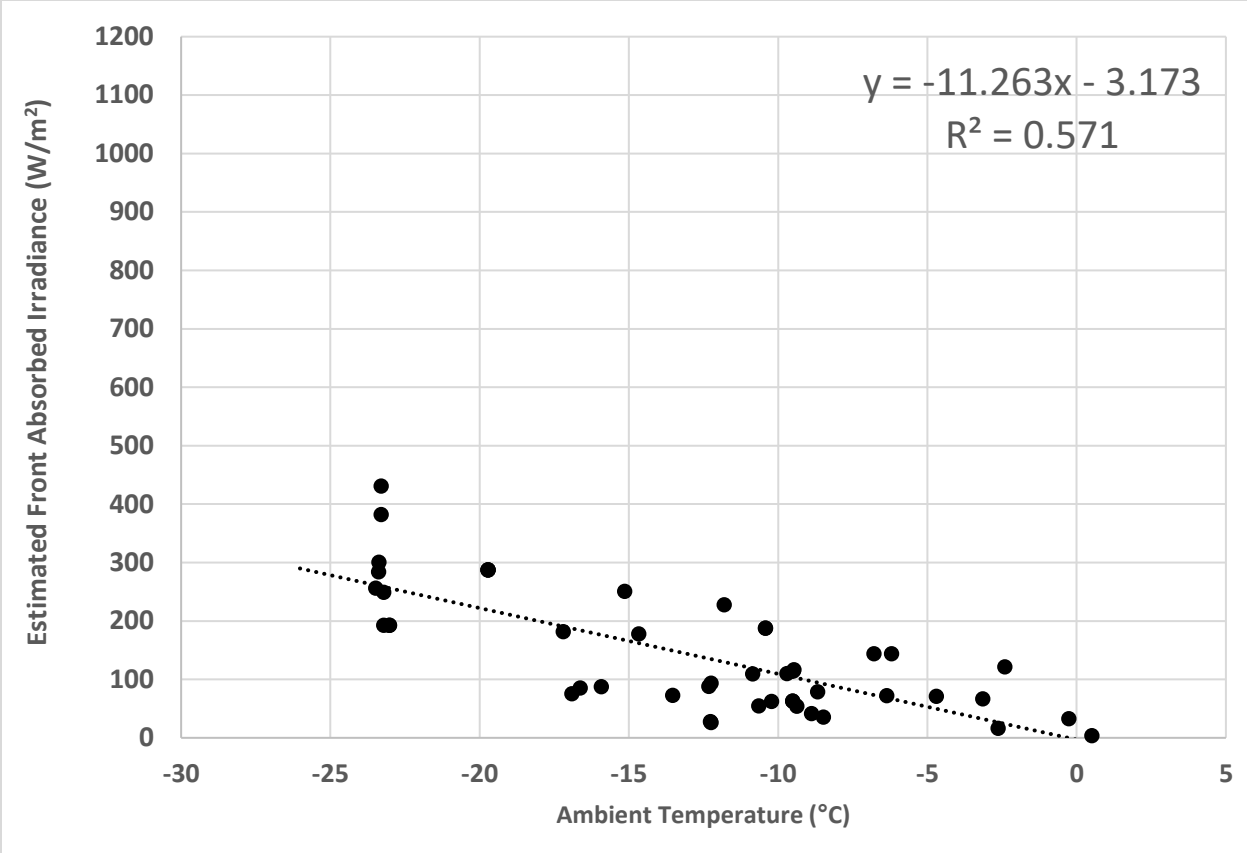
Figure 5.5 Front Absorbed Irradiance as a Function of Ambient Temperature
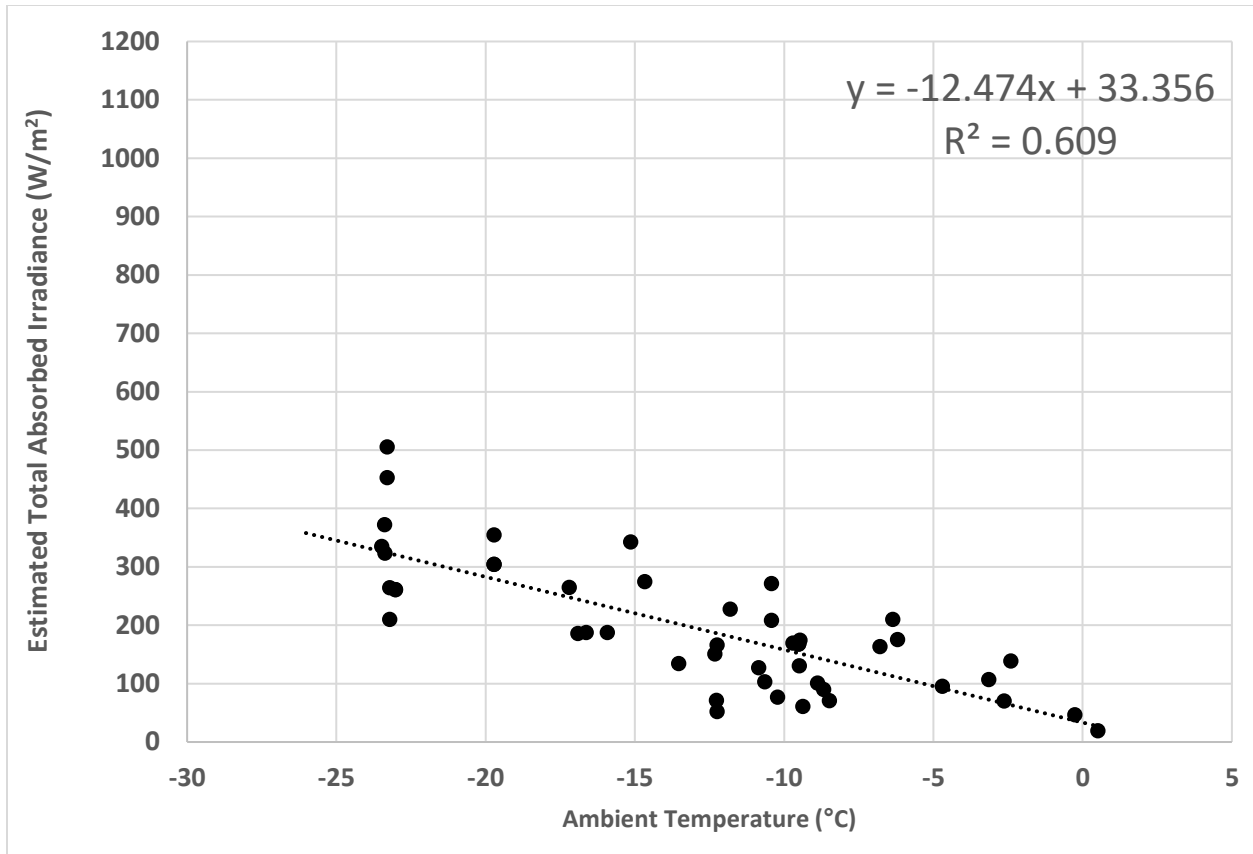
Figure 5.6 Total Absorbed Irradiance as a Function of Ambient Temperature

By observation of the three plots, the data from both the absorbed irradiance plots follow a more clear linear trend between decreasing ambient temperature and increasing absorbed irradiance. In contrast, the front irradiance data appears more like an elongated data cloud and has a much weaker relationship to the trend line.

5.6.1. Results Summary

Table 5.2 contains the values of several metrics on which the performance of the different types of models can be compared. The coefficients of determination of all the absorbed irradiance datasets fit their respective linear models substantially better than the front irradiance model. However, the improvement of the total absorbed irradiance case was only marginal over that of the front absorbed irradiance case.

The root mean squared error (RMSE) and the y-axis offset from the line in which 90% of the observations are within (P90) is significantly smaller for the absorbed irradiance cases, however, the magnitude of absorbed irradiance is also substantially smaller. To be able to compare the models, a normalized version of these variables was calculated ($RMSE_N$ and $P90_N$), the formulas for the normalized values are shown in Table 5.2. Only the $RMSE_N$ of the total absorbed irradiance case was smaller than the front irradiance case, the $RMSE_N$ of the front absorbed irradiance case was slightly higher (which is not believed to be significant). The $P90_N$ of the front absorbed irradiance model was the largest; the total absorbed irradiance model had a similar $P90_N$ to the front irradiance model. A similar relationship between the models was observed with $P95_N$ values. Finally, the F-statistic is a measure of the statistical significance of the relationship between the data and the model. All three F-statistics are significantly higher than three, which means that there is greater than 98% confidence that the relationship between the models and the data is not statistically insignificant.

Table 5.2 Results Summary Table

Irradiance Type:	Coefficient of determination (R^2)	RMSE	RMSE Normalized ($RMSE_N$) $$RMSE_N = \frac{RMSE}{\bar{I}}$$	90th Percentile Offset (P90)	Normalized 90th Percentile Offset ($P90_N$) $$P90_N = \frac{P90}{\bar{I}}$$	F-statistic
Front Irradiance	0.16	203	0.443	275	0.60	9
Front Absorbed	0.57	66	0.464	102	0.72	60
Total Absorbed	0.61	67	0.343	114	0.59	70

By observing the intercept of the linear model (b), it is clear that in all the absorbed irradiance models the intercept is substantially closer to 0 W/m^2 than in the front (plane-of-array) irradiance

model, even if it is normalized. Although based on a first principle understanding of longwave radiation the intercept should be greater than 0 W/m^2, it should be only slightly greater. If the intercepts were fixed to 0 W/m^2, none of the absorbed irradiance models would experience a significant change in slope or precision. However, for the front irradiance model, setting the intercept to 0 W/m^2 would have a significant negative impact on the model performance, in fact, the coefficient of determination (R^2) would become negative.

5.7. Discussion

The results of this study suggest that significant improvements to snow clearing prediction models can be achieved by considering the amount of irradiance reaching the panel surface and being absorbed. Furthermore, the analysis shows that the amount of irradiance being absorbed by the back surface of the panel can offer a further small improvement to the model. However, the front absorbed irradiance model offers nearly the same improvement as the total absorbed model (as can be seen in Table 5.2) and is less challenging to apply to new designs, as there is no need for a fitted shading coefficient.

The irradiance absorbed by the back surface may be more relevant in situations where shading of the area behind the panel is less prevalent, and more irradiance is absorbed by the back surface. Another situation where the back-surface irradiance may be more important is when the snow accumulations on the panel are thicker, resulting in little front absorbed irradiance; in this case, the back absorbed irradiance may be the panels primary heat input. The snow accumulations within the utilized dataset were generally thin, with an average thickness of 1.2 cm, with only one accumulation thicker than 3 cm.

Included in the results of this model are perhaps some uncertainty resulting from the use of an approximated value for irradiance and an estimation of the transmittance of the snow layer. The

many variables associated with these approximations make it difficult to specify the amount of error. The error in the magnitude of the irradiance calculation is subject to differences in the angle of incidence, cloud cover condition, and ground snow cover condition for example. The RMSE is likely 20% of the actual value but would be heavily dependant on the characteristics of the snow and the meteorological conditions. The research developed to understand the transmittance of fresh snow is very limited, and the characteristics of snow (for example density, water content, and crystal shape) are extremely variable. If more characteristics of the snow or the conditions under which it formed could be included in the determination of the transmittance value of snow accumulations the approximation of transmittance would likely improve significantly. Due to the limited types of data recorded by typical weather stations and the need for a widely applicable model, research relating the transmittance of snow to its characteristics would not be as useful for this model as linking transmittance to the conditions under which the snow fell (for example, ambient temperature and wind speed).

Although it is not unreasonable for a large system operator to perhaps measure the front (plane-of-array) irradiance and absorbed irradiance on a panel, it is not practical for small system operators to measure these parameters. For this reason, the approach used in this analysis to calculate the absorbed irradiance, which depends on variables readily available from thousands of weather stations, has a wide range of applicability with all types of PV system operators in many different regions.

It may be possible to attain a moderately accurate approximation of the absorbed irradiance through the front surface of the panel on PV systems that have a maximum power point tracking (MPPT) inverter and are uniformly covered with snow. In this case, the amount of electricity generation from the snow-covered panel could be compared with the plane-of-array irradiance on

the panel to approximate the absorbed irradiance (and the transmittance of the snow layer). However, it is essential to consider that the spectral response of PV panels and the spectral transmittance of snow are not uniform, making this calculation more complicated than a simple ratio.

5.8. Conclusion

Modelling and forecasting the electricity generation of PV systems with sufficient accuracy is critical for their broadened integration into electricity grids. Without a high level of accuracy in electricity generation forecasts, it is challenging to depend on PV generation in grid management decisions, like offsetting other forms of electricity generation.

The addition of threshold type snow cover prediction models can significantly increase the accuracy of PV system electricity generation predictions for panels subjected to snow accumulations. In these models, irradiance and ambient temperature exclusively or nearly exclusively define the threshold between clearing and not. These short-term models are unique because they can be used with historical data to determine the expected effect of snow on electricity generation or used with short-term forecasts to predict the amount of electricity generation for 24 to 48 hours into the future [14].

The results of this study suggest that the use of absorbed irradiance as a replacement for front (plane-of-array) irradiance can substantially reduce the uncertainty in when snow begins clearing; the coefficient of determination was improved by very nearly a factor of four. Furthermore, the procedure outlined to compute absorbed irradiance from GHI measurements allows the model to be applicable in many regions. The different models presented can be paired with the linear relationship developed by Marion et al. [5] to determine the rate of snow clearing. From this, the amount of electricity generation loss for a given time can be approximated. The presented model

could be further improved by research of the effect meteorological conditions during the formation

of the snow accumulation have on its transmittance.

Chapter 6: First Principle Model

6.1. Symbols

t	time of the simulated panel temperature
T_{t-n}	Panel temperature "n" time-steps before the simulated time (°C)
E_{t-n}	Total absorbed irradiance "n" time-steps before the simulated time (W/m^2)
h_{cr}	Combined convective and longwave radiant heat transfer coefficient (W/m^2/°C)
T_{amb}	Ambient temperature (°C)
C	Heat Capacity of the panel (J/m^2/°C)
Δt	Time-step length (seconds)
p_n	cumulative effect of preceding irradiance on the predicted temperature
c_n	proportional effect of a timestep on panel temperature

6.2. Introduction

Existing empirical models that simulate the effect of snow on PV system electricity generation are extremely useful for system operators and designers. Empirical models can either be grey-box models or black box models. Grey-box models use first principle relationships to determine the structure of the model and use a population of data to estimate the coefficients. Black-box models rely solely on the data to develop the structure of the model and determine coefficients. Grey-box and black-box models generally require experimental data showing the effect of a parameter before the parameter can be simulated, which can limit the usefulness of grey and black box models to researchers studying mitigation methods.

Researchers interested in developing mitigation methods to prevent the accumulation of snow on PV panels would benefit from having a first-principle based model, which simulates the heat and mass transfer related behaviours of both the panel and the snow. However, a comprehensive model would be exceptionally complicated when considering that there are many processes which are difficult to simulate, that occur throughout the melting process, such as phase change, mass flow, convective heat loss, and transmitted irradiance. The resulting model would be dependent on many assumptions, and the output would likely be heavily dependent on approximated inputs. Previously two first principle models have been developed [23,63]; however, neither model is universally

applicable, they either do not consider irradiance or do not consider latent heat and transient heat flow.

Past research into the modelling of the impact of snow has suggested that clearing (sliding or melting) will occur when the panel temperature reaches 0°C for a tilted panel [112]. If this is used as an assumption, along with the panel being subject to uniform heat-flux, then a simple first-principle model which simulates panel temperature could be used to simulate when clearing begins to occur.

In this chapter, a simple first-principle thermal model, which simulates the PV panel temperature before and until melting begins, is described and validated with experimental observations. The developed first principle model is used to enhance the proposed empirical threshold models discussed in Chapter 5. The improvements to the threshold models are achieved by including a weighted value of the preceding and current absorbed irradiance values to account for the heat capacity of the panels.

6.3. Methodology

Transient heat transfer is used in the model to simulate the temperature of snow-covered PV panels before and until melting begins. The model takes into account the solar radiation transmitted through the snow cover and absorbed by the PV panels. Also, the radiation absorbed by the back of the PV panels is included. The data collected from the experiment described in Chapter 3 will be used to validate the model.

6.3.1. Assumptions

One key assumption was made to maximize the applicability of the model, and avoid it depending on input information that is impractical to collect. It was assumed that all heat loss from the panel was through the back surface of the panel. Snow acts as an excellent insulator with a thermal

conductivity of only 0.03 to 0.04 W/m/°C [122], as such, even with a thin 1 cm thick snow accumulation, the heat transfer coefficient would be less than 3 W/m²/°C. Furthermore, the heat lost to the snow is assumed to be insignificant; this is justified because of the combined effect of the low thermal conductivity and low heat capacity of snow. The heat capacity of fresh snow is low (less than 200 kJ/m³/°C), this is the result of the low density of snow [23]. The result is that a snow accumulation 1 cm in thickness would accumulate, at most, only 8-13% the amount of heat accumulated in the panel, which is insignificant for this model.

6.3.2. Model Structure

The model is a transient heat transfer model, and as such, it is dependent on both current and past conditions to simulate panel temperature. The prediction is based on one hour of preceding data and uses a 5-minute time-step, resulting in thirteen time-steps (present time and the twelve preceding timesteps). Ambient temperature and solar irradiance are the required measured inputs for this model. Ambient temperature is relatively stable, and as such, the ambient temperature at the time being simulated (t) was used for all of the timesteps.

Using 1 hour of preceding timesteps provided sufficient time for the simulated panel temperature (T_t) to stabilize from the initial condition. In simulations performed for ambient temperatures between 0°C and -35°C, and a constant level of absorbed irradiance, reducing the absorbed irradiance by 50% for the first 5-minute interval, changed the final simulated panel temperature by less than 0.001°C.

The initial panel temperature condition (T_{t-12}) (the approximate panel temperature 12 timesteps, 60 minutes before the simulated time (t)) is established using steady-state heat transfer. The initial condition is a function of the total absorbed irradiance (E_{t-12}) (measured in W), and ambient temperature (T_{amb}) as described in Eqn. (6.1). Note that the absorbed irradiance (E_{t-12}) values can

either be the front absorbed irradiance (E_F), or the total absorbed irradiance (E_T) as defined in Chapter 5.

$$T_{t-12} = \left(\frac{E_{t-12}}{h_{cr}}\right) + T_{amb} \qquad \textbf{(6.1)}$$

The input ambient temperature can be measured on site or by a nearby weather station. The absorbed irradiance can be calculated from global horizontal irradiance (GHI) measurements using the procedure outlined in Chapter 5. GHI should be measured on site or from a site near enough to experience the same cloud cover conditions.

The combined radiation and convective heat transfer coefficient (h_{cr}) was chosen to be 16 W/m^2/°C; this is within the range of the values suggested by past research given that the testing apparatus was on the ground, surrounded on three sides by obstructions to the wind [123-125]. If in a given application, local wind speed and direction is known for a PV system then the formulas for the combined heat transfer coefficient developed by Lui and Harris [123] or Blocken et al. [126] could be employed.

After the initial condition is calculated, a transient heat transfer calculation is performed for the panel temperature in the remaining timesteps (T_{t-11} to T_t). T_{t-11} to T_t depend on absorbed irradiance (E_n), the past timestep's panel temperature prediction (T_{t-n-1}), ambient temperature (T_{amb}), heat capacity (C), and the duration of the timestep (Δt) as described by Eqn. (6.2). This relationship is depicted in Figure 6.1.

$$T_{t-n} = T_{t-n-1} + \left(\frac{E_{t-n} - h_{cr}(T_{t-n-1} - T_{amb})}{C}\right) \times \Delta t \quad for\ n < 12 \qquad \textbf{(6.2)}$$
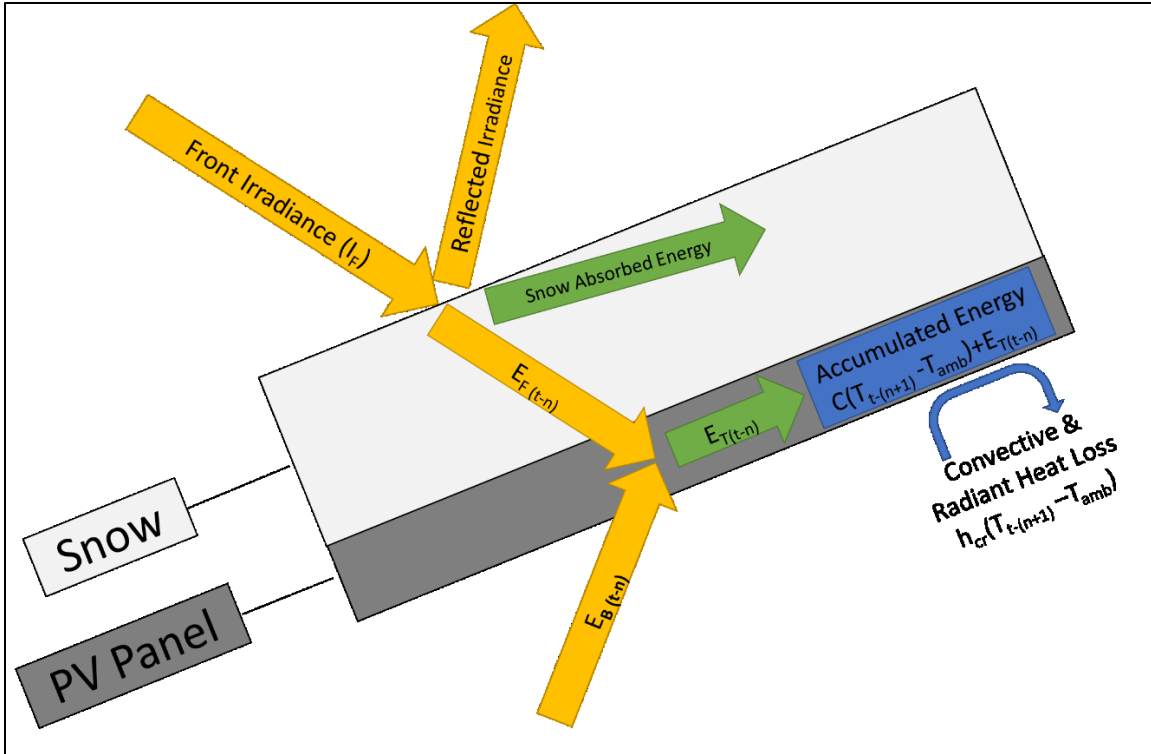
Figure 6.1 Schematic of Transient Heat Flow

The heat capacity of the panel (C) can be determined using the heat capacity, density, and thickness of its components. The heat capacity values used in this analysis were derived from Kant et al. [127]; however, the actual thickness of the glass was used. It is recommended that the actual glass thickness should be used in the computation of heat capacity, due to its significant effect on the panels heat capacity. For the three panels used in the experiment, the framed PV panel has an approximated heat capacity of 7730 $J/m^2/°C$, the glass panel has an approximated heat capacity of 12000 $J/m^2/°C$, and the frameless PV panel has an approximated heat capacity of 12230 $J/m^2/°C$. The framed PV panel has a heat capacity similar to a typical PV panel.

6.3.3. Model Validation

The model was validated using the same dataset as that used to develop the empirical model in Chapter 5. The dataset is the meteorological conditions under which visual signs of clearing were first observed. To use this dataset to validate the model, the assumption must be made that clearing begins when the panel temperature reaches 0°C, which has been suggested indirectly by previous

research [5,14,19]. Furthermore, of all the observations of snow clearing, only three occurred without melting.

Figure 6.2 is a histogram of the values of the predicted panel temperature for each of the 47 observations of snow clearing (i.e. the PV panel is assumed to be 0°C). Figure 6.3 depicts the predicted panel temperatures when clearing was observed (T_t) as a function of ambient temperature (T_{amb}).
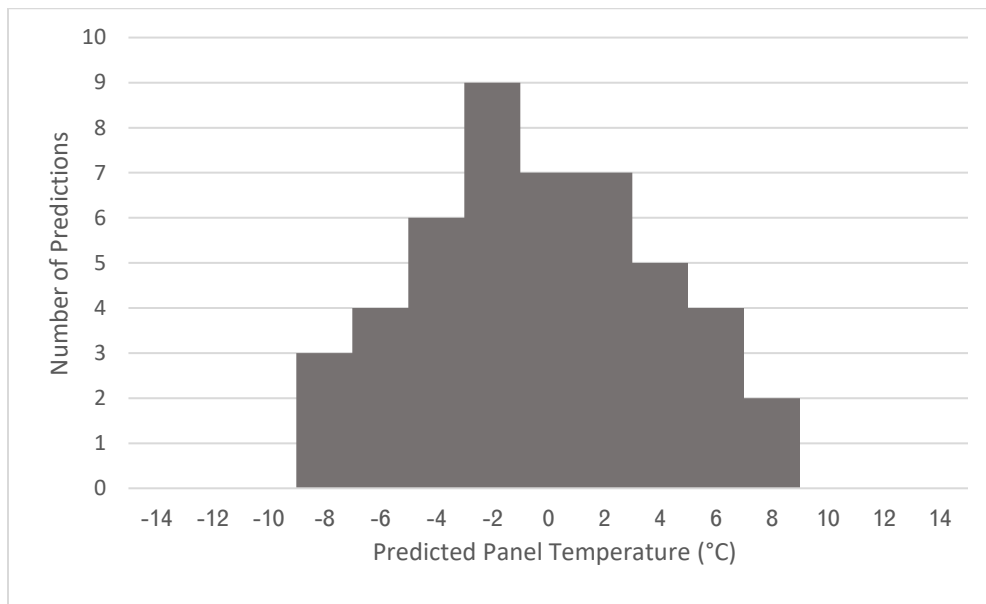

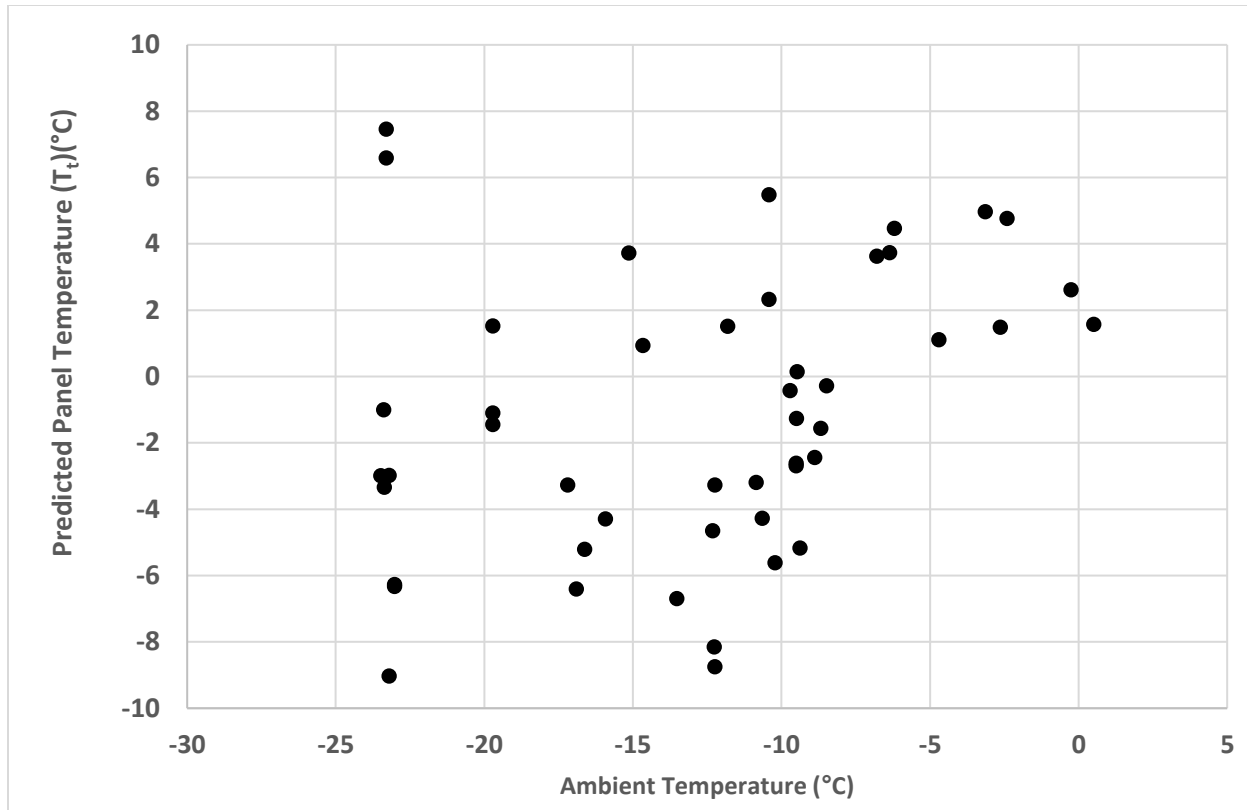*Figure 6.2 Histogram of Predicted Panel Temperature*

Figure 6.3 Predicted Panel Temperature as a function of Ambient Temperature

Figure 6.2 shows that the majority (72%) of the predictions were within 4°C of 0°C. When considering that the average ambient temperature was -12.9°C the results are acceptable but not excellent. Figure 6.3 shows that the precision of the predictions appears correlated with ambient temperature; furthermore, there appears to be a linear trend increasing to the right. The trend is most likely the result of using too high of a combined heat transfer coefficient (h_{cr}) for the heat transfer at the back of the panels but could also be the result of using too high of a heat capacity value (C) for the panels. Too high of a heat capacity would cause the rise in temperature to be slower in conditions where the absorbed irradiance is increasing. The root mean squared error (RMSE) of the model was 4.3°C, as calculated by Eqn. **(6.3)**.

$$RMSE = \sqrt{\frac{\sum_{i=1}^{K}\left(T_{t,i} - (0°C)\right)^2}{K}} \tag{6.3}$$

Where K is the size of the dataset

6.4. Weighted Empirical Threshold Model

First-principle models, like the one described, can be used to improve empirical models by quantitatively incorporating into them first principle relationships, like thermal lag due to the thermal capacity of panels. For this analysis, the first principle model was used to calculate the relative importance of the preceding irradiance on the meteorological conditions that sliding occurred at.

This analysis was performed by first determining the absorbed irradiance for each timestep (E_{t-n}) that is required to increase the panel temperature (T_t) to 0°C. The required irradiance depends on the ambient temperature, profile of the absorbed irradiance (how it is changing over time), and the heat capacity (C) of the panel. Ambient temperatures between -5°C and -35°C were tested. The average increase in absorbed irradiance was 46% in the hour preceding the observations of clearing in the validation dataset, this rate of increase was used for this computation. The heat capacity of the framed panel (7730 J/m^2/°C), the glass (12000 J/m^2/°C), and the frameless panel (12230 J/m^2/°C) were simulated.

With the required absorbed irradiance values determined, the impact of the absorbed irradiance in each timestep on the predicted panel temperature was determined by replacing the absorbed irradiance with 0 W/m^2 one timestep at a time. The resulting change in the final simulated panel temperature (T_t) was divided by the temperature difference between the ambient temperature used for the simulation and 0°C. The result was the effect (c_n) that the irradiance in each timestep contributes to increasing the predicted panel temperature (T_t) from the ambient temperature to 0°C

(this can be thought of as accumulated energy in the panel). Calculations for different ambient temperatures show that these proportions were not dependent on ambient temperature. The proportional effect (c_n) of each timestep on the panel temperature (T_t) is shown in Table 6.1 and Figure 6.4; the increased effect of timestep 12 is the result of it forming the initial condition for the simulation.

Table 6.1 Proportional Effect (c_n) of Individual Timesteps on Panel Temperature (T_t)

Timestep (n)	c_n (C=7730 J/m²/°C)	(c_n) (C=12000 J/m²/°C)	(c_n) (C=12230 J/m²/°C)
0	0.595	0.394	0.388
1	0.241	0.239	0.237
2	0.098	0.145	0.145
3	0.039	0.088	0.089
4	0.016	0.053	0.055
5	0.006	0.032	0.033
6	0.003	0.019	0.020
7	0.001	0.012	0.013
8	0.000	0.007	0.008
9	0.000	0.004	0.005
10	0.000	0.003	0.003
11	0.000	0.002	0.002
12	0.000	0.003	0.003
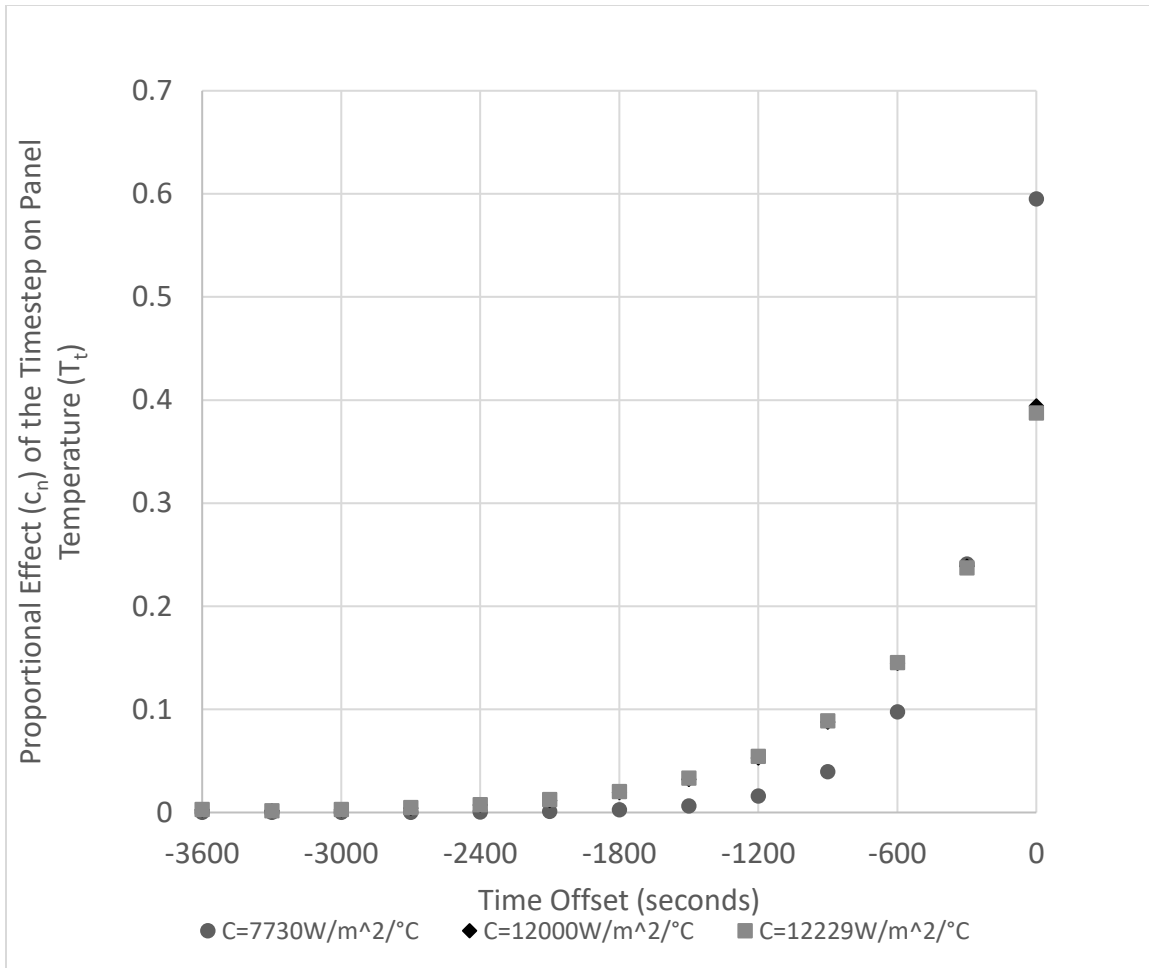
Figure 6.4 Proportional Effect (c_n) of Individual Timesteps on Panel Temperature (Tt)

For datasets with measurement intervals other than 5 minutes Figure 6.5 depicts the cumulative effect of preceding irradiance values on the predicted panel temperature as a function of the time offset. The lines are defined by Eqn. (6.4), Eqn. (6.5), and Eqn. (6.6). From Figure 6.5, given the accuracy of the model, only irradiance conditions within the preceding 20 minutes (1200 seconds) have a significant impact on the panel temperature. The effect of a single timestep (c_n) can be computed with Eqn. (6.7).
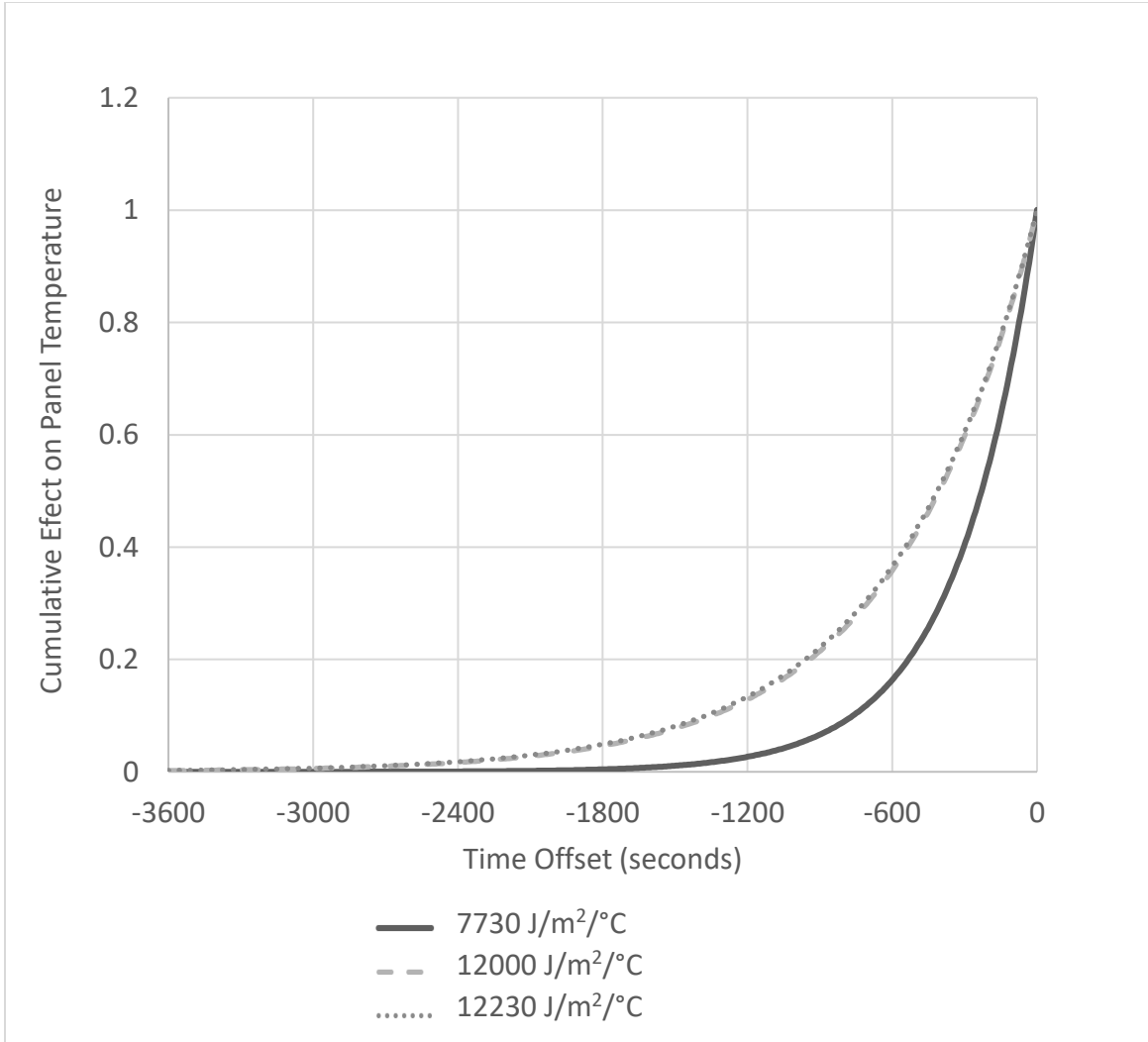
Figure 6.5 Cumulative Effect (p_n) of Irradiance from Preceding Measurements on Predicted Panel Temperature

$$p_n = e^{3.02 \times 10^{-3}(\Delta t \times n)} \quad for\ C = 7730\ \frac{J}{(m^2)(°C)} \tag{6.4}$$

$$p_n = e^{1.71 \times 10^{-3}(\Delta t \times n)} \quad for\ C = 12000\ \frac{J}{(m^2)(°C)} \tag{6.5}$$

$$p_n = e^{1.68 \times 10^{-3}(\Delta t \times n)} \quad for\ C = 12230\ \frac{J}{(m^2)(°C)} \tag{6.6}$$

$$c_n = p_n - p_{n-1} \tag{6.7}$$

The threshold models discussed in Chapter 5 make use of the current irradiance condition and ambient temperature to determine if sliding would occur. Using a singular irradiance value, or average irradiance measurements that are short in length (for example 5 minutes), does not account for the thermal heat capacity of PV panels. PV panels can have a thermal heat capacity of between 7.7 and 12.2 $KJ/m^2/°C$ (as calculated from Kant et al. [127]). As a result, the temperature response of PV panels is not immediate. For example, with an ambient temperature of -20°C and a panel temperature of -10°C, a typical PV panel with a 3 mm thick glass surface (C=7730 $J/m^2/°C$) would take 420 W/m^2 of absorbed irradiance for a length of 5 minutes to warm to 0°C, or 310 W/m^2 for 15 minutes. The result is that moderate levels of irradiance for sustained periods can result in clearing, and rapid increases in irradiance (e.g. due to a break in cloud cover) may not. The heat capacity and the resulting lag in panel temperature should be accommodated for in a model. The heat capacity can be accounted for by considering both present radiation conditions and preceding radiation conditions from a relevant timeframe.

To account for the heat capacity of PV panels, a weighted average of past and current estimated absorbed irradiance can be used. Eqn. (6.8) describes the weighted absorbed irradiance formula. The effect of timesteps (c_n) on the predicted panel temperature (T_t) was used as the weighting coefficients. The coefficients from the second column (C=7730 $J/m^2/°C$) of Table 6.1 were used; using the coefficients of a different heat capacity value, had no significant effect on the model. 7730 $J/m^2/°C$ was used because it represents the heat capacity of a typical PV panel. Only four preceding timesteps (20 minutes) were used because, as can be seen in Figure 6.5, the effect of irradiance before this is small in comparison to the other errors in the model.

$$E_{weighted} = \frac{\sum_0^4 c_{t-n}E_{t-n}}{\sum_0^4 c_{t-n}} = \frac{\sum c_{t-0}E + c_{t-1}E_{t-1} \ldots c_{t-4}E_{t-4}}{\sum c_{t-0} + c_{t-1} \ldots c_{t-4}} \qquad \textbf{(6.8)}$$

Figure 6.6 shows the weighted front absorbed irradiance as a function of ambient temperature, and Figure 6.7 shows the weighted total irradiance as a function of ambient temperature. These figures have the same format as the model charts in Chapter 5 (i.e. Figure 5.4, Figure 5.5, and Figure 5.6); they display the conditions under which clearing was observed, the fitted threshold model, and the equation for the threshold model.
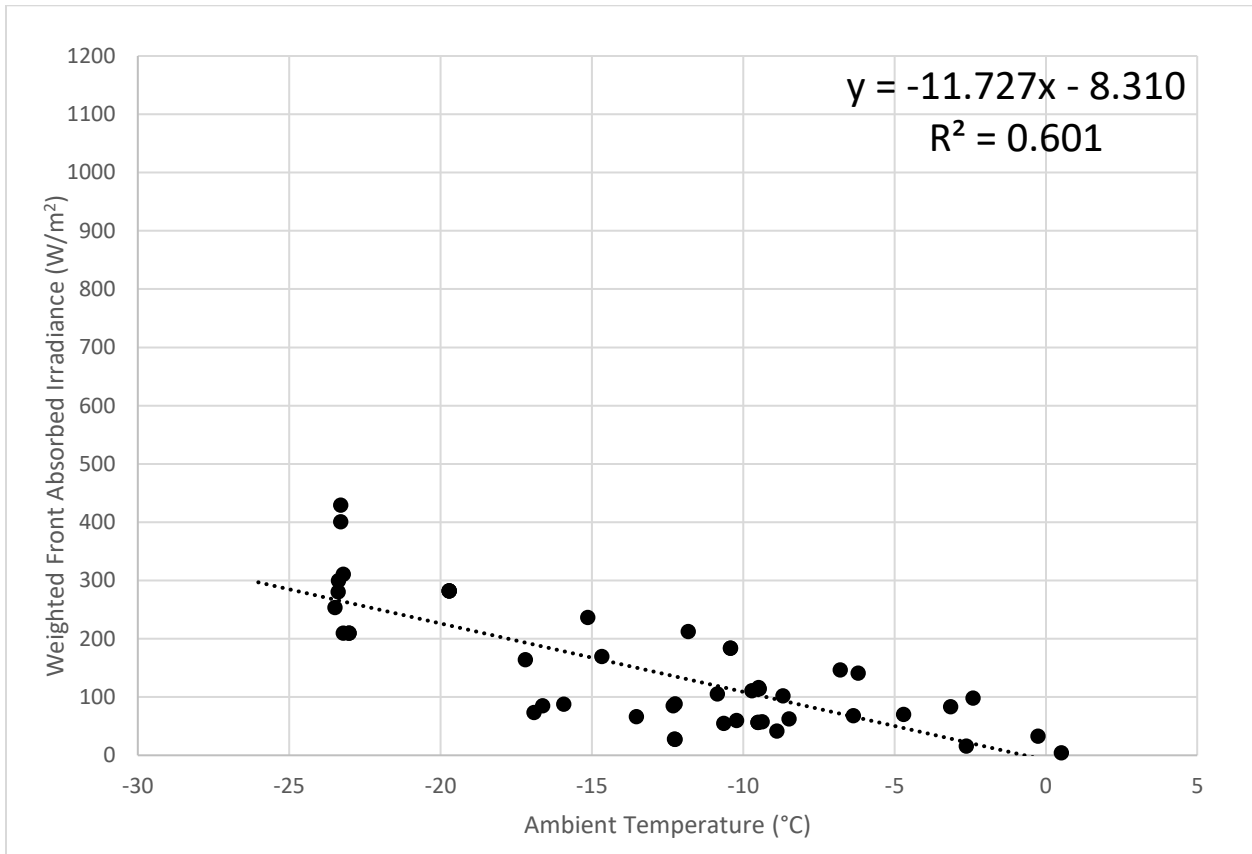
Figure 6.6 Weighted Front Absorbed Irradiance as a Function of Ambient Temperature
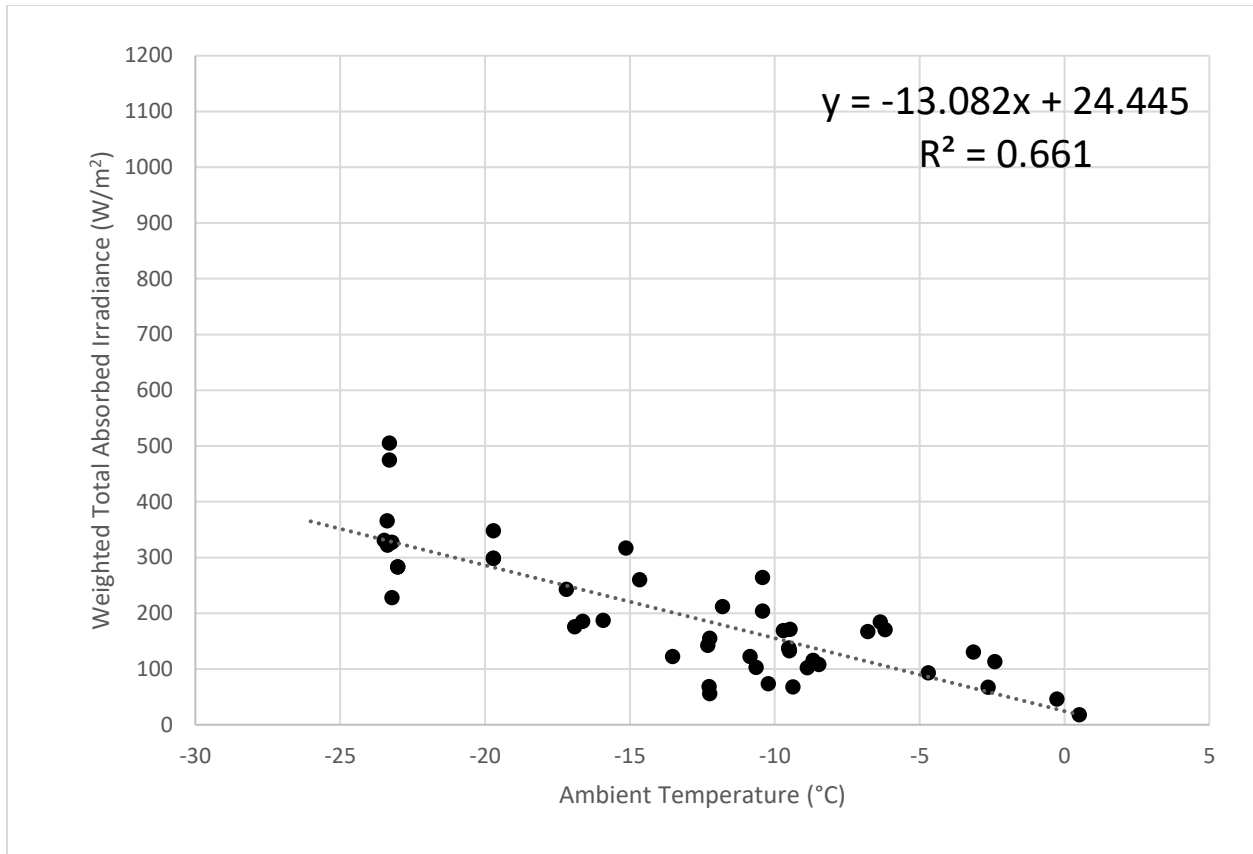
Figure 6.7 Weighted Total Absorbed Irradiance as a Function of Ambient Temperature

Table 6.2 contains the values of several metrics on which the performance of the different types of models can be compared. The models discussed in both Chapter 5 and in this Chapter (Chapter 6) are contained in this table to facilitate comparison. The coefficients of determination (R^2) of the two weighted absorbed irradiance models both exceed that of their respective un-weighted absorbed irradiance model.

To compare the models, which have different magnitudes, a normalized version of RMSE and P90 were calculated ($RMSE_N$ and $P90_N$). The formulas for the normalized values are shown in Table 6.2. Neither of these metrics showed a significant difference between the weighted and unweighted models, except the $P90_N$ of the weighted total absorbed irradiance model which was moderately better than the unweighted total absorbed irradiance. Both the unweighted and weighted total absorbed irradiance models $P95_N$ were 0.65, slightly lower than the front irradiance $P95_N$ of 0.72.

The front absorbed irradiance and weighted front absorbed irradiance models had $P95_N$ values of 0.78 and 0.80 respectively, slightly higher than the front irradiance case. The F-statistic of all the models is high enough that there is no evidence suggesting the models are not representative of the data.

Table 6.2 Results Summary Table

Irradiance Type:	Coefficient of determination (R^2)	RMSE	RMSE Normalized ($RMSE_N$) $$RMSE_N = \frac{RMSE}{\bar{I}}$$	90th Percentile Offset (P90)	Normalized 90th Percentile Offset ($P90_N$) $$P90_N = \frac{P90}{\bar{I}}$$	F-statistic
Front Irradiance	0.16	203	0.443	275	0.60	9
Front Absorbed	0.57	66	0.464	102	0.72	60
Total Absorbed	0.61	67	0.343	114	0.59	70
Weighted Front Absorbed	0.60	65	0.453	104	0.73	68
Weighted Total Absorbed	0.66	64	0.329	102	0.53	88

6.5. Discussion

Beyond being useful for determining the relative importance of preceding irradiance on panel temperature, simple first principle models can be used to optimize the design and operation of mitigation methods (e.g. heating). Furthermore, they can be useful for identifying outliers in data used to train empirical models.

A slight variation of this model (to include a term for external heat inputs) could be used to optimize the design and operation of heating devices used to clear snow from PV panels. First-principle models can be used in the design phase of a PV system to select a heating system with

an optimized heat flux value. To effectively operate heating devices, the energy consumed to cause the panel to clear must be less valuable than the additional energy the panel will generate as a result of clearing it with heat. A first principle model could be used with forecasted meteorological parameters to decide whether heaters should be operated, and what timeframe would result in the most significant benefit.

Manually removing outliers from model training datasets can be time-consuming and extremely tedious. First principle models can be used to remove data-points that are not possibly the result of the parameters being simulated. For example, in the dataset used, outliers could have been identified by simulating the panel temperature using the measured conditions under which clearing was observed. The difference between 0°C and the simulated temperature would be much larger for outliers than it would be for the remaining data in the dataset. Outliers can be the result of external actions causing snow to clear, like wind and vibrations.

In a small minority of observations snow slid clear of the panels with no signs of melting. The sliding process was rapid, and large sections of the snow accumulations broke free from the panel and cleared completely from the panel within seconds. In all the cases, the meteorological conditions during and after the snowfall were such that there was likely a lack of moisture available for icing to form at the interface between the panel and the snow accumulation (due to snow accumulation). The lack of ice means the lack of the possible adhesive forces caused by ice. The hypothesis was that in cases where there is no moisture for icing to occur, the snow accumulation is weakly held in place on the panel, and a minor disruption due to vibrations or wind would be sufficient to cause the snow to break free from the panel.

The described first principle model has several limitations key of which is not being able to simulate the period of clearing after the melting process begins. Simulating the melting process

103

requires the consideration of latent and sensible heat transfer within the snow, which significantly increases the complexity of a model. Furthermore, many uncertainties are introduced due to the characteristics of the snow and how the water flows while interacting with the snow and the panel surface.

Before developing this model, an effort was made to develop a first principle model that could simulate non-uniform heating over the surface of a panel; with the top of the panel being heated by an external heat input, and the remainder being only heated naturally by irradiance. The purpose of the model was to simulate the effectiveness of an absorber plate attached to the top of the panel, which would remain clear of snow and absorb sunlight, conducting heat to warm the top of the panel. Simulations showed that an insulated absorber could be an effective means to melt snow accumulations from the PV panels. The model showed that the heat transferred to the panel would cause the snow accumulation at the top of the panel to melt, and the sensible and latent heat transferred down the slope of the panel would be sufficient for sliding to occur in many meteorological conditions. The vast majority of the heat transferred down the panel was due to the water flow, with only a small fraction being the result of heat conduction within the panel. The model assumed that the water flowed down the panel in a uniform layer; however, observations of the melting process disproved this assumption. The observations showed when melting occurred, channels of water formed between the melting areas and the bottom of the panel (see Figure 4.5), which would result in ineffective heat transfer, and would prevent the panel from clearing.

Past research has developed complex models to simulate the snow clearing process, but the previous models have not simulated the effect that water has on sliding and cannot simulate non-uniform heating of the panel. These processes are believed to be incredibly complex, and further research on various topics pertaining to the interaction between snow and the panel surface must

be established before a first-principle model could be developed to simulate these processes. Being able to model the flow of water at the interface and furthering the understanding of how adhesion affects snow accumulations would contribute significantly to the ability to develop a first principle model

6.6. Conclusion

The model developed within this chapter shows that the panel temperature at the point of melting can be simulated with a RMSE of 4.3°C. This level of accuracy is sufficient to be able to use the model to incorporate heat capacity into empirical threshold type snow clearing prediction models. Simple physical models can also be used to remove outliers from training datasets used in the development of empirical models. Furthermore, first-principle models can be a valuable tool in the design and operation of heating and potentially other mitigation methods for snow accumulations on PV panels.

The proposed empirical model further incorporates first-principle radiant and transient state thermal heat-transfer relationships into an empirical model, making it a mix between a purely empirical model and a grey-box model. Ultimately, a simple yet accurate first-principle based model of snow-covered panels and their clearing process would be of exceptional value to researchers developing methods of mitigating the effects of snow on PV panels. First principle models are advantageous because they can be applied to any configuration and can be easily adapted for specific cases. The research performed by Ross [23] and Rahmatmand et al. [63] have made significant achievements towards developing a first-principle model that is widely applicable; however, there are still limitations to the functionality of their models.

Chapter 7: Conclusions

Solar PV plays a significant role in the renewable energy market because of the recent reductions in system cost and its scalability. The reductions in cost have made it cost-effective in more applications. The scalability has resulted in PV being relatively easy to apply in both utility-scale projects and point-of-use projects, which is something unique to solar PV in the realm of renewable energy. However, the electricity generation attained from solar PV systems is wholly dependant on the amount of irradiance that is reaching the PV cells. Snow accumulation on PV panels significantly reduces the irradiance reaching the cells, and as a result, reduces the quantity and predictability of PV generation. Existing irradiance forecasts are sufficient to predict the electricity generation of PV systems under most conditions. Models which predict the effect of snow are still subject to significant under and over predictions. There is a need to improve the modelling of snow on PV panels before their electricity generation can be more heavily depended on, by regional electricity grids, to meet the demand requirements of consumers and industry during winter months.

This thesis begins with a comprehensive literature review that describes the current level of understanding in a wide variety of topics pertaining to the impact of snow on PV system electricity generation. The purpose of the remainder of this thesis is to enhance the understanding and modelling of the snow clearing process. Experimental results showed that the formation of ice at the interface between the panel and snow was a recurring phenomenon, which could be the cause of snow accumulations. The key contribution of this thesis is the substantial improvement to modelling precision that can be achieved from using the absorbed irradiance instead of the plane-of-array (front irradiance) in threshold type snow cover prediction models. In addition, it is shown

that simple first-principle models can be used to incorporate heat capacity into empirical models and achieve modest improvements to their precision.

The literature review quantifies the impact of snow on PV panel electricity generation and identifies factors that influence the impact of snow. The review also describes existing methods of modelling the effect of snow and summarizes existing and potential mitigation methods to reduce the adverse effect that snow has on PV generation. The review gives PV system designers and operators tools to understand how to mitigate the impact of snow on PV panels. It also identifies shortcomings in existing research and areas of opportunity for future research.

Various experimental observations create the foundation of the analyses performed in this thesis. The experimental setup is described in detail including the apparatus and data logging equipment. The use of non-conventional measurement and data logging is discussed, highlighting its advantages and disadvantages.

The coefficients of friction between snow and PV panels introduced by past researchers would not result in snow accumulations remaining on tilted panels. Adhesion is believed to be a significant contributor to snow accumulations remaining on PV panels. This study presents, for the first time to the author's knowledge, the formation of ice at the interface between the panel and the snow accumulation. The study showed that icing formed in five out of seven observations. Contact melting, existing snow accumulation melting, and pre-existing icing were identified as being the source of moisture for the icing in the experimental observations. Understanding the formation of ice between PV panels and snow accumulations will enhance researchers' ability to model the impact of snow on PV systems and focus efforts towards the development of effective mitigation strategies.

Threshold type empirical models have been shown to be effective at predicting when snow accumulations clear from PV panels; they can be coupled with an electricity generation model to predict future generation with acceptable levels of accuracy. The analysis presented within suggests that using the irradiance absorbed by the PV panel to develop threshold models, rather than plane-of-array irradiance (front irradiance), can substantially improve the precision of models used to determine when clearing will begin.

The coefficients of determination (R^2) for the absorbed irradiance models were nearly four times that of the plane-of-array irradiance (front irradiance) model. The absorbed irradiance through the front surface considers the transmittance of the snow accumulation. The absorbed irradiance through the back surface was also considered. In addition, a process is introduced that predicts the absorbed irradiance by the front and back surface of the panel with parameters readily available from most weather stations, with the only irradiance measurement requirement being GHI. The results of this analysis have the potential to improve the modelling of the effect of snow on PV panels in two ways: improved precision and broadened applicability. Improved precision in threshold models results in the state of the snow cover on PV systems being more frequently predicted correctly—leading to better approximations of electricity generation. Broadened applicability is attained by being able to approximate incident irradiance and absorbed irradiance based on readily available data from most weather stations; this could allow modelling to be performed in many more regions than models that are dependant on complex measurements, or site-specific measurements.

First principle models can excel above empirical models because they are theoretically applicable to any situation. An effective but simple first principle model of the snow clearing process would provide researchers with a method to simulate mitigation strategies for snow on PV systems. Two

existing first principle models serve the purpose for which they were created but are not universally applicable due to the exclusion of certain parameters which are essential to the snow clearing process, for example, latent heat or the effect of solar irradiance.

A simple first-principle thermal heat transfer model is developed, which predicts PV panel temperatures before and until melting begins. Panel temperature is critical because past research suggests that panel temperature is related to when snow accumulations clear. The model simulates the panel temperature with an RMSE of 4.3°C. However, the purpose of this model was not to accurately predict panel temperature, but rather to facilitate the inclusion of the heat capacity of the PV panels in empirical threshold models. The inclusion of heat capacity modestly improved modelling precision. The developed first-principle model could also be useful to exclude outliers from datasets used to train empirical models, and optimize the operation of mitigation methods for snow on PV panels (e.g. heating).

Solar PV electricity generation has the potential to be a significant contributor to meeting the electricity demands of regions. Significant improvements have been made to both efficiency and streamlined production methods which have resulted in significant reductions in upfront cost. Vested interest from society has supported interdisciplinary research in all aspects of PV design and operation. This research will further the application of solar PV. One essential requirement for the extensive use of PV generation in electricity grids is the ability to predict short-term generation accurately. The beginning of this thesis highlights the current state of understanding of how to manage and predict the effect of snow on solar PV electricity generation. The literature review intends to offer researchers entering the field with a summary of the field and highlight the deficiencies in existing knowledge. The remainder of this thesis advances the level of understanding of the cause and prediction of snow accumulations on PV panels; in this regard,

there is still progress to be made; suggestions for future research and studies are included at the end of each chapter.

Bibliography

[1] International Energy Agency. Market Report Series: Renewables 2017 2017;2017.

[2] SolarPower Europe. Global Market Outlook For Solar Power / 2018 - 2022. Solar Power Europe 2018.

[3] Fu R, Feldman D, Margolis R. U.S. Solar Photovoltaic System Cost Benchmark: Q1 2018. National Renewable Energy Laboratory 2018.

[4] Heidari N, Gwamuri J, Townsend T, Pearce JM. Impact of Snow and Ground Interference on Photovoltaic Electric System Performance. IEEE Journal of Photovoltaics 2015;5:1680-1685.

[5] Marion B, Schaefer R, Caine H, Sanchez G. Measured and modeled photovoltaic system energy losses from snow for Colorado and Wisconsin locations. Solar Energy 2013;97:112-121.

[6] Taylor MP. Statistical Relationship Between Photovoltaic Generation and Electric Utility Demand in
Minnesota (1996-2002). Proceedings of the Solar 2003 Conference 2003.

[7] Andrews RW, Pollard A, Pearce JM. A new method to determine the effects of hydrodynamic surface coatings on the snow shedding effectiveness of solar photovoltaic modules. Solar Energy Materials & Solar Cells 2013;113:71-78.

[8] Sugiura T, Yamada T, Nakamura H, Umeya M, Sakuta K, Kurokawa K. Measurements, analyses and evaluation of residential PV systems by Japanese monitoring program. Solar Energy Materials and Solar Cells 2003;75:767-779.

[9] Matthews T. Solar Photovoltaic Reference Array Report. Northern Alberta Institute of Technology 2016.

[10] Powers L, Newmiller J, Townsend T. Measuring and modeling the effect of snow on photovoltaic system performance. PVSC 2010:973.

[11] Townsend T, Powers L. Photovoltaics and snow: An update from two winters of measurements in the SIERRA. PVSC 2011:3231.

[12] Marion B, Rodriguez J, Pruett J. Instrumentation for Evaluating PV System Performance Losses from Snow. Proceedings of the Solar 2009 Conference, 11-16 May 2009, Buffalo, New York (CD-ROM) 2009.

[13] Bosman L, Darling S. Difficulties and recommendations for more accurately predicting the performance of solar energy systems during the snow season. ICRERA 2016:567-571.

[14] Lorenz E, Heinemann D, Kurz C. Local and regional photovoltaic power prediction for large scale grid integration: Assessment of a new algorithm for snow detection. Progress in Photovoltaics: Research and Applications 2012;20:760-769.

[15] Renewable Energy Policy Network for the 21st Century. Renewables 2017 Global Status Report 2017.

[16] Fu R, Feldman D, Margolis R, Woodhouse M, Kristen A. U.S. Solar Photovoltaic System Cost Benchmark. National Renewable Energy Laboratory 2017.

[17] Becker G, Schiebelsberger B, Weber W. An Approach to the Impact of Snow on the Yield of Grid Connected PV Systems. Bavarian Association for the Promotion of Solar Energy 2006.

[18] Andrews RW, Pollard A, Pearce JM. The effects of snowfall on solar photovoltaic performance. Solar Energy 2013;92:84-97.

[19] Ryberg D, Freeman J. Integration, Validation, and Application of a PV Snow Coverage Model in SAM. National Renewable Energy Laboratory 2017.

[20] Government of Canada Environment and Natural Resources. Canadian Climate Normals 1981-2010 Station Data 2017;2018.

[21] Wirth G, Weigl T, Weizenbeck J, Zehner M, Schroedter-Homscheidt M, Becker G. Mapping of Snow Cover Periods for Yield Assessment and Dimensioning of PV Systems 2009.

[22] Brench BL. Snow-covering effects on the power output of solar photovoltaic arrays 1979.

[23] Ross MMD. Snow and ice accumulation on photovoltaic arrays: An assessment of the TN conseil passive melting technology. Energy Diversification Research Laboratory, CANMET, Natural Resources Canada 1995.

[24] Pisklak S. Commercial implementation of a snow impact model for PV performance prediction. PVSC 2016:1002-1006.

[25] Andrews RW. Photovoltaic system performance enhancement: Validated modeling methodologies for the improvement of PV system design 2015.

[26] Weatherbase. Weatherbase;2017.

[27] Cedar Lake Ventures Inc. Average Weather at Munich International Airport ;2017.

[28] National Renewable Energy Laboratory. National Solar Radiation Data Base 2006;2017.

[29] Rohm S, Knoflach C, Nachbauer W, Hasler M, Kaserer L, van Putten J, et al. Effect of Different Bearing Ratios on the Friction between Ultrahigh Molecular Weight Polyethylene Ski Bases and Snow. ACS Appl Mater Interfaces 2016;8:12552-12557.

[30] Buhl D, Rhyner H, Ammann WJ, Adams EE[. Measuring the coefficient of friction of polyethylen on snow. Measuring The Coefficient Of Friction Of Polyethylen On Snow 2000:412-415.

[31] Jelle BP. The challenge of removing snow downfall on photovoltaic solar cell roofs in order to maximize solar energy efficiency - Research opportunities for the future. Energy & Buildings 2013;67:334-351.

[32] Mellor M. A review of basic snow mechanics. International Symposium on Snow Mechanics, Grindelwald 1975;19:15-66.

[33] Kako T, Nakajima A, Irie H, Kato Z, Uematsu K, Watanabe T, et al. Adhesion and sliding of wet snow on a super-hydrophobic surface with hydrophilic channels. Journal of Materials Science 2004;39:547-555.

[34] Andrews RW, Pearce JM. Prediction of energy effects on photovoltaic systems due to snowfall events. PVSC 2012:3386.

[35] Pietruszko SM, Fetlinski B, Bialecki M. Analysis of the performance of grid connected photovoltaic system.
2009:48.

[36] Yosida Z. Physical Studies on Deposited Snow; 1955.

[37] Dufresne S. Clearing snow off panels using the wind/venturi effect 2011;2017.

[38] He Z, Xiao S, Gao H, He J, Zhang Z. Multiscale crack initiator promoted super-low ice adhesion surfaces. Soft Matter 2017;13:6562-6568.

[39] Beemer DL, Wang W, Kota AK. Durable gels with ultra-low adhesion to ice. J. Mater. Chem. A 2016;4:18253-18258.

[40] Urata C, Dunderdale GJ, England MW, Hozumi A. Self-lubricating organogels (SLUGs) with exceptional syneresis-induced anti-sticking properties against viscous emulsions and ices. J. Mater. Chem. A 2015;3:12626-12630.

[41] Wang Y, Yao X, Chen J, He Z, Liu J, Li Q, et al. Organogel as durable anti-icing coatings. Sci China Mater 2015;58:559-565.

[42] Johnston S. Output performance and payback analysis of a residential photovoltaic system in Colorado. PVSC 2012:1452.

[43] Libby C, Kurtz S, Coley S. Field testing of flat-plate and concentrator photovoltaic systems at the Solar Technology Acceleration Center. PVSC 2015:1-6.

[44] Weiss A, Weiss H. Photovoltaic cell electrical heating system for removing snow on panel including verification. ICRERA 2016:995-1000.

[45] Shishavan AA, Foresman EC, Toor F. Performance analysis of crystalline silicon and amorphous silicon photovoltaic systems in Iowa: 2011 to 2014. PVSC 2016:2625-2630.

[46] Hosokawa K, Tomabechi T. Research on the installation technology of photovoltaic systems in consideration of snow. AIJ Journal of Technology and Design 2010;16:197-200.

[47] Wang YJ, Hsu PC. Analytical modelling of partial shading and different orientation of photovoltaic modules. IET Renewable Power Generation 2010;4:272-282.

[48] Barreiro C, Jansson PM, Thompson A, Schmalzel JL. PV by-pass diode performance in landscape and portrait modalities. PVSC 2011:3097.

[49] Nakagawa S, Tokoro T, Nakano T, Hayama K, Ohyama H, Yamaguchi T. An Effect of Snow on the Generation of Electric Energy by 40kw Pv System 2003:2447-2450.

[50] Woyte A, Nijs J, Belmans R. Partial shadowing of photovoltaic arrays with different system configurations: literature review and field test results. Solar Energy 2003;74:217-233.

[51] Torres Lobera D, Mäki A, Huusari J, Lappalainen K, Suntio T, Valkealahti S. Operation of TUT Solar PV Power Station Research Plant under Partial Shading Caused by Snow and Buildings. International Journal of Photoenergy 2013;2013:1-13.

[52] Maghami MR, Hizam H, Gomes C, Radzi MA, Rezadad MI, Hajighorbani S. Power loss due to soiling on solar panel: A review. Renewable and Sustainable Energy Reviews 2016;59:1307-1316.

[53] Thevenard D, Pelland S. Estimating the uncertainty in long-term photovoltaic yield predictions. Solar Energy 2011;91:432.

[54] Pelland S, Galanis G, Kallos G. Solar and photovoltaic forecasting through post-processing of the Global Environmental Multiscale numerical weather prediction model. Progress in Photovoltaics: Research and Applications 2013;21:284-296.

[55] Ryberg D, Freeman J. Integration, validation, and application of a PV snow coverage model in SAM. National Renewable Energy Laboratory 2015.

[56] Thevenard D, Driesse A, Turcotte D, Poissant Y. Uncertainty in long-term photovoltaic yield predictions. CanmetENERGY 2010.

[57] Lorenz E, Scheidsteger T, Hurka J, Heinemann D, Kurz C. Regional PV power prediction for improved grid integration. Progress in Photovoltaics: Research and Applications 2011;19:757-771.

[58] Kostylev V, Pavlovski A. Solar Power Forecasting Performance – Towards Industry Standards. 1st International Workshop on the Integration of Solar Power into Power Systems 2011.

[59] Wirth G, Schroedter-Homscheidt M, Zehner M, Becker G. Satellite-based snow identification and its impact on monitoring photovoltaic systems. Solar Energy 2010;84:215-226.

[60] Natural Renewable Energy Laboratory. System Advisor Model 2017.

[61] Hong T, Koo C, Lee M. Estimating the Loss Ratio of Solar Photovoltaic Electricity Generation through Stochastic Analysis. Journal of Construction Engineering and Project Management 2013;3:23-34.

[62] Zamo M, Mestre O, Arbogast P, Pannekoucke O. A benchmark of statistical regression methods for short-term forecasting of photovoltaic electricity production, part I: Deterministic forecast of hourly production. Solar Energy 2014;105:792-803.

[63] Rahmatmand A, Harrison SJ, Oosthuizen P. An Improved Numerical Method for Predicting Snow Melting on Photovoltaic Panels
. Proceedings of the eSim 2016 Building Performance Simulation Conference 2016:286-296.

[64] Jelle BP, Gao T, Mofid SA, Kolås T, Stenstad PM, Ng S. Avoiding Snow and Ice Formation on Exterior Solar Cell Surfaces – A Review of Research Pathways and Opportunities. Procedia Engineering 2016;145:699-706.

[65] United States. Army. Corps of Engineers. Snow Hydrology : Summary Report of the Snow Investigations North Pacific Division, Corps of Engineers, U.S. Army: Portland, Ore.; 1956.

[66] Ross M, Usher EP. Photovoltaic Array Icing and Snow Accumulation: A Study of a Passive Melting Technology. Proceedings of the 21st Annual Conference of the Solar Energy Society of Canada 1995:21-26.

[67] Ross MMD, Usher EP. Modelled and Observed Operation of a Passive Melting Technology for Photovoltaic Arrays. Proceedings of the 7th International Workshop on Atmospheric Icing of Structures 1996:245-250.

[68] Ross MMD. Solar Irradiance of a Photovoltaic Panel's Rear Face: Models Applicable to Snow Removal and Bifacial Technologies. Proceedings of the 22nd Annual Conference of the Solar Energy Society of Canada 1996.

[69] Bergevin B, Hosatte P, Vallieres N. Photovoltaic system using reflected solar rays of the surroundings and method therefor, to dispose of snow, frost and ice 1994.

[70] Skoplaki E, Palyvos JA. On the temperature dependence of photovoltaic module electrical performance: A review of efficiency/power correlations. Solar Energy 2009;83:614-624.

[71] Alfred. Effect of Temperature on Solar Panels 2010;2016.

[72] Nakajima A. Design of a Transparent Hydrophobic Coating. Journal of the Ceramic Society of Japan 2004;112:533-540.

[73] Fillion RM, Riahi AR, Edrisy A. A review of icing prevention in photovoltaic devices by surface engineering. Renewable & Sustainable Energy Reviews 2014;32:797-809.

[74] Golovin K, Kobaku SPR, Lee DH, DiLoreto ET, Mabry JM, Tuteja A. Designing durable icephobic surfaces. Science advances 2016;2:e1501496.

[75] Kenny RP, Ioannides A, Müllejans H, Zaaiman W, Dunlop ED. Performance of thin film PV modules. Thin Solid Films 2006;511:663-672.

[76] Failla MC. Snow and Ice on Photovoltaic Devices: Analysis of a Challenge and Proposals for Solutions 2016.

[77] Xiao S, He J, Zhang Z. Nanoscale deicing by molecular dynamics simulation. Nanoscale 2016;8:14625-14632.

[78] Krasowska M, Zawala J, Malysa K. Air at hydrophobic surfaces and kinetics of three phase contact formation. Advances in Colloid and Interface Science 2009;147:155-169.

[79] Kako T, Nakajima A, Kato Z, Uematsu K, Watanabe T, Hashimoto K. Adhesion and Sliding of Snow on Hydrophobic Solid Surface. JOURNAL- CERAMIC SOCIETY JAPAN 2002;110:186-192.

[80] Perovich DK. Light reflection and transmission by a temperate snow cover. Journal of Glaciology 2007;53:201-210.

[81] Croft S, Dorn R, Gur I, Hachtmann B, Hollars D, Jaiswal S, et al. Photovoltaic modules with integrated devices 2009.

[82] Hoppins D, Le T, Kaiser F. Solar power systems optimized for use in cold weather conditions 2011.

[83] Kautzor Enterprise Int. Automatic Solar Panel Snow Removal 2015;2017.

[84] Nobuyoshi Takehara, Naoki Manabe. Photovoltaic power generating system 1999.

[85] Takehara N, Manabe N. Photovoltaic power generating system 2000;US 09/258,210.

[86] Ball JT, Ball BJ. Photovoltaic module with heater 2012.

[87] Krzysztof Skupien, Pawel Boratynski, Edyta Stanek, Dawid Cycon. Application of fluorine doped tin (iv) oxide sno2:f for making a heating layer on a photovoltaic panel, and the photovoltaic panel 2012;US 14/373,061.

[88] McKarris George. Intelligent & self-cleaning solar panels 2012.

[89] Townsend BP. Solar defrost panels 2011.

[90] Adler JS, Baird HR. Autonomous winter solar panel 2014;US 13/507,958.

[91] Hickman Nicoleta. Hybrid Solar Cell Integrating Photovoltaic and Thermoelectric Cell Elements for High Efficiency and Longevity 2007;US 13/861,594.

[92] Husu AG, Stan MF, Cobianu C, Fidel N, Nedelcu O. An inedited solution to increase the energy efficiency of photovoltaic panels for regions with snow. EMES 2015:1-4.

[93] Nickel B. Snow melt system for solar collectors 2012;US 13/834,386.

[94] Warfield DB, Garvison P. Photovoltaic module mounting unit and system 2005.

[95] Lund J. Pavement Snow Melting
. Geo-Heat Center Quarterly Bulletin 2000.

[96] Mazumder M, K. Self-cleaning solar panels and concentrators with transparent electrodynamic screens 2012.

[97] Higashiyama Y, Yanase S, Sugimoto T. Behavior of water droplets located on a hydrophobic insulating plate under DC field. Conference Record of 1998 IEEE Industry Applications Conference. Thirty-Third IAS Annual Meeting (Cat. No.98CH36242) 1998;3:1813 vol.3.

[98] Keim S, Koenig D. The dynamic behaviour of water drops in an AC field. CEIDP 2001:613-616.

[99] Mizuno Y, Iwatani M, Nagata M, Naito K, Kondo K, Ito S. Behavior of water droplets on silicone rubber sheet under AC voltage application. 1998 Annual Report Conference on Electrical Insulation and Dielectric Phenomena (Cat. No.98CH36257) 1998;1:99 vol. 1.

[100] Dufresne S. Solar snow pre-melter experiments 2014;2017.

[101] Visa I, Burduhos B, Neagoe M, Moldovan M, Duta A. Comparative analysis of the infield response of five types of photovoltaic modules. Renewable Energy 2016;95:178-190.

[102] Efron R, Adel M, Klier S, Klier Z. Method of removal of snow or ice coverage from solar collectors 2012.

[103] Köntges M, Kajari-Schröder S, Kunze I, Jahn U. Crack Statistic of Crystalline Silicon Photovoltaic Modules. 26th European Photovoltaic Solar Energy Conference and Exhibition 2011:3290-3294.

[104] Taylor DA. Snow on sloping roofs 1987.

[105] Abe O. Shear strength and angle of repose of snow layers including graupel. Annals of Glaciology 2004;38:305-308.

[106] Kuroiwa D, Yukiko M, Masao T. Micromeritical Properties of Snow. Physics of Snow and Ice : proceedings 1967:751-772.

[107] Andrews RW, Pearce JM. The effect of spectral albedo on amorphous silicon and crystalline silicon solar photovoltaic device performance. Solar Energy 2013;91:233-241.

[108] Alberta Agriculture and Forestry. Current and Historical Alberta Weather Station Data Viewer 2018.

[109] University of Alberta. Earth and Atmospheric Science Weather station archive 2018;2018.

[110] Raspberry Pi Foundation. Penguin Lifelines 2014;2019.

[111] Environment and Natural Resources Canada. Canadian Weather 2018;2018.

[112] Pawluk R, Chen Y, She Y. Photovoltaic Electricity Generation Loss Due to Snow – A Literature Review on Influence Factors, Estimation, and Mitigation. Renewable and Sustainable Energy Reviews 2019.

[113] NREL. National Renewable Energy Laboratory - System Advisor Model (SAM) Release Notes 2018;2018.

[114] Perovich DK. Light reflection and transmission by a temperate snow cover. Journal of Glaciology 2007;53:201-210.

[115] Warren G. S. Optical properties of snow. REVIEWS OF GEOPHYSICS AND SPACE PHYSICS 1982:67-89.

[116] Perez RR, Ineichen P, Maxwell EL, Seals RD, Zelenka A. Dynamic global-to-direct irradiance conversion models 1992.

[117] Perez R, Ineichen P, Moore K, Kmiecik M, Chain C, George R, et al. A new operational model for satellite-derived irradiances: description and validation. Solar Energy 2002;73:307-317.

[118] Myers DR. Solar radiation modeling and measurements for renewable energy applications: data and model quality. Energy 2005;30:1517-1531.

[119] F. Holmgren W, W. Hansen C, A. Mikofski M. pvlib python: a python package for modeling solar energy systems. Journal of Open Source Software 2018;3:884.

[120] Perez R, Ineichen P, Seals R, Michalsky J, Stewart R. Modeling daylight availability and irradiance components from direct and global irradiance. Solar Energy 1990;44:271-289.

[121] Burg BR, Ruch P, Paredes S, Michel B. Effects of radiative forcing of building integrated photovoltaic systems in different urban climates. Solar Energy 2017;147:399-405.

[122] Chernov RA. Metamorphism and thermal properties of fresh snow (study in the Moscow region). Ld i Sneg, Vol 56, Iss 2, Pp 199-206 (2016) 2016:199.

[123] Liu Y, Harris DJ. Full-scale measurements of convective coefficient on external surface of a low-rise building in sheltered conditions. Building and Environment 2007;42:2718-2736.

[124] Vasan N, Stathopoulos T. Experimental study of wind effects on unglazed transpired collectors. Solar Energy 2014;101:138-149.

[125] Kalogirou SA, Aresti L, Christodoulides P, Florides G. The Effect of Air Flow on a Building Integrated PV-panel. Procedia IUTAM 2014;11:89-97.

[126] Blocken B, Defraeye T, Derome D, Carmeliet J. High-resolution CFD simulations for forced convective heat transfer coefficients at the facade of a low-rise building. Building and Environment 2009;44:2396-2412.

[127] Kant K, Shukla A, Sharma A, Biwole PH. Thermal response of poly-crystalline silicon photovoltaic panels: Numerical simulation and experimental study. Solar Energy 2016;134:147-155.